



1 **Two-way coupled meteorology and air quality models in Asia: a systematic review**  
2 **and meta-analysis of impacts of aerosol feedbacks on meteorology and air quality**  
3 Chao Gao<sup>1</sup>, Aijun Xiu<sup>1,\*</sup>, Xuelei Zhang<sup>1,\*</sup>, Qingqing Tong<sup>1</sup>, Hongmei Zhao<sup>1</sup>, Shichun Zhang<sup>1</sup>,  
4 Guangyi Yang<sup>1,2</sup>, and Mengduo Zhang<sup>1,2</sup>

5  
6 <sup>1</sup>Key Laboratory of Wetland Ecology and Environment, Northeast Institute of Geography and Agroecology, Chinese  
7 Academy of Sciences, Changchun, 130102, China

8 <sup>2</sup>University of Chinese Academy of Sciences, Beijing, 100049, China

9 Correspondence to: A.J. Xiu (xiuajun@iga.ac.cn) & X.L. Zhang (zhangxuelei@iga.ac.cn)

10  
11 **Abstract**

12 Atmospheric aerosols can exert influence on meteorology and air quality through aerosol-  
13 radiation interactions (ARI) and aerosol-cloud interactions (ACI) and this two-way feedback has  
14 been studied by applying two-way coupled meteorology and air quality models. As one of regions  
15 with high aerosol loading in the world, Asia has attracted many researchers to investigate the aerosol  
16 effects with several two-way coupled models (WRF-Chem, WRF-CMAQ, GRAPES-CUACE and  
17 WRF-NAQPMS) over the last decade. This paper attempts to offer bibliographic analysis regarding  
18 the current status of applications of two-way coupled models in Asia, related research focuses,  
19 model performances and the effects of ARI or/and ACI on meteorology and air quality. There are  
20 total 157 peer-reviewed articles published between 2010 and 2019 in Asia meeting the inclusion  
21 criteria, with more than 81 % of papers involving the WRF-Chem model. The number of relevant  
22 publications has an upward trend annually and East Asia, India, China, as well as the North China  
23 Plain are the most studied areas. The effects of ARI and both ARI and ACI induced by natural  
24 aerosols (particularly mineral dust) and anthropogenic aerosols (bulk aerosols, different chemical  
25 compositions and aerosols from different sources) are widely investigated in Asia. Through the  
26 meta-analysis of surface meteorological and air quality variables simulated by two-way coupled  
27 models, the model performance affected by aerosol feedbacks depends on different variables,  
28 simulation time lengths, selection of two-way coupled models, and study areas. Future research  
29 perspectives with respect to the development, improvement, application, and evaluation of two-way  
30 coupled meteorology and air quality models are proposed.

31 **1 Introduction**

32 Atmospheric pollutants can affect local weather and global climate via many mechanisms as  
33 extensively summarized in the Intergovernmental Panel on Climate Change (IPCC) reports (IPCC,  
34 2007, 2014, 2021), and also exhibit impacts on human health and ecosystems (Lelieveld et al., 2015;  
35 Wu and Zhang, 2018). Atmospheric pollutants can modify the radiation energy balance, thus  
36 influence meteorological conditions (Gray et al., 2010; Yiğit et al., 2016). Compared to other climate  
37 agents, the short-lived and localized aerosols could induce changes in meteorology and climate  
38 through aerosol-radiation interactions (ARI, Satheesh and Moorthy, 2005; Tremback et al., 1986)  
39 and aerosol-cloud interactions (ACI, Lohmann and Feichter, 2005; Martin and Leight, 1949) or both  
40 (Haywood and Boucher, 2000; Sud and Walker, 1990). ARI (previously known as direct effect and  
41 semi-direct effect) are based on scattering and absorbing solar radiation by aerosols as well as cloud  
42 dissipation by heating (Ackerman et al., 2000; Koch and Genio, 2010; McCormick and Ludwig,  
43 1967; Wilcox, 2012), and ACI (known as indirect effect) are concerned with aerosols altering albedo  
44 and lifetime of clouds (Albrecht, 1989; Lohmann and Feichter, 2005; Twomey, 1977). As our  
45 knowledge base of aerosol-radiation-cloud interactions that involve extremely complex physical  
46 and chemical processes has been expanding, accurately assessing the effects of these interactions  
47 still remains a big challenge (Chung, 2012; Fan et al., 2016; Kuniyal and Guleria, 2019; Rosenfeld  
48 et al., 2019, 2008).

49 The interactions between air pollutants and meteorology can be investigated by observational  
50 analyses and/or air quality models. So far, many observational studies using measurement data from  
51 a variety of sources have been conducted to analyze these interactions (Bellouin et al., 2008; Groß  
52 et al., 2013; Rosenfeld et al., 2019; Wendisch et al., 2002). Yu et al. (2006) reviewed research work  
53 that adopted satellite and ground-based measurements to estimate the ARI-induced changes of  
54 radiative forcing and the associated uncertainties in the analysis. Yoon et al. (2019) analyzed the  
55 effects of aerosols on the radiative forcing based on the Aerosol Robotic Network observations and  
56 demonstrated that these effects depended on aerosol types. On the other hand, since the uncertainties  
57 in ARI estimations were associated with ACI (Kuniyal and Guleria, 2019), the simultaneous  
58 assessments of both ARI and ACI effects were needed and had gradually been conducted via satellite



59 observations (Illingworth et al., 2015; Kant et al., 2019; Quaas et al., 2008; Sekiguchi et al., 2003).  
60 In the early stages, observational studies of ACI effects were based on several cloud parameters  
61 mainly derived from surface-based microwave radiometer (Kim et al., 2003; Liu et al., 2003) and  
62 cloud radar (Feingold et al., 2003; Penner et al., 2004). Later on, with the further development of  
63 satellite observation technology and enhanced spatial resolution of satellite measurement comparing  
64 against traditional ground observations, the satellite-retrieved cloud parameters (effective cloud  
65 droplet radius, liquid water path (LWP) and cloud cover) were utilized to identify the ACI effects  
66 studies on cloud scale. (Goren and Rosenfeld, 2014; Rosenfeld et al., 2014). Moreover, in order to  
67 clarify whether aerosols affect precipitation positively or negatively, the effects of ACI on cloud  
68 properties and precipitation were widely investigated but with various answers (Andreae and  
69 Rosenfeld, 2008; Casazza et al., 2018; Fan et al., 2018; Rosenfeld et al., 2014). Analyses of satellite  
70 and/or ground observations revealed that increased aerosols could suppress (enhance) precipitation in  
71 drier (wetter) environments (Donat et al., 2016; Li et al., 2011; Rosenfeld, 2000; Rosenfeld et al.,  
72 2008). Most recently, Rosenfeld et al. (2019) further used satellite-derived cloud information  
73 (droplet concentration and updraft velocity at cloud base, LWP at cloud cores, cloud geometrical  
74 thickness and cloud fraction) to single out ACI under a certain meteorological condition, and found  
75 that the cloudiness change caused by aerosol in marine low-level clouds was much greater than  
76 previous analyses (Sato and Suzuki, 2019). Despite the fact that aforementioned studies had  
77 significantly improved our understanding of aerosol effects, many limitations still exist, such as low  
78 temporal resolution of satellite data, low spatial resolution of ground monitoring sites and lack of  
79 vertical distribution information of aerosol and cloud (Rosenfeld et al., 2014; Sato and Suzuki, 2019;  
80 Yu et al., 2006).

81 Numerical models can also be used to study the interactions between air pollutants and  
82 meteorology. Air quality models simulate physical and chemical processes in the atmosphere (ATM)  
83 and are classified as offline and online models (El-Harbawi, 2013). Offline models (also known as  
84 traditional air quality models) require outputs from meteorological models to subsequently drive  
85 chemical models (Byun and Schere, 2006; ENVIRON, 2008; Seaman, 2000). Comparing to online  
86 models, offline models usually are computationally efficient but incapable of capturing two-way  
87 feedbacks between chemistry and meteorology (North et al., 2014). Online models or coupled  
88 models are designed and developed to consider the two-way feedbacks and attempted to accurately  
89 simulate both meteorology and air quality (Briant et al., 2017; Grell et al., 2005; Wong et al., 2012).  
90 Two-way coupled models can be generally categorized as integrated and access models based on  
91 whether using a coupler to exchange variables between meteorological and chemical modules  
92 (Baklanov et al., 2014). Currently, there are three representative two-way coupled meteorology and  
93 air quality models, namely the Weather Research and Forecasting-Chemistry (WRF-Chem) (Grell  
94 et al., 2005), WRF coupled with Community Multiscale Air Quality (CMAQ) (Wong et al., 2012)  
95 and WRF coupled with a multi-scale chemistry-transport model for atmospheric composition  
96 analysis and forecast (WRF-CHIMERE) (Briant et al., 2017). The WRF-Chem is an integrated  
97 model that includes various chemical modules in the meteorological model (i.e., WRF) without  
98 using a coupler. For the remaining two models, which belong to access model, the WRF-CMAQ  
99 uses a subroutine called *aqprep* (Wong et al., 2012) as its coupler while the WRF-CHEMERE  
100 a general coupling software named Ocean Atmosphere Sea Ice Soil-Model Coupling Toolkit (Craig  
101 et al. 2017). With more growing interest in coupled models and their developments, applications  
102 and evaluations, two review papers thoroughly summarized the related works published before 2008  
103 (Zhang, 2008) and 2014 (Baklanov et al., 2014). Zhang (2008) overviewed the developments and  
104 applications of five coupled models (WRF-Chem; Gas, Aerosol, Transport, Radiation, General  
105 Circulation, Mesoscale, and Ocean Model; Community Atmosphere Model version3; the Model for  
106 Integrated Research on Atmospheric Global Exchanges; Caltech unified General Circulation Model)  
107 in the United States (US) and the treatments of chemical and physical processes in these coupled  
108 models with emphasis on the ACI related processes. Another paper presented a systematic review  
109 on the similarities and differences of eighteen integrated or access models in Europe and discussed  
110 the descriptions of interactions between meteorological and chemical processes in these models as  
111 well as the model evaluation methodologies involved (Baklanov et al., 2014). Some of these coupled  
112 models can not only be used to investigate the interactions between air quality and meteorology at  
113 regional scales but also at global and hemispheric scales (Grell et al., 2011; Jacobson, 2001; Mailler  
114 et al., 2017; Xing et al., 2015a), but large scale studies were not included in the two review papers  
115 by Zhang (2008) and Baklanov et al. (2014). These reviews only focused on application and



116 evaluation of coupled models in US and Europe but there is still no systematic review targeting two-  
117 way coupled model applications in Asia.

118 Compared to US and Europe, Asia has been suffering more severe air pollution in the past three  
119 decades (Bollasina et al., 2011; Gurjar et al., 2016; Rohde and Muller, 2015) due to the rapid  
120 industrialization, urbanization and population growth together with unfavorable meteorological  
121 conditions (Jeong and Park, 2017; Lelieveld et al., 2018; Li M. et al., 2017). Then, the interactions  
122 between atmospheric pollution and meteorology in Asia, which have received a lot of attention from  
123 scientific community, are investigated using extensive observations and a certain number of  
124 numerical simulations (Li et al., 2016; Nguyen et al., 2019a; Wang et al., 2010). Based on airborne,  
125 ground-based, and satellite-based observations, multiple important experiments have been carried  
126 out to analyze properties of radiation, cloud and aerosols in Asia, as briefly reviewed by Lin N. et  
127 al. (2014). Recent observational studies confirmed that increasing aerosol loadings play important  
128 roles in radiation budget (Benas et al., 2020; Eck et al., 2018), cloud properties (Dahutia et al., 2019;  
129 Yang et al., 2019), precipitation intensity along with vertical distributions of precipitation types  
130 (Guo et al., 2018, 2014). According to previous observational studies in Southeast Asia (SEA), Tsay  
131 et al. (2013) and Lin N. et al. (2014) comprehensively summarized the spatiotemporal characteristics  
132 of biomass burning (BB) aerosols and clouds as well as their interactions. Li et al. (2016) analyzed  
133 how ARI or ACI influenced climate/meteorology in Asia utilizing observations and climate models.  
134 With regard to the impacts of aerosols on cloud, precipitation and climate in East Asia (EA), a  
135 detailed review of observations and modeling simulations has also been presented by Li Z. et al.  
136 (2019). Since the 2000s, substantial progresses have been made in the climate-air pollution  
137 interactions in Asia based on regional climate models simulations, which have been summarized by  
138 Li et al. (2016). Moreover, starting from year of 2010, with the development and availability of two-  
139 way coupled meteorology and air quality models, more and more modeling studies have been  
140 conducted to explore the ARI or/and ACI effects in Asia (Nguyen et al., 2019a; Sekiguchi et al.,  
141 2018; Wang et al., 2010; Wang J. et al., 2014). In recent studies, a series of WRF-Chem and WRF-  
142 CMAQ simulations were performed to assess the consequences of ARI on radiative forcing,  
143 planetary boundary layer height (PBLH), precipitation, and fine particulate matter (PM<sub>2.5</sub>) and ozone  
144 concentrations (Huang et al., 2016; Nguyen et al., 2019a; Sekiguchi et al., 2018; J. Wang et al.,  
145 2014). Different from current released version of WRF-CMAQ model (based on WRF version 4.3  
146 and CMAQ version 5.3.2, Wong et al., 2012) that only includes ARI, WRF-Chem with ACI (starting  
147 from WRF-Chem version 3.0, Chapman et al., 2009) has been implemented for analyzing the  
148 complicated aerosol effects that lead to variations of cloud properties, precipitations and PM<sub>2.5</sub>  
149 concentrations (Bai et al., 2020; Liu Z. et al., 2018; Park et al., 2018; Zhao et al., 2017). To quantify  
150 the individual or joint effects of ARI or/and ACI on meteorological variables and pollutants  
151 concentrations, several modeling studies have been performed in Asia (Chen et al., 2019a; Ma et al.,  
152 2016; Zhang B. et al., 2015; Zhang et al., 2018). In addition, model comparisons (including offline  
153 and online models) targeting EA have been carried out recently under the Model Inter-Comparison  
154 Study for Asia (MICS-Asia) phase III (Chen et al., 2019b; Gao M. et al., 2018a; Li J. et al., 2019).  
155 As mentioned above, even though there are already several reviews regarding the observational  
156 studies of ARI or/and ACI (Li et al., 2016; Li Z. et al., 2019S; Lin N. et al., 2014; Tsay et al., 2013)  
157 it is necessary to conduct a systematic review in Asia focusing on applications of two-way coupled  
158 meteorology and air quality models as well as simulated variations of meteorology and air quality  
159 induced by aerosol effects.

160 This paper is constructed as follows: Section 2 describes the methodology for literature  
161 searching, paper inclusion, and analysis; Section 3 summarizes the basic information about  
162 publications as well as developments and applications of coupled models in Asia and Section 4  
163 provides the recent overviews of their research points. Sections 5 to 6 present systematic review and  
164 meta-analysis of the effects of aerosol feedbacks on model performance, meteorology and air quality  
165 in Asia. The summary and perspective are provided in Section 7.

## 166 2 Methodology

### 167 2.1 Criteria and synthesis

168 Since 2010, in Asia, regional studies of aerosol effects on meteorology and air quality based  
169 on coupled models have been increasing gradually, therefore in this study we performed a systematic  
170 search of literatures to identify relevant studies from January 1, 2010 to December 31, 2019. In  
171 order to find all the relevant papers in English, Chinese, Japanese and Korean, we deployed several  
172 science-based search engines, including Google Scholar, the Web of Science, the China National



173 Knowledge Infrastructure, the Japan Information Platform for S&T Innovation, the Korean Studies  
174 Information Service System. The different keywords and their combinations for paper searching are  
175 as follows: (1) model-related keywords including “coupled model”, “two-way”, “WRF”, “NU-  
176 WRF”, “WRF-Chem”, “CMAQ”, “WRF-CMAQ”, “CAMx”, “CHIMERE” and “WRF-  
177 CHIMERE”; (2) effect-related keywords including “aerosol radiation interaction”, “ARI”, “aerosol  
178 cloud interaction”, “ACI”, “aerosol effect” and “aerosol feedback”; (3) air pollution-related  
179 keywords including “air quality”, “aerosol”, “PM2.5”, “O3”, “CO”, “SO2”, “NO2”, “dust”, “BC”,  
180 “black carbon”, “blown carbon”, “carbonaceous”, “primary pollutants”; (4) meteorology-related  
181 keywords including “meteorology”, “radiation”, “wind”, “temperature”, “specific humidity”,  
182 “relative humidity”, “planetary boundary layer”, “cloud” and “precipitation”; (5) region-related  
183 keywords including “Asia”, “East Asia”, “Northeast Asia”, “South Asia”, “Southeast Asia”, “Far  
184 East”, “China”, “India”, “Japan”, “Korea”, “Singapore”, “Thailand”, “Malaysia”, “Nepal”, “North  
185 China Plain”, “Yangtze River Delta”, “Pearl River Delta”, “middle reaches of the Yangtze River”,  
186 “Sichuan Basin”, “Guanzhong Plain”, “Northeast China”, “Northwest China” “East China”, “Tibet  
187 Plateau”, “Taiwan”, “northern Indian”, “southern Indian”, “Gangetic Basin”, “Kathmandu Valley”.

188 After applying the search engines and the keywords combinations mentioned above, we found  
189 943 relevant papers. In order to identify which paper should be included or excluded in this paper,  
190 following criteria were applied: (1) duplicate literatures were deleted; (2) studies of using coupled  
191 models in Asia with aerosol feedbacks turned on were included, and observational studies of aerosol  
192 effects were excluded; (3) publications involving coupled climate model were excluded. According  
193 to these criteria, not only regional studies, but also studies using the coupled models at global or  
194 hemispheric scales involving Asia or its subregions were included. Then, we carefully examined all  
195 the included papers and further checked the listed reference in each paper to make sure that no  
196 related paper was neglected. A flowchart that illustrated the detailed procedures applied for article  
197 identification is presented in Appendix A (Note: Although the deadline for literature searching is  
198 2019, any literature published in 2020 is also included.). There was a total of 157 publications  
199 included in our study.

## 200 2.2 Analysis method

201 To summarize the current status of coupled models applied in Asia and quantitatively analyze  
202 the effects of aerosol feedbacks on model performance as well as meteorology and air quality, we  
203 carried out a series of analyses based on data extracted from the selected papers. We firstly compiled  
204 the publication information of the included papers as well as the information regarding model name,  
205 simulated time period, study region, simulation design, and aerosol effects. Secondly, we  
206 summarized the important findings of two-way coupled model applications in Asia according to  
207 different aerosol sources and components to clearly acquire what are the major research focuses in  
208 past studies. Finally, we gathered all the simulated results of meteorological and air quality variables  
209 with/without aerosol effects and their statistical indices (SI). For questionable results, the quality  
210 assurance was conducted after personal communications with original authors to decide whether  
211 they were deleted and/or corrected. All the extracted publication and statistical information were  
212 exported into an Excel file, which was provided in Supplement Table S1. Moreover, we performed  
213 quantitative analyses of the effects of aerosol feedbacks through following steps. (1) We discussed  
214 whether meteorological and air quality variables were overestimated or underestimated based on  
215 their SI. Then, variations of the SI of these variables were further analyzed in detail with/without turning  
216 on ARI or/and ACI in two-way coupled models. (2) We investigated the SI of simulation results at  
217 different simulation time lengths and spatial resolutions in coupled models. (3) More detailed inter-  
218 model comparisons of model performance based on the compiled SI among different coupled  
219 models are conducted. (4) Differences in simulation results with/without aerosol feedbacks were grouped  
220 by study regions and time scales (yearly, seasonal, monthly, daily and hourly). Toward a better  
221 understanding of the complicated interactions between air quality and meteorology in Asia, the  
222 results sections in this paper are organized following above analysis methods (1) - (3) and  
223 represented in Section 5, and the results following method (4) were represented in Section 6. In  
224 addition, Excel and Python were used to conduct data processing and plotting in this study.

## 225 3 Statistics of published literature

### 226 3.1 Summary of applications of coupled models in Asia

227 A total of 157 articles were selected according to the inclusion criteria, and their basic  
228 information was compiled in Table 1. In these studies, two commonly used two-way coupled models  
229 were WRF-Chem and WRF-CMAQ, and two locally developed models global-regional assimilation



230 and prediction system coupled with the Chinese Unified Atmospheric Chemistry Environment  
 231 forecasting system (GRAPES-CUACE) and WRF coupled with nested air-quality prediction  
 232 modeling system (WRF-NAQPMS). 127 out of total 157 papers involved the applications of WRF-  
 233 Chem in Asia since its two-way coupled version was publicly available in 2006 (Fast et al., 2006).  
 234 WRF-CMAQ was applied in only 16 studies due to its later initial release in 2012 (Wong et al.,  
 235 2012). GRAPES-CUACE was developed by the China Meteorological Administration and  
 236 introduced in details in Zhou et al. (2008, 2012, 2016), then firstly utilized in Wang et al. (2010) to  
 237 estimate impacts of aerosol feedbacks on meteorology and dust cycle in EA. The coupled version  
 238 of WRF-NAQPMS was developed by the Institute of Atmospheric Physics, Chinese Academy of  
 239 Sciences and could improve the prediction accuracy of haze pollution in the North China Plain (NCP)  
 240 (Wang Z.F. et al., 2014). Note that GRAPES-CUACE and WRF-NAQPMS were only applied in  
 241 China. In the included papers, 92, 31, 29 studies targeted various areas in China, EA and India,  
 242 respectively. There were 72 papers regarding effects of ARI, 60 both ARI and ACI, 18 ACI, and 7  
 243 health. ACI studies were much less than ARI related ones, which indicated that ACI related studies  
 244 need to be paid with more attention in the future. Considering that the choices of cloud microphysics  
 245 and radiation schemes can affect coupled models' results (Baró et al., 2015; Jimenez et al., 2016),  
 246 these schemes used in the selected studies were also summarized in Table 1. This table presents a  
 247 concise overview of coupled models' applications in Asia with the purpose of providing basic  
 248 information regarding models, study periods and areas, aerosol effects, scheme selections, and  
 249 reference.

250 It should be noted that in Table 1 there were four model inter-comparison studies that aimed at  
 251 evaluating model performance, identifying error sources and uncertainties, and providing optimal  
 252 model setups. By comparing simulations from two coupled models (WRF-Chem and Spectral  
 253 Radiation-Transport Model for Aerosol Species) (Takemura et al., 2003) in India (Govardhan et al.,  
 254 2016), it was found that the spatial distributions of various aerosol species (black carbon (BC),  
 255 mineral dust and sea salt) were similar with the two models. Based on the intercomparisons of WRF-  
 256 Chem simulations in different areas, Yang et al. (2017) revealed that aerosol feedbacks could  
 257 enhance PM<sub>2.5</sub> concentrations in the Indo-Gangetic Plain but suppress the concentrations in the  
 258 Tibetan Plateau (TP). Targeting China and India, Gao M. et al. (2018b) also applied the WRF-Chem  
 259 model to quantify the contributions of different emission sectors to aerosol radiative forcings,  
 260 suggesting that reducing the uncertainties in emission inventories were critical, especially for India.  
 261 Moreover, for the NCP region, Gao M. et al. (2018a) presented a comparison study with multiple  
 262 online models under the MICS-Asia Phase III and pointed out noticeable discrepancies in the  
 263 simulated secondary inorganic aerosols under heavy haze conditions and the importance of accurate  
 264 wind speed at 10 meters above surface (WS10) predictions by these models. Comprehensive  
 265 comparative studies for Asia have been emerging lately but are still limited, comparing to those for  
 266 North America and Europe, such as the Air Quality Model Evaluation International Initiative Phase  
 267 II (Brunner et al., 2015; Campbell et al., 2015; Forkel et al., 2016; Im et al., 2015a, 2015b; Kong et  
 268 al., 2015; Makar et al., 2015a, 2015b; Wang K. et al., 2015).

Table 1. Basic information of coupled model applications in Asia during 2010-2019.

No.	Model	Study period	Study region	Aerosol effect	Radiation scheme	Microphysics scheme	Reference
1	WRF-Chem	2013	India	ARI	Dudhia/RRTM	Thompson	Singh et al. (2020)*
2	WRF-Chem	12/2015	India	ARI	Goddard/RRTM	Lin	Bharali et al. (2019)
3	WRF-Chem	10/13/2016 to 11/20/2016	India	ARI	RRTMG	Unmentioned	Shahid et al. (2019)
4	WRF-Chem	12/27/2017 to 12/30/2017	NCP	ARI	RRTMG	Lin	Wang D. et al. (2019)
5	WRF-Chem	12/05/2015 to 01/04/2016	NCP	ARI	Goddard	WSM 6-class graupel scheme	Wu et al. (2019a)
6	WRF-Chem	12/05/2015 to 01/04/2016	NCP	ARI	Goddard	WSM 6-class graupel scheme	Wu et al. (2019b)
7	WRF-Chem	06/01/2006 to 12/31/2011	NWC	ARI	RRTMG	Morrison	Yuan et al. (2019)
8	WRF-Chem	07/2016, 10/2016, 01/2017, 04/2017	NCP	ARI	Goddard/RRTM	Lin	Zhang et al. (2019)
9	WRF-Chem	02/17/2014 to 02/26/2014, 10/21/2014 to 10/25/2014, 11/05/2014 to 11/11/2014,	NCP	ARI	RRTMG	Morrison	Zhou et al. (2019)
10	WRF-Chem	12/18/2015 to 12/24/2015	WA	ARI	RRTMG	Morrison	Bran et al. (2018)
11	WRF-Chem	03/15/2012 to 03/25/2012	China & India	ARI	RRTMG	Lin	Gao M. et al. (2018b)



12	WRF-Chem	05/01/2007 to 05/07/2007	CA	ARI	RRTM	Lin	Li and Sokolik (2018)
13	WRF-Chem	06/02/2012 to 06/15/2012	YRD	ARI	RRTMG	Lin	Li M. et al. (2018)
14	WRF-Chem	12/15/2016 to 12/21/2016	NCP	ARI	RRTMG	Morrison	Liu Q. et al. (2018)
15	WRF-Chem	11/30/2016 to 12/04/2016	NCP	ARI	RRTMG	Lin	Miao et al. (2018)
16	WRF-Chem	2010	India	ARI	RRTMG	Morrison	Soni et al. (2018)
17	WRF-Chem	01/01/2013 to 01/31/2013	NCP	ARI	Goddard/RRTM	Lin	Wang L. et al. (2018)
18	WRF-Chem	12/2013	EC	ARI	RRTMG	Lin	Wang Z. et al. (2018)
19	WRF-Chem	2013	TP	ARI	RRTMG	Morrison	Yang et al. (2018)
20	WRF-Chem	03/11/2015 to 03/26/2015	EA	ARI	RRTMG	Lin	Zhou et al. (2018)
21	WRF-Chem	01/2013	EC	ARI	RRTMG	Lin	Gao et al. (2017a)
22	WRF-Chem	03/16/2014 to 03/18/2014	YRD	ARI	RRTMG	Lin	Li M. M. et al. (2017a)
23	WRF-Chem	10/15/2015 to 10/17/2015	YRD	ARI	Goddard/RRTM	Lin	Li M. M. et al. (2017b)
24	WRF-Chem	02/21/2014 to 02/27/2014	NCP	ARI	RRTMG	Lin	Qiu et al. (2017)
25	WRF-Chem	07/21/2012	NCP	ARI	RRTMG	Lin	Yang and Liu (2017a)
26	WRF-Chem	07/21/2012	NCP	ARI	RRTMG	Lin	Yang and Liu (2017b)
27	WRF-Chem	05/30/2013 to 06/27/2013	EC	ARI	RRTMG	Lin	Yao et al. (2017)
28	WRF-Chem	11/15/2013 to 12/30/2013	SEC	ARI	RRTMG	Lin	Zhan et al. (2017)
29	WRF-Chem	03/2012	India	ARI	RRTMG	Thompson	Feng et al. (2016)
30	WRF-Chem	1960-2010	NCP	ARI	Goddard/RRTM	Lin	Gao M. et al. (2016a)
31	WRF-Chem	01/2008, 04/2008, 07/2008, 10/2008	EA	ARI	Goddard/RRTM	Lin	Liu X. et al. (2016)
32	WRF-Chem	04/2011	NC	ARI	RRTMG	Single-Moment 5-class	Liu L. et al. (2016)
33	WRF-Chem	09/21/2011 to 09/23/2011	NCP	ARI	RRTMG	Lin	Miao et al. (2016)
34	WRF-Chem	03/2005	EA	ARI	Goddard/RRTM	Morrison	Wang et al. (2016)
35	WRF-Chem	06/23/2008 to 07/20/2008	NWC	ARI	RRTMG	Morrison	Yang et al. (2016)
36	WRF-Chem	01/2007, 04/2007, 07/2007, 10/2007	EA	ARI	RRTM	Lin	Zhong et al. (2016)
37	WRF-Chem	05/2011, 10/2011	India	ARI	RRTMG	Thompson	Govardhan et al. (2015)
38	WRF-Chem	2006	China	ARI	RRTMG	Lin	Huang et al. (2015)
39	WRF-Chem	2007 to 2011	EA	ARI	Goddard/RRTM	Lin	Chen et al. (2014)
40	WRF-Chem	11/2007 to 12/2008	EA	ARI	RRTMG	Lin	Gao et al. (2014)
41	WRF-Chem	10/2006	SEA	ARI	RRTM	Lin	Ge et al. (2014)
42	WRF-Chem	04/17/2010 to 04/22/2010	India	ARI	RRTM	Thompson	Kumar et al. (2014)
43	WRF-Chem	01/11/2013 to 01/14/2013	NCP	ARI	Goddard/RRTM	Lin	Li and Liao (2014)
44	WRF-Chem	03/15/2008 to 03/18/2008	EA	ARI	RRTMG	Morrison	Lin C. et al. (2014)
45	WRF-Chem	07/21/2006 to 07/30/2006	NWC	ARI	RRTMG	Morrison	Chen et al. (2013)
46	WRF-Chem	05/12/2009 to 05/22/2009	India	ARI	Goddard/RRTM	Milbrandt-Yau	Dipu et al. (2013)
47	WRF-Chem	2008	India	ARI	Goddard/RRTM	Thompson	Kumar et al. (2012a)
48	WRF-Chem	2008	India	ARI	Goddard/RRTM	Thompson	Kumar et al. (2012b)
49	WRF-Chem	1999	India	ARI	Goddard/*	Lin	Seethala et al. (2011)
50	WRF-Chem	2006	China	ARI	*	*	Zhuang et al. (2011)
51	WRF-Chem	12/14/2013 to 12/16/2013	PRD	ARI & ACI	RRTMG	Morrison	Liu et al. (2020)*
52	WRF-Chem	11/30/2009 to 12/01/2009	NCP	ARI & ACI	Goddard/RRTM	Morrison	Jia et al. (2019)
53	WRF-Chem	11/25/2013 to 12/26/2013	EC	ARI & ACI	RRTMG	Lin	Wang Z. et al. (2019)
54	WRF-Chem	01/2014	China	ARI & ACI	RRTMG	Morrison	Archer-Nicholls et al. (2019)
55	WRF-Chem	12/01/2016 to 12/09/2016, 12/19/2016 to 12/24/2016	YRD	ARI & ACI	RRTMG	Lin	Li M. et al. (2019)
56	WRF-Chem	05/06/2013 to 20/06/2013, 24/08/2014 to 08/09/2014	India	ARI & ACI	RRTM	Lin	Kedia et al. (2019a)
57	WRF-Chem	06/2010 to 09/2010	India	ARI & ACI	RRTM	Lin, Morrison, Thompson	Kedia et al. (2019b)
58	WRF-Chem	04/2013	PRD	ARI & ACI	RRTMG	Lin	Huang et al. (2019)
59	WRF-Chem	11/30/2013 to 12/10/2013	EC	ARI & ACI	RRTMG	Morrison	Ding et al. (2019)
60	WRF-Chem	12/01/2015	NCP	ARI & ACI	RRTMG	Lin	Chen et al. (2019a)
61	WRF-Chem	04/12/2015 to 27/12/2015	EA	ARI & ACI	Goddard	WSM 6-class graupel scheme	An et al. (2019)
62	WRF-Chem	06/2015 to 02/2016	MRYR	ARI & ACI	Goddard/RRTM	WSM 6-class graupel scheme	Liu L. et al. (2018)
63	WRF-Chem	06/2008, 06/2009, 06/2010, 06/2011, 06/2012	PRD	ARI & ACI	RRTMG	Morrison	Liu Z. et al. (2018)
64	WRF-Chem	01/2014, 04/2014, 07/2014, 10/2014	China	ARI & ACI	RRTMG	Lin	Zhang et al. (2018)
65	WRF-Chem	10/01/2015 to 10/26/2015	YRD	ARI & ACI	RRTMG	Lin	Gao J. et al. (2018)
66	WRF-Chem	2001, 2006, 2011	EA	ARI & ACI	RRTMG	Morrison	Zhang et al. (2017)
67	WRF-Chem	06/01/2011 to 06/06/2011	EC	ARI & ACI	Goddard/RRTM	Lin	Wu et al. (2017)
68	WRF-Chem	11/27/2013 to 12/12/2013	YRD	ARI & ACI	Goddard/RRTM	Single-Moment 5-class	Sun et al. (2017)
69	WRF-Chem	2005 & 2009	YRD	ARI & ACI	RRTMG	Morrison	Zhong et al. (2017)
70	WRF-Chem	11/05/2014 to 11/11/2014	NCP	ARI & ACI	Goddard/RRTM	Lin	Gao et al. (2017b)
71	WRF-Chem	01/2013	NCP	ARI & ACI	Goddard/RRTM	Lin	Gao et al. (2017c)
72	WRF-Chem	01/2010, 07/2010	China	ARI & ACI	†	†	Ma and Wen (2017)
73	WRF-Chem	06/01/2008 to 07/05/2008	India	ARI & ACI	†	†	Lau et al. (2017)
74	WRF-Chem	01/2013	NCP	ARI & ACI	Goddard/RRTM	Morrison	Kajino et al. (2017)
75	WRF-Chem	03/01/2009 to 03/31/2009	TP & India	ARI & ACI	RRTMG	Morrison	Yang et al. (2017)
76	WRF-Chem	2001, 2006, 2011	EA	ARI & ACI	RRTMG	Morrison	He et al. (2017)
77	WRF-Chem	05/2008 to 08/2008	YRD	ARI & ACI	†	†	Campbell et al. (2017)



78	WRF-Chem	12/07/2013 to 12/09/2013	EC	ARI & ACI	Goddard/RRTM	Morrison	Zhang Yue et al. (2016)
79	WRF-Chem	01/2006, 04/2006, 07/2006, 10/2006	China	ARI & ACI	Goddard/RRTM	Lin	Ma et al. (2016)
80	WRF-Chem	01/2005, 04/2005, 07/2005, 10/2005	EA	ARI & ACI	Goddard/RRTM	Lin	Zhang Yang et al. (2016a)
81	WRF-Chem	01/2005, 04/2005, 07/2005, 10/2005	EA	ARI & ACI	Goddard/RRTM	Lin	Zhang Yang et al. (2016b)
82	WRF-Chem	06/2012	EC	ARI & ACI	RRTMG	Lin	Huang et al. (2016)
83	WRF-Chem	01/2010, 07/2010	YRD	ARI & ACI	Goddard/RRTM	Lin	Xie et al. (2016)
84	WRF-Chem	11/12/2012 to 11/16/2012, 11/02/2013 to 11/06/2013	India	ARI & ACI	Goddard/RRTM	Lin	Srinivas et al. (2016)
85	WRF-Chem	07/2010	India	ARI & ACI	RRTMG	Lin	Kedia et al. (2016)
86	WRF-Chem	05/20/2008 to 08/31/2015	India	ARI & ACI	Goddard/RRTM	Lin	Jin et al. (2016a)
87	WRF-Chem	05/20/2008 to 08/31/2015	India	ARI & ACI	Goddard/RRTM	Lin	Jin et al. (2016b)
88	WRF-Chem	01/2010	NCP	ARI & ACI	Goddard/RRTM	Lin	Gao M. et al. (2016b)
89	WRF-Chem	01/05/2008 to 01/09/2008	NCP	ARI & ACI	RRTMG	Lin	Gao Y. et al. (2016)
90	WRF-Chem	12/2013	EC	ARI & ACI	RRTMG	Lin	Ding et al. (2016)
91	WRF-Chem	02/15/2013 to 02/17/2013	NCP	ARI & ACI	Goddard/RRTM	†	Yang et al. (2015)
92	WRF-Chem	01/2010, 04/2010, 07/2010, 10/2010	NCP	ARI & ACI	Goddard/RRTM	Lin	Shen et al. (2015)
93	WRF-Chem	2006, 2011	EA	ARI & ACI	RRTMG	Morrison	Zhang Y. et al. (2015a)
94	WRF-Chem	2006, 2011	EA	ARI & ACI	RRTMG	Morrison	Chen Y. et al. (2015)
95	WRF-Chem	06/27/2008 to 06/28/2008	NCP	ARI & ACI	RRTM	Lin	Zhong et al. (2015)
96	WRF-Chem	05/20/2008 to 08/31/2015	India	ARI & ACI	Goddard/RRTM	Lin	Jin et al. (2015)
97	WRF-Chem	03/2005, 04/2005, 05/2005	India	ARI & ACI	Goddard/RRTM	Thompson	Jena et al. (2015)
98	WRF-Chem	01/02/2013 to 01/26/2013	NCP	ARI & ACI	RRTMG	Morrison	Gao Y. et al. (2015)
99	WRF-Chem	07/08/2013 to 07/09/2013	SWC	ARI & ACI	RRTMG	†	Fan et al. (2015)
100	WRF-Chem	01/2010, 04/2010, 07/2010, 10/2010	NCP	ARI & ACI	Goddard/RRTM	Lin	Chen D. et al. (2015)
101	WRF-Chem	01/2013	EC	ARI & ACI	Goddard/RRTM	Lin	Zhang B. et al. (2015)
102	WRF-Chem	2006, 2007	EA	ARI & ACI	Goddard/*	Lin	Wu et al. (2013)
103	WRF-Chem	09/27/2010 to 10/22/2010	India	ARI & ACI	Goddard/RRTM	Lin	Beig et al. (2013)
104	WRF-Chem	12/1/2009	NCP	ARI & ACI	Goddard/RRTM	Lin	Jia and Guo, (2012)
105	WRF-Chem	01/2001, 07/2001	EA	ARI & ACI	Goddard/RRTM	Lin	Zhang et al. (2012)
106	WRF-Chem	11/10/2007 to 01/01/2008	China	ARI & ACI	RRTMG	Lin	Gao et al. (2012)
107	WRF-Chem	06/18/2018 to 06/19/2018	MRYR	ACI	Goddard/RRTM	†	Bai et al. (2020)*
108	WRF-Chem	06/07/2017 to 06/12/2017	YRD	ACI	RRTMG	Morrison	Liu et al. (2019)
109	WRF-Chem	03/2010 to 05/2010	EA	ACI	RRTMG	Morrison	Wang K. et al. (2018)
110	WRF-Chem	03/09/2012 to 04/30/2012	EA	ACI	RRTMG	Thompson	Su and Fung (2018a)
111	WRF-Chem	03/09/2012 to 04/30/2012	EA	ACI	RRTMG	Thompson	Su and Fung (2018b)
112	WRF-Chem	05/18/2015 to 06/13/2015	NEA	ACI	RRTMG	Morrison	Park et al. (2018)
113	WRF-Chem	08/2008	EC	ACI	RRTMG	Lin	Gao and Zhang (2018)
114	WRF-Chem	10/03/2013 to 10/07/2013	SEC	ACI	RRTMG	Morrison	Shen et al. (2017)
115	WRF-Chem	01/2013, 07/2013	China	ACI	Fu-Liou-Gu	Morrison	Zhao et al. (2017)
116	WRF-Chem	06/04/2004 to 07/10/2004	India	ACI	Goddard	Lin	Bhattacharya et al. (2017)
117	WRF-Chem	09/20/2013 to 09/23/2013	PRD	ACI	RRTMG	Lin	Jiang et al. (2016)
118	WRF-Chem	2005, 2010	EA	ACI	RRTMG	Morrison	Y. Zhang et al. (2015b)
119	WRF-Chem	08/20/2009 to 08/29/2008	India	ACI	Goddard/RRTM	Morrison	Sarangi et al. (2015)
120	WRF-Chem	01/2001, 04/2001, 07/2001, 10/2001, 01/2005, 04/2005, 07/2005, 10/2005, 01/2008, 04/2008, 07/2008, 10/2008	EA	ACI	†	†	Zhang et al. (2014)
121	WRF-Chem	07/2008	EC	ACI	RRTMG	Morrison	Lin et al. (2014)
122	WRF-Chem	1980 to 2010	SEC	ACI	†	†	Bennartz et al. (2011)
123	WRF-Chem	2008, 2050	China	Health	†	†	Zhong et al. (2019)
124	WRF-Chem	2015, 2050	India	Health	RRTM	Thompson	Conibear et al. (2018a)
125	WRF-Chem	2014	India	Health	RRTM	Thompson	Conibear et al. (2018b)
126	WRF-Chem	2011	India	Health	Goddard/RRTM	Thompson	Glude et al. (2016)
127	WRF-Chem	2013	NCP	Health	RRTMG	†	Gao M. et al. (2015)
128	WRF-CMAQ	03/2006, 04/2006 to 03/2010, 04/2010	EA	ARI	†	†	Dong et al. (2019)
129	WRF-CMAQ	04/10/2016 to 06/19/2016	NEA	ARI	RRTMG	Single-Moment 3-class	Jung et al. (2019)
130	WRF-CMAQ	2014	EA	ARI	RRTMG	Morrison	Nguyen et al. (2019a)
131	WRF-CMAQ	2014	SEA	ARI	RRTMG	Morrison	Nguyen et al. (2019b)
132	WRF-CMAQ	02/2015	NEA	ARI	RRTMG	Single-Moment 5-class	Yoo et al. (2019)
133	WRF-CMAQ	01/2014, 02/2014, 03/2014	EA	ARI	RRTMG	Morrison	Sekiguchi et al. (2018)
134	WRF-CMAQ	2006 to 2010, 2013	EA	ARI	RRTMG	Morrison	Hong et al. (2017)
135	WRF-CMAQ	01/2013, 07/2013	China	ARI	RRTMG	Morrison	Xing et al. (2017)
136	WRF-CMAQ	1990 to 2010	EC	ARI	RRTMG	Morrison	Xing et al. (2016)
137	WRF-CMAQ	1990 to 2010	EC	ARI	RRTMG	Morrison	Xing et al. (2015a)
138	WRF-CMAQ	1990 to 2010	EC	ARI	RRTMG	Morrison	Xing et al. (2015b)
139	WRF-CMAQ	1990 to 2010	EC	ARI	RRTMG	Morrison	Xing et al. (2015c)
140	WRF-CMAQ	01/2013	China	ARI	RRTMG	Morrison	J. Wang et al. (2014)
141	WRF-CMAQ	01/2013, 04/2013, 07/2013, 10/2013	China	ACI	RRTMG	Morrison	Chang (2018)
142	WRF-CMAQ	2050	China	Health	RRTMG	Morrison	Hong et al. (2019)
143	WRF-CMAQ	1990 to 2010	EC	Health	RRTMG	Morrison	Wang et al. (2017)



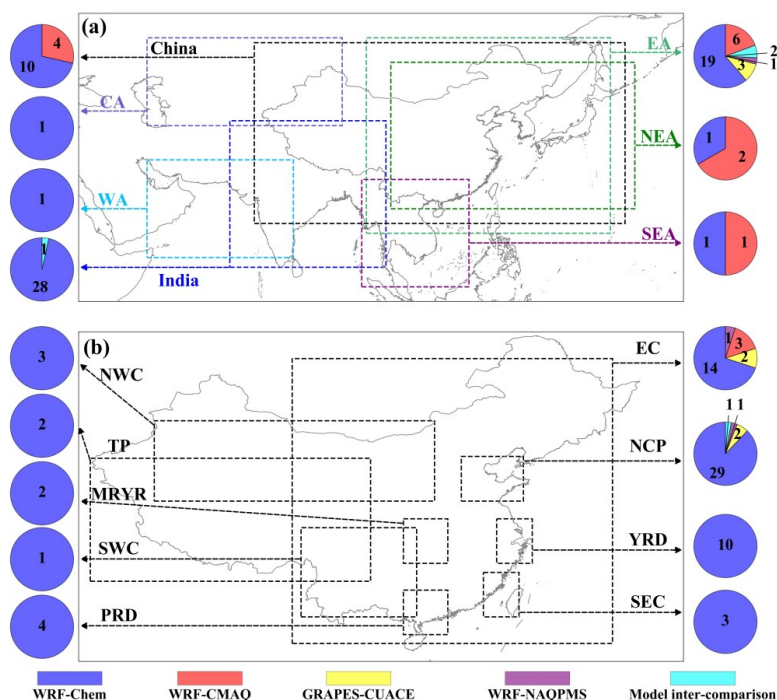
144	GRAPES-CUACE	12/15/2016 to 12/24/2016	NCP	ARI	Goddard	†	H. Wang et al. (2018)
145	GRAPES-CUACE	07/07/2008 to 07/11/2008	NCP	ARI	CLIRAD	†	H. Wang et al. (2015)
146	GRAPES-CUACE	04/26/2006	EA	ARI	Goddard/*	†	Wang and Niu (2013)
147	GRAPES-CUACE	04/26/2006	EA	ARI	Goddard/*	†	Wang et al. (2013)
148	GRAPES-CUACE	07/13/2008 to 07/31/2008	NC	ARI	†	†	Zhou et al. (2012)
149	GRAPES-CUACE	04/26/2006	EA	ARI	Goddard/*	†	Wang et al. (2010)
150	GRAPES-CUACE	01/2013	EC	ACI	†	Single-Moment 6-class	Zhou et al. (2016)
151	WRF-NAQPMS	2013	EA	ARI	†	†	Li J. et al. (2018)
152	WRF-NAQPMS	09/27/2013 to 10/01/2013	NCP	ARI	Goddard/RRTM	Lin	Wang Z. et al. (2014)
153	WRF-NAQPMS	01/01/2013	EC	ARI	Goddard/RRTM	Lin	Wang Z. F. et al. (2014)
154	Multi-model comparison	2010	EA	ARI & ACI	†	†	Chen et al. (2019b)
155	Multi-model comparison	2010	EA	ARI & ACI	†	†	Li J. et al., (2019)
156	Multi-model comparison	01/2010	NCP	ARI & ACI	†	†	Gao et al. (2018a)
157	Multi-model comparison	05/2011	India	ARI & ACI	†	†	Govardhan et al. (2016)

†: Not mentioned; \*: A preprint version of this study was available online on October 31, 2019, and was formally published on January 1, 2020. (EA: East Asia, NEA: Northeast Asia, SEA: Southeast Asia, EC: East China, NCP: North China Plain, YRD: Yangtze River Delta, SEC: Southeast China, NWC: Northwest China, TP: Tibetan Plateau, MRYR: middle reaches of the Yangtze River, SWC: Southwest China; PRD: Pearl River Delta).

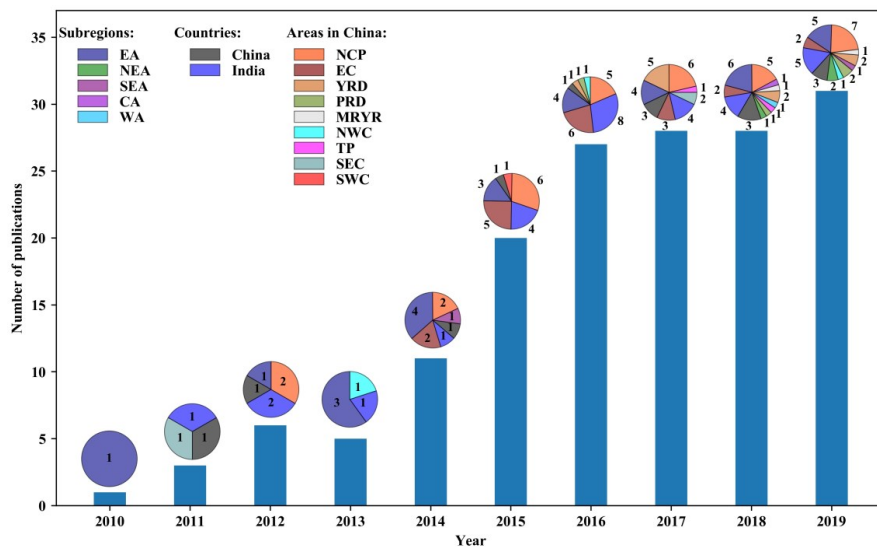
### 3.2 Spatiotemporal distribution of publications

To gain an overall understanding of applications of coupled models in Asia, the spatial distributions of study areas of the selected literatures and the temporal variations of the annual publication numbers were extracted from Table 1 and summarized. Figure 1 illustrates the spatial distributions of study regions as well as the number of papers involving coupled models in Asia (Fig. 1a) and China (Fig. 1b). In this figure, the color and number in the pie charts represent individual (WRF-Chem, WRF-CMAQ, GRAPES-CUACE and WRF-NAQPMS) or multiple coupled models and the quantity of corresponding articles, respectively. At subregional scales, most studies targeted EA where high anthropogenic aerosol loading occurred in recent decades, mainly using WRF-Chem and WRF-CMAQ (Fig. 1a). For other subregions, such as Northeast Asia (NEA), SEA, Central Asia (CA), and West Asia (WA), there were rather limited research activities taking into account aerosol feedbacks with two-way coupled models. National scale applications of two-way coupled models targeted mostly modeling domains covering India and China but much less work were carried out in other countries, such as Japan and Korea, where air pollution levels are much lower. With respect to various areas in China (Fig. 1b), the research activities concentrated mostly in NCP and secondly in the East China (EC), then in the Yangtze River Delta (YRD) and Pearl River Delta (PRD) areas. WRF-Chem was the most popular model applied in all areas, but there were a few applications of GPRAPES-CUACE and WRF-NAQPMS in EC and NCP.

Figure 2 depicts the temporal variations of research activities with two-way coupled models in Asia over the period of 2010 to 2019. The total number of papers related to two-way coupled models had an obvious upward trend in the past decade. Prior to 2014, applications of two-way coupled models in Asia were scarce, with about 1 to 6 publications per year. A noticeable increase of research activities emerged starting from 2014 and the growth was rapid from 2014 to 2016, at a rate of 7-9 more papers per year, especially in China. It could be related to the Action Plan on Prevention and Control of Atmospheric Pollution (2013-2017) implemented by the Chinese government. The growth was rather flat during 2016-2018 before reaching a peak of 31 articles in 2019. In addition, the pie charts in Fig. 2 indicates that modeling activities had been picking up with a diversified pattern in study domain from 2010 to 2019. The modeling domains extended from EA to China and India and then several subregions in Asia and various areas in China. For EA and India, investigations of aerosol feedbacks based on two-way coupled models rose from 1-2 papers per year during 2010-2013 to 4-8 during 2014-2019. Since 2014, most model simulations were carried out towards areas with severe air pollution in China, especially the NCP area where attracted 5-7 publications per year.



310  
 311  
 312 Figure 1. The spatial distributions of study domains as well as the two-way coupled modeling publication numbers  
 313 in different subregions or countries of Asia (a) and areas of China (b). (EA: East Asia, NEA: Northeast Asia, SEA:  
 314 Southeast Asia, EC: East China, NCP: North China Plain, YRD: Yangtze River Delta, SEC: Southeast China, NWC:  
 315 Northwest China, TP: Tibetan Plateau, MRYS: middle reaches of the Yangtze River, SWC: Southwest China, PRD:  
 316 Pearl River Delta).



317  
 318 Figure 2. The temporal variations of study activities adopting two-way coupled models in Asia during 2010-2019.  
 319 (EA: East Asia, NEA: Northeast Asia, SEA: Southeast Asia, EC: East China, NCP: North China Plain, YRD: Yangtze  
 320 River Delta, SEC: Southeast China, NWC: Northwest China, TP: Tibetan Plateau, MRYS: middle reaches of the  
 321 Yangtze River, SWC: Southwest China; PRD: Pearl River Delta).



## 322 4 Overview of research focuses in Asia

### 323 4.1 Feedbacks of natural aerosols

#### 324 4.1.1 Mineral dust aerosols

325 Due to the fact that dust storm events frequently occurred over Asia during 2000-2010, the  
326 research community has focused on dust transportation and associated climatic effects (Choobari et  
327 al., 2014; Gong et al., 2003; Lee et al., 2010; Yasunari and Yamazaki, 2009; Zhang et al., 2003a,  
328 2003b). Also the detailed processes and physiochemical mechanisms of dust storms had been well  
329 understood and reviewed in detail (Chen et al., 2017a; Huang et al., 2014; Shao and Dong, 2006;  
330 Uno et al., 2006). To probe into the radiative feedbacks of dust aerosols in Asia, Wang et al. (2013,  
331 2010) initiated modeling studies by a two-way coupled model, i.e., the GRAPES-CUAUE model,  
332 to simulate direct radiative forcing (DRF) of dust, and revealed that the feedback effects of dust  
333 aerosols could lead to decreasing of surface wind speeds and then suppress dust emissions. Further  
334 modeling simulations by the same model (Wang and Niu, 2013) indicated that considering dust  
335 radiative effects did not substantially improve the model performance of the air temperature at 2  
336 meters above the surface (T2), even with assimilating data from in-situ and satellite observations  
337 into the model. Subsequently, several similar studies based on another two-way coupled model  
338 (WRF-Chem with The Georgia Tech/Goddard Global Ozone Chemistry Aerosol Radiation and  
339 Transport scheme) were conducted to investigate dust radiative forcing (including shortwave  
340 radiative forcing (SWRF) and longwave radiative forcing (LWRF)) and ARI effects of dust on  
341 meteorological variables (PBLH, T2 and WS10) in different regions of Asia (Bran et al., 2018; Chen  
342 et al., 2014; Jin et al., 2016a, 2015; Kumar et al., 2014; Liu L. et al., 2016; Su and Fung, 2018a,  
343 2018b; Zhou et al., 2018). These studies demonstrated that dust aerosols could induced negative  
344 radiative forcing (cooling effect) at top of atmosphere (TOA) as well as the surface (including both  
345 Earth's and sea surfaces) and positive radiative forcing (warming effect) in the ATM (Bran et al.,  
346 2018; Chen et al., 2014; Kumar et al., 2014; Li and Sokolik, 2018; Li M.M. et al., 2017a; Su and  
347 Fung, 2018a; Wang et al., 2013). More thorough analyses of the radiative effects of dust in Asia (Li  
348 and Sokolik, 2018; Wang et al., 2013) pointed out that dust aerosols played opposite roles in the  
349 shortwave and longwave bands, so that the dust SWRF at TOA and the surface (cooling effects) as  
350 well as in the ATM (warming effects) was offset partially by the dust LWRF (warming effects at  
351 TOA and the surface but cooling effects in the ATM). It was noteworthy that adding more detailed  
352 mineralogical composition into the dust emission for WRF-Chem could alter the dust SWRF at TOA  
353 from cooling to warming and then lead to a positive net radiative forcing at TOA (Li and Sokolik,  
354 2018). These different conclusions showed some degrees of uncertainties in the coupled model  
355 simulations of dust aerosols' radiative forcing that need to be further investigated in the future.

356 Dust aerosols can act not only as water-insoluble cloud condensation nuclei (CCN) (Kumar et  
357 al., 2009) but also as ice nuclei (IN) (Lohmann and Diehl, 2006) since they are referred to as ice  
358 friendly (Thompson and Eidhammer, 2014). Therefore, activation and heterogeneous ice nucleation  
359 parameterizations (INPs) with respect to dust aerosols were developed and incorporated into WRF-  
360 Chem to explore ACI effects as well as both ARI and ACI effects of dust aerosols in Asia (Jin et al.,  
361 2016a, 2015; Su and Fung, 2018a, 2018b; Wang K. et al., 2018; Zhang Y. et al., 2015b). During dust  
362 storms, including the adsorption activation of dust particles played vital roles in the simulations of  
363 ACI-related cloud properties and a 45 % of increase of cloud droplet number concentration (CDNC),  
364 comparing to a simpler aerosols activation scheme in WRF-Chem (Wang K. et al., 2018). More  
365 sophisticated INPs implemented in WRF-Chem that taking dust particles into account as IN resulted  
366 in substantial modifications of cloud and ice properties as well as surface meteorological variables  
367 and air pollutant concentrations in model simulations (Su and Fung, 2018b; Zhang Y. et al., 2015b).  
368 Zhang Y. et al. (2015b) delineated that dust aerosols acting either as CCN or IN made model results  
369 rather different regarding radiation, T2, precipitation, and number concentrations of cloud water and  
370 ice. Su and Fu (2018b) described that the ACI effects of dust had less impacts on the radiative forcing  
371 than its ARI effects and dust particles could promote (demote) ice (liquid) clouds in mid-upper (low-  
372 mid) troposphere over EA. With turning on both ARI and ACI effects of dust, less low-level clouds  
373 and more mid- and high-level clouds were detected that contributed to cooling at the Earth's surface  
374 and in the lower atmosphere and warming in the mid-upper troposphere (Su and Fung, 2018b).  
375 Mineral dust particles transported by the westerly and southwesterly winds from the Middle East  
376 (ME) affected the radiative forcing at TOA and the Earth's surface and in the ATM by the dust-  
377 induced ARI and ACI in the Arabian Sea and the India subcontinent, and subsequently changed the  
378 circulation patterns, cloud properties, and characteristics related to the India summer monsoon (ISM);



379 Jin et al., 2015, 2016b). Moreover, the effects of dust on precipitation are not only complex but also  
380 highly uncertain, evidencing from several modeling investigations targeting a variety of areas in  
381 Asia (Jin et al., 2016a, 2016b, 2015; Su and Fung, 2018b; Zhang Y. et al., 2015b). Less precipitation  
382 from model simulations including dust effects was found at EA and dust particles acting mainly as  
383 CCN or IN influenced precipitation in a rather different way (Zhang Y. et al., 2015b). A positive  
384 response of ISM rainfall to dust particles from the ME was reported by Jin et al. (2015) and less  
385 affected by dust storms from the local sources and NWC (Jin et al., 2016a). Jin et al. (2016b) further  
386 elucidated that the impacts of ME dust on ISM rainfall were highly sensitive to the imaginary  
387 refractive index of dust setting in the model, so that accurate simulations of the dust-rainfall  
388 interaction depended on more precise representation of radiative absorptions of dust in two-way  
389 coupled models. About 20 % of increase or decrease in rainfall due to the dust effects were detected  
390 in different areas over EA from the WRF-Chem simulations (Su and Fung, 2018b). However, it  
391 should be mentioned that a few studies that targeting DRF of dust in Asia based on WRF-Chem  
392 simulations but without enabling aerosol-radiation feedbacks (Ashrafi et al., 2017; Chen S. et al.,  
393 2017b; Tang et al., 2018) were not included in this paper.

394 Along with the modeling research on the effects of dust aerosols on meteorology, their impacts  
395 on air quality in Asia were explored using two-way coupled models (Chen et al., 2014; Kumar et  
396 al., 2014; Li and Sokolik, 2018; Li M. M. et al., 2017a; Wang et al., 2013). Many early modeling  
397 research work involving two-way coupled models with dust only looked into the ARI or direct  
398 radiative effects of dust particles, which are described as follows. Taking a spring-time dust storm  
399 from the Thar Desert into consideration in WRF-Chem, the modeled aerosol optical depth (AOD)  
400 and Angstrom exponent (as indicators of aerosol optical properties and unique proxies of the surface  
401 particulate matter pollution) demonstrated that turning on the ARI effects of dust could reduce biases  
402 in their simulations, but were underestimated in North India (Kumar et al., 2014). Wang et al. (2013)  
403 pointed out that in EA, including the longwave radiative effects of dust in the  
404 GRAPES\_CUACE/dust model lowered relative errors of the modeled AOD by 15 %, as compared  
405 to simulations that only considering shortwave effects of dust. Comparisons against both satellite  
406 and in situ observations depicted that the WRF-Chem model was able to capture the general  
407 spatiotemporal variations of the optical properties and size distribution of dust particles over the  
408 main dust sources in EA, such as the Taklimakan Desert and Gobi Desert, but overestimated AOD  
409 during summer and fall and also exhibited positive (negative) biases in the fine (coarse) mode of  
410 dust particles (Chen et al., 2014). Besides the ARI effects of dust, the heterogeneous chemistry on  
411 dust particles' surface added in WRF-Chem was accounted for 80 % of the net reductions of O<sub>3</sub>,  
412 NO<sub>2</sub>, NO<sub>3</sub>, N<sub>2</sub>O<sub>5</sub>, HNO<sub>3</sub>, ·OH, HO<sub>2</sub>· and H<sub>2</sub>O<sub>2</sub> when a springtime dust storm striking the Nanjing  
413 megacity of EC (Li M. M. et al., 2017a). In CA, AOD was overestimated by WRF-Chem model but  
414 its simulation was improved when more detailed mineral components of dust particles were  
415 incorporated in the model (Li and Sokolik, 2018). Later on, more investigations started to focus on  
416 both ARI and ACI effects of dust aerosols. With consideration of ARI as well as both ARI and ACI  
417 of dust particles from the ME, during the ISM period, the WRF-Chem model reproduced AOD's  
418 spatial distributions but underpredicted (overpredicted) AOD over the Arabian Sea (the Arabian  
419 Peninsula) comparing with satellite observations and AOD reanalysis data (Jin et al., 2016a, 2016b,  
420 2015). In EA, Wang K. et al. (2018) demonstrated that including both ARI and ACI effects of dust  
421 in WRF-Chem caused lower O<sub>3</sub> concentrations and by incorporating INPs, the WRF-Chem model  
422 well simulated the surface PM<sub>10</sub> concentrations (Su and Fung, 2018a) with reduced (elevated)  
423 surface concentrations of OH, O<sub>3</sub>, SO<sub>4</sub><sup>2-</sup>, and PM<sub>2.5</sub> (CO, NO<sub>2</sub>, and SO<sub>2</sub>) (Zhang Y. et al., 2015b). It  
424 is worth noting that how to partition dust particles into fine mode and coarse mode or initialize their  
425 size distribution in coupled models can affect simulations in many ways and requires more detailed  
426 measurements at the source areas and further modeling studies.

#### 427 **4.1.2 Wildfire, sea salt and volcanic ash**

428 In the Maritime SEA region, peat and forest fire triggered by El Niño induced drought  
429 conditions released huge amount of smoke particles, which promoted dire air pollution problems in  
430 the downstream areas, and their ARI (including direct and semi-direct) effects simulated by WRF-  
431 Chem enhanced (reduced) radiative forcing at the TOA and the atmospheric stability (radiation  
432 reaching the ground and sensible and latent heat fluxes, turbulence, PBLH, T<sub>2</sub>) (Ge et al., 2014).  
433 Ge et al. (2014) also pointed out the ARI effects of these fires impaired (intensified) sea breeze at  
434 daytime (land breeze at nighttime) over this region so that their impacts on cloud cover could be  
435 positive or negative in different areas and time period (day or night). Sea salt and volcanic ash are



436 also important natural aerosols for regions near seashores and active volcanoes and surrounding  
437 areas but modeling studies of their ARI and ACI effects are relatively scarce in Asia. Based on WRF-  
438 Chem simulations, Kedia et al. (2019a) demonstrated that the feedbacks of sea salt aerosols  
439 impacted convective and nonconvective precipitation rather variously in different areas of the India  
440 subcontinent. Jiang et al. (2019a, 2019b) also used WRF-Chem with/without sea-salt emissions to  
441 evaluate the effects of sea salt on rainfall in Guangdong Province of China, but unfortunately, no  
442 feedbacks were considered in the simulations. So far there is no investigation targeting aerosol  
443 effects of volcanic ash from volcano eruptions in Asia using coupled models.

#### 444 4.2 Feedbacks of anthropogenic aerosols

445 Atmospheric pollutants from anthropogenic sources are the leading causes of heavy pollution  
446 events occurring in Asia due to the acceleration of urbanization, industrialization, and population  
447 growth in recent decades, particularly in China and India, and their ARI or/and ACI effects on  
448 meteorology and air quality had been quantitatively examined using two-way coupled models  
449 (Archer-Nicholls et al., 2019; Bharali et al., 2019; Gao M. et al., 2016b; Kumar et al., 2012a, 2012b;  
450 Li and Liao, 2014; Wang J. et al., 2014; Wang Z. et al., 2018; Zhang B. et al., 2015; Yao et al., 2017;  
451 Zhong et al., 2016). These modeling research work had been primarily focused on the ARI or/and  
452 ACI effects of anthropogenic aerosols, their specific chemical components (especially the light-  
453 absorbing aerosols, i.e., BC and brown carbon (BrC)) and aerosols originated from different sources.  
454 The major findings in these research are outlined as follows, with respect to the effects of  
455 anthropogenic aerosol feedbacks on meteorology and air quality.

456 Concerning the meteorological responses, most papers treated anthropogenic aerosols as a  
457 whole to explore their effects on meteorological variables based on coupled model simulations with  
458 enabling ARI or/and ACI in WRF-Chem, WRF-CMAQ, WRF-CMAQ, GRAPES-CUACE and  
459 WRF-NAQPMS (Bai et al., 2020; Gao M. et al., 2016b; Kumar et al., 2012a; Nguyen et al., 2019a,  
460 2019b; Wang H. et al., 2015; J. Wang et al., 2014; Wang Z. F. et al., 2014; Zhang B. et al., 2015;  
461 Zhang et al., 2018; Zhao et al., 2017). Generally, the main ARI effects of anthropogenic aerosols  
462 resulted in decreases of SWRF, T2 and WS10, and PBLH, as well as increases of surface relative  
463 humidity (RH2) and temperature in the ATM, which further suppressed PBL development (Gao Y.  
464 et al., 2015; Li M. M. et al., 2017b; Nguyen et al., 2019a, 2019b; Xing et al., 2015c; Zhang et al.,  
465 2018). Wang H. et al. (2015) utilized GRAPES/CUACE with ARI to study a summer haze case in  
466 the NCP area and discovered that the ARI effects made the subtropical high less intense (-14 hPa)  
467 to help pollutants in the area to dissipate. In Asia, ACI effects of anthropogenic aerosols on cloud  
468 properties and precipitation are relatively complex. On the one hand, anthropogenic aerosols, that  
469 being activated as CCN, enhanced CDNC and LWP and then slowed down the precipitation onset,  
470 but their impacts on precipitation amounts varied in different seasons and areas in China (Zhao et  
471 al., 2017). Targeting a summertime rainstorm in the middle reaches of the Yangtze River (MRYSR)  
472 in China, sensitivity studies using WRF-Chem unveiled that CDNC, cloud water contents, and  
473 precipitation decreased (increased) with low (high) anthropogenic emission scenarios due to the  
474 ACI effects and these variations tended to depend on atmospheric humidity (Bai et al., 2020). The  
475 modeling investigations with WRF-Chem aiming at the ISM (Kedia et al., 2019) and a disastrous  
476 flood event in Southwest China (SWC) (Fan et al., 2015) pointed out that the simulated convective  
477 process was suppressed and convective (nonconvective) precipitation was inhibited (enhanced) by  
478 the ARI and ACI effects of accumulated anthropogenic aerosols, but these effects could invigorate  
479 convection and rainfall in the downwind mountainous area at nighttime (Fan et al., 2015). On the  
480 other hand, how anthropogenic aerosols act in the ice nucleation processes is still open to question  
481 (Zhao et al., 2019) and these process need to be represented accurately in two-way coupled models,  
482 however until now no study had been performed to simulate the ACI effects of anthropogenic  
483 aerosol serving as IN in Asia using two-way coupled models. Therefore, in Asia, further  
484 investigations are needed that targeting cloud or/and ice processes involving anthropogenic aerosols  
485 (including their size, composition, and mixing state) in two-way coupled models. Meanwhile,  
486 several studies not only discussed aerosol feedbacks but also focused on the additional effects of  
487 topography or urban heat island on meteorology (Wang D. et al., 2019; Zhong et al., 2017, 2015).

488 Hitherto there were several attempts to ascertain the effects of different chemical components  
489 of anthropogenic aerosols on meteorology in Asia (Archer-Nicholls et al., 2019; Ding et al., 2019;  
490 Ding et al., 2016; Gao J. et al., 2018; Huang et al., 2015; Wang Z. et al., 2018). First of all, Asia is  
491 the region in the world with the highest BC emissions due to burning of large amount of fossil fuels  
492 and biomass and this has increasingly attracted many researchers to probe into the ARI or/and ACI



493 effects of BC (Boucher et al., 2013). As the most important absorbing aerosol, BC induced the  
494 largest positive, positive and negative mean DRF at the TOA (followed by sulfate and other types  
495 of aerosols with negative DRF), in the ATM (followed by mineral dust), and at the surface,  
496 respectively, over China during 2006 (Huang et al., 2015). Ding et al. (2016) and Wang Z. et al.  
497 (2018) further applied WRF-Chem with feedbacks to investigate how aerosol-PBL interactions  
498 involving BC prohibited the PBL development, which deteriorated air quality in Chinese cities and  
499 was described as “dome effect” (namely BC warms the atmosphere and cools the surface, suppresses  
500 the PBL development and eventually results in more accumulation of pollutants). This “dome effect”  
501 of BC promoted the advection-radiation fog and fog-haze formation in the YRD area through  
502 altering the land-sea circulation pattern and increasing the moisture level (Ding et al., 2019). Gao J.  
503 et al. (2018) also pointed out BC in the ATM modified the vertical profiles of heating rate and  
504 equivalent potential temperature in Nanjing, China. In India, the ARI effects of BC enhanced  
505 convective activities, meridional flows, and rainfall in North-East India during the pre-monsoon  
506 season but could either enhance or suppress precipitation during the monsoon season in different  
507 parts of the India subcontinent (Soni et al., 2018). Moreover, the ARI effects of BC on surface  
508 meteorological variables were larger than its ACI effects in EC (Archer-Nicholls et al., 2019; Ding  
509 et al., 2019). Besides BC, the BrC portion of organic aerosols (OA) emitted from agriculture residue  
510 burning (ARB) were included in WRF-Chem with the parameterization scheme suggested by Saleh  
511 et al. (2014) and the model simulations in EC revealed that at the TOA, the net DRF of OA was -  
512  $0.22 \text{ W}\cdot\text{m}^{-2}$  (absorption and scattering DRF were  $+0.21 \text{ W}\cdot\text{m}^{-2}$  and  $-0.43 \text{ W}\cdot\text{m}^{-2}$  respectively), but  
513 the BC’s DRF was still the highest ( $+0.79 \text{ W}\cdot\text{m}^{-2}$ ) (Yao et al., 2017). As mentioned above, it is  
514 obvious that ARI and ACI effects of different aerosol components are substantially distinctive, and  
515 many other aerosol compositions (e.g., sulfate, nitrate and ammonium) besides BC and BrC should  
516 be taken into considerations in future modeling studies in Asia.

517 ARB is a common practice in many Asian countries after harvesting and before planting and  
518 can deteriorate air quality quickly as one of the most important sources of anthropogenic aerosols,  
519 so that it has been attracting much attention among the public and scientists worldwide (Chen J. et  
520 al., 2017; Hodshire et al., 2019; Koch and Del Genio, 2010; Reid et al., 2005; Yan et al., 2018).  
521 Recently, the effects of ARB aerosols on meteorology had widely been explored using the two-way  
522 coupled model (WRF-Chem) in many Asian countries and regions, such as EC (Huang et al., 2016;  
523 Li M. et al., 2018; Wu et al., 2017; Yao et al., 2017), South China (SC) (Huang et al., 2019), and  
524 South Asia (SA) (Singh et al., 2020). In general, when ARB occurred, the WRF-Chem simulations  
525 from all the studies showed that the changes in radiative forcing induced by ARB aerosols were  
526 greater than by those from other anthropogenic sources, especially in the ATM. Also all the modeling  
527 studies indicated that ARB aerosols reduced (increased) radiative forcing at the surface (in the ATM),  
528 cooled (warmed) the surface (the atmosphere), and increased (decreased) atmospheric stability  
529 (PBLH). Furthermore, the WRF-Chem simulations with ARI demonstrated that light-absorbing  
530 carbonaceous aerosols (CAs) from ARB caused daytime (nighttime) precipitation decreased  
531 (increased) over Nanjing in EC during a post-harvest ARB event (Huang et al., 2016). Yao et al.  
532 (2017) pointed out their WRF-Chem simulations in EC exhibited larger DRE induced by BC from  
533 ARB at the TOA than previous studies. Lately, several modeling studies using WRF-Chem had  
534 targeted the effects of ARI and both ARI and ACI due to ARB aerosols from countries in the  
535 Indochina, SEA, and SA regions during the planting and harvesting time (Dong et al., 2019; Huang  
536 et al., 2019; Singh et al., 2020; Zhou et al., 2018). Zhou et al. (2018) investigated how ARB aerosols  
537 from SEA mixed with mineral dust and other anthropogenic aerosols while being lifted to the mid-  
538 low troposphere over the source region and transported to the YRD area and then affected  
539 meteorology and air quality there. The influences of ARI and ACI caused by ARB aerosols from  
540 Indochina were contrary, namely, the ARI (ACI) effects made the atmosphere over SC warmer  
541 (cooler) and drier (wetter), and the ARI effects hindered cloud formation and suppressed  
542 precipitation there (Huang et al., 2019). Dong et al. (2019) found the warming ARI effects of ARB  
543 aerosols were smaller over the source region (i.e., SEA) than the downwind region (i.e., SC) with  
544 cloudier conditions. Annual simulations regarding the ARI effects of ARB aerosols from SA  
545 (especially Myanmar and Punjab) indicated that CAs released by ARB reduced the radiative forcing  
546 at the TOA but did not change the precipitation processes much when only the ARI effects were  
547 considered in WRF-Chem (Singh et al., 2020).

548 Besides ARB, to our best knowledge, there were only a few research work quantitatively  
549 assessing the effects of anthropogenic aerosols from different emission sources on meteorology



550 using WRF-Chem. Gao M. et al. (2018b) evaluated the responses of radiative forcing in China and  
551 India to aerosols from five emission sectors (power, industry, residential, BB, and transportation),  
552 and found that the power (residential) sector was the dominate contributor to the negative (positive)  
553 DRF at the TOA over both countries due to high emissions of sulfate and nitrate precursors (BC)  
554 and the total sectoral contributions were in the order of power > residential > industry > BB >  
555 transportation (power > residential > transportation > industry > BB) for China (India) during 2013.  
556 To pinpoint the ARI and ACI effects, Archer-Nicholls et al. (2019) reported that during January  
557 2014, the aerosols from the residential emission sector induced larger SWRF (+1.04 W·m<sup>-2</sup>) than  
558 LWRF (+0.18 W·m<sup>-2</sup>) at the TOA and their DRF (+0.79 W·m<sup>-2</sup>) was the largest, followed by their  
559 semidirect effects (+0.54 W·m<sup>-2</sup>) and indirect effects (-0.29 W·m<sup>-2</sup>) over EC. This study further  
560 emphasized a realistic ratio of BC to total carbon from the residential emission was critical for  
561 accurate simulations of the ARI and ACI effects with two-way coupled models.

562 In terms of anthropogenic aerosol effects on air quality, the responses of PM<sub>2.5</sub> had been widely  
563 investigated (Chen et al., 2019a; Gao J. et al., 2018; Gao M. et al., 2016b; Gao Y. et al., 2015;  
564 Nguyen et al., 2019a, 2019b; Wang H. et al., 2015; Wang J. et al., 2014; Wang Z. F. et al., 2014;  
565 Wu et al., 2019a; Zhang B. et al., 2015; Zhang et al., 2018; Zhao et al., 2017) but less studies  
566 explored the responses of O<sub>3</sub> and other species (Kumar et al., 2012b; Li J. et al., 2018; Nguyen et  
567 al., 2019a, 2019b; Xing et al., 2017; Zhang B. et al., 2015). As summarized by Wu et al. (2019a) in  
568 their Table 1, observations and model simulations with WRF-Chem, WRF-CMAQ, WRF-CMAQ,  
569 GRAPES-CUACE, and WRF-NAQPMS all pointed out that the ARI effects promoted higher PM<sub>2.5</sub>  
570 concentrations in China (Chen et al., 2019a; Gao M. et al., 2016b; Gao Y. et al., 2015; Wang H. et  
571 al., 2015; Wang J. et al., 2014; Wang Z.F. et al., 2014; Zhang B. et al., 2015; Zhang et al., 2018) and  
572 this was also true in other areas of Asia (e.g., India, EA, Continental SEA) (Gao M. et al., 2018b;  
573 Nguyen et al., 2019a, 2019b) during different seasons. At the same time, all the modeling  
574 investigations revealed that the positive aerosol-meteorology feedbacks could further exacerbate  
575 pollution problems during heavy haze episodes. Based on WRF-Chem simulations, the ACI effects  
576 on PM<sub>2.5</sub> was negligible comparing to the ARI effects over EC (Zhang B. et al., 2015) but was  
577 subject to a certain degree of uncertainty if no consideration of the ACI effects induced by cumulus  
578 clouds in the model (Gao Y. et al., 2015). Annual WRF-Chem simulations for 2014 by Zhang et al.  
579 (2018) indicated that even though the ARI effects had bigger impacts on PM<sub>2.5</sub> during wintertime  
580 than the ACI effects, the ARI and ACI impacts on PM<sub>2.5</sub> were similar during other seasons and the  
581 increase of PM<sub>2.5</sub> due to the ACI effects was more noticeable in wet season than dry season. Using  
582 the process analysis method to distinguish the contributions of different physical and chemical  
583 processes to PM<sub>2.5</sub> over the NCP area, Chen et al. (2019a) applied WRF-Chem with ARI and ACI  
584 and found that besides local emissions and regional transport processes, vertical mixing contributed  
585 the most to the accumulation and dispersion of PM<sub>2.5</sub>, comparing to chemistry and advection, and  
586 the ARI effects changed the vertical mixing contribution to daily PM<sub>2.5</sub> variation from negative to  
587 positive. Regarding surface O<sub>3</sub> concentrations, all the two-way coupled models with ARI, ACI, and  
588 both ARI and ACI predicted reduced photolysis rate and O<sub>3</sub> concentrations under heavy pollution  
589 conditions, through the radiation attenuation induced by aerosols and clouds. Further analyses  
590 indicated that the ARI effects impacted O<sub>3</sub> positively through reducing vertical dispersions (WRF-  
591 CMAQ, Xing et al., 2017), reduced O<sub>3</sub> more during wintertime than summertime in EC (WRF-  
592 NAQPMS, Li J. et al., 2018), and suppressed (enhanced) O<sub>3</sub> in dry (wet) season in continental SEA  
593 (WRF-CMAQ, Nguyen et al., 2019b). Xing et al. (2017) applied the process analysis method in  
594 WRF-CMAQ with ARI and revealed that the impacts of ARI on the contributions of atmospheric  
595 dynamics and photochemistry processes to O<sub>3</sub> over China varied in winter and summer months and  
596 ARI induced largest changes in photochemistry (dry deposition) of surface O<sub>3</sub> at noon time in  
597 January (July). The process analysis in WRF-Chem with ARI and ACI identified that the vertical  
598 mixing process played the most important role among the other physical and chemical processes  
599 (advection and photochemistry) in surface O<sub>3</sub> growth during 10-14 local time in Nanjing, China  
600 (Gao J. et al., 2018). ARI and ACI not only affected PM<sub>2.5</sub> and O<sub>3</sub>, but also other chemical species.  
601 For instance, CO and SO<sub>2</sub> increased due to ARI and ACI over EC (Zhang B. et al., 2015), ARI  
602 caused midday (daily average) OH increased (decreased) in July (January) over China (Xing et al.,  
603 2017), SO<sub>2</sub>, NO<sub>2</sub>, BC, SO<sub>4</sub><sup>2-</sup>, NO<sub>3</sub><sup>-</sup> were enhanced but OH was reduced over China by ACI (Zhao  
604 et al., 2017), and ARI impacted SO<sub>2</sub> and NO<sub>2</sub> positively over EA (Nguyen et al., 2019a). Wu et al.  
605 (2019b) further analyzed how the aerosol liquid water involved in ARI and chemical processes (i.e.,  
606 photochemistry and heterogeneous reactions) and influenced radiation and PM<sub>2.5</sub> (esp. secondary



607 aerosols) over NCP during an intense haze event. Moreover, evaluations and sensitivity studies  
608 indicated that turning on aerosol feedbacks could improve the model performance for surface  $PM_{2.5}$ ,  
609 particularly during severe haze episodes (Li J. et al., 2018; Wang H. et al., 2018; Zhang B. et al.,  
610 2015; Zhang et al., 2018).

611 With reference to the feedback effects of anthropogenic aerosol compositions on air quality,  
612 most modeling research work with WRF-Chem had focused on the ARI and ACI effects of BC and  
613 BrC, especially the “dome effect” that prompted the accumulation of pollutants (aerosols and  $O_3$ )  
614 near surface and in PBL (Ding et al., 2016; Ding et al., 2019; Gao J. et al., 2018; Li and Liao, 2014;  
615 Wang Z. et al., 2018). At the same time, the ARI effects of BC undermined the low-level wind  
616 convergence and then led to decrease of aerosols (sulfate and nitrate) and  $O_3$  (Li and Liao, 2014).  
617 With the process analysis methodology in WRF-Chem, Gao J. et al. (2018) indicated that comparing  
618 to simulations without BC, the BC and PBL interaction slowed the  $O_3$  growth from late morning to  
619 early afternoon somewhat before reaching its maximum value in afternoon due to less vertical  
620 mixing in PBL, even though more  $O_3$  precursors were trapped in PBL that promoted photochemical  
621 reaction of  $O_3$ .

622 Studies on the feedback effects of aerosols from different emission sectors on air quality were  
623 relatively limited and mainly involved with ARB emissions and assessments of emission controls  
624 during certain major air pollution events. Jena et al. (2015) applied WRF-Chem with aerosol  
625 feedbacks and investigated  $O_3$  and its precursors in SA due to regional ARB. Based on WRF-Chem  
626 simulations with enabling ARI and ACI, Wu et al. (2017) denoted that aerosols emitted from ARB  
627 could be mixed or/and coated with urban aerosols while being transported to cities and contributed  
628 to heavy air pollution events there, such as in Nanjing, China. The ARI effects induced by ARB  
629 aerosols on  $O_3$  and  $NO_2$  concentrations (-1 % and 2 %, respectively) were small compared to the  
630 contribution of precursors emitted from ARB to  $O_3$  chemistry (40 %) in the ARB zone (Li M. et al.,  
631 2018). Pollutants emitted from natural and anthropogenic BB over Indochina affected pollution  
632 levels over SC and their ACI effects removed aerosols more efficiently than the ARI effects that  
633 could make BB aerosols last longer in the ATM (Huang et al., 2019). Gao et al. (2017a) and Zhou  
634 et al. (2019) both utilized WRF-Chem to evaluate what role the ARI effects played when dramatic  
635 emission reductions implemented during the week of Asia Pacific Economic Cooperation Summit  
636 and concluded that the ARI reduction induced by decreased emission led to 6.7-10.9 % decline in  
637  $PM_{2.5}$  concentrations in Beijing.

#### 638 4.3 Human health effects

639 Poor air quality poses risks to human health (Brunekreef and Holgate, 2002; Manisalidis et al.,  
640 2020), therefore, in the past several decades, air quality models had been used in epidemiology  
641 related research to establish quantitative relationships between concentrations of various pollutants  
642 and burden of disease (including mortality or/and morbidity) as well as associated economic loss  
643 (Conti et al., 2017). In Asia, there were several studies that applied coupled air quality models with  
644 feedbacks to assess human health effects of air pollutants under historical and future scenarios  
645 (Conibear et al., 2018a, 2018b; Gao et al., 2017b; Gao M. et al., 2015; Ghude et al., 2016; Hong et  
646 al., 2019; Wang et al., 2017; Xing et al., 2016; Zhong et al., 2019). By applying WRF-Chem with  
647 ARI and ACI, M. Gao et al. (2015) estimated the health and financial impacts induced by an intense  
648 air pollution event happened in the NCP area during January, 2013 and concluded that the mortality,  
649 morbidity, and financial loss over Beijing area were 690, 69070, and 253.8 million US\$,  
650 respectively. Targeting the same case, Gao M. et al. (2017b) pointed out that turning on the data  
651 assimilation of surface  $PM_{2.5}$  observations in WRF-Chem not only improved model simulations but  
652 also made the premature death numbers increased by 2 % in the NCP area, comparing to simulations  
653 without the  $PM_{2.5}$  data assimilation. In India, WRF-Chem simulations with aerosol feedbacks and  
654 updated population data revealed that the premature (COPD related) deaths caused by  $PM_{2.5}$  ( $O_3$ )  
655 were 570,000 (12,000), resulting in shortened life expectancy ( $3.4 \pm 1.1$  years) and financial  
656 expenses (640 million US\$) during 2011 (Ghude et al., 2016). Based on WRF-CMAQ simulations  
657 with ARI for 21 years (1990-2010), Xing et al. (2016) pointed out that in EA the population-  
658 weighted  $PM_{2.5}$  induced mortality had an upward trend from 1990 (+3187) to 2010 (+3548) and the  
659 mean mortality caused by ARI-enhanced  $PM_{2.5}$  was 3.68 times more than that decreased by ARI-  
660 reduced temperature. The same 21 year simulations also showed that from 1990 to 2010, the  $PM_{2.5}$   
661 related mortalities in EA and SA rose by 21 % and 85 %, respectively, while they declined in  
662 Europe and high-income North America by 67 % and 58 %, respectively (Wang et al., 2017).  
663 Conibear et al. (2018a) applied WRF-Chem with ARI to study how different emission sectors



664 affected human health in India and demonstrated that the residential energy use sector played the  
665 most critical role among other sectors and could cause 511,000 premature deaths in 2014.  
666 Furthermore, Conibear et al. (2018b) investigated future PM<sub>2.5</sub> pollution levels as well as health  
667 impacts in India under different emission scenarios (business as usual and two emission control  
668 pathways) and deduced that the burden of disease driven by PM<sub>2.5</sub> and population factors (growth  
669 and aging) in 2050 increased by 75 % under the business as usual scenario but decreased by 9 %  
670 and 91 % under the International Energy Agencies New Policy Scenario and Clean Air Scenario,  
671 respectively, comparing with that in 2015. The sensitivity study using WRF-Chem with ARI under  
672 a variety of emission scenarios, population projections, and concentration-response functions  
673 (CRFs) for the years of 2008 and 2050 demonstrated that CRFs (future emission projections) were  
674 the main sources of uncertainty in the total mortality estimations related to PM<sub>2.5</sub> (O<sub>3</sub>) in China  
675 (Zhong et al., 2019). Applying a suite of models, including WRF-CMAQ with ARI, climate and  
676 epidemiology, Hong et al. (2019) inferred that under Representative Concentration Pathway 4.5,  
677 the future mortalities could be 12100 and 8900 per year in China led by PM<sub>2.5</sub> and O<sub>3</sub>, respectively,  
678 and the climate-driven weather extremes could add 39 % and 6 % to future mortalities due to stable  
679 atmosphere and heat waves, respectively.

#### 680 **5 Effects of aerosol feedbacks on model performance**

681 Even though there are a certain number of research papers using two-way coupled models to  
682 quantify the effects of aerosol feedbacks on regional meteorology and air quality in Asia, model  
683 performances impacted by considering aerosol effects varied to some extent. This section provides  
684 a summary of model performance comparisons by using the SI (meteorology and air quality as  
685 shown in data file (Table C2.xlsx)) collected from the published papers that supplying these indices  
686 and being defined as “papers with SI (PSI) (listed in Appendix Tables B2-B3). As aforementioned  
687 in Section 3, investigations of ACI effects were very limited and no former studies simultaneously  
688 exploring aerosol feedbacks with and without both ARI and ACI turned on. Here, we only compared  
689 the SI for simulations with and without ARI in the same study, as summarized in Appendix Tables  
690 B4-B5. It should be pointed out that all the reported evaluation results either from individual model  
691 or inter-model comparison studies were extracted and put into the Table C2.xlsx file.

#### 692 **5.1 Model performance for meteorology variables**

693 With certain emissions, accurate simulations of meteorological elements are critical to air  
694 quality modeling and prediction (Appel et al., 2017; Bauer et al., 2015; Saylor et al., 2019; Seaman,  
695 2000). Targeting meteorological variables, we summarized their SI and further analyzed the  
696 variations of SI on different simulated time scales and among multiple models.

#### 697 **5.1.1 Overall performance**

698 Figure 3 shows the compiled statistical indicators (correlation coefficient (R) is in black, and  
699 mean bias (MB) and root mean square error (RMSE) are in blue) of T2 (°C), RH2(%) and specific  
700 humidity (SH2, g·kg<sup>-1</sup>) at 2 meters, and WS10 (m·s<sup>-1</sup>) from PSI (a-d), and simulations with and  
701 without ARI (marked as ARI and NO-ARI in e-h). In this figure and following figures, NP and NS  
702 are number of publications and samples with SI, respectively and summed up in Appendix Table  
703 B2. In these two tables, we also listed the NS of positive (red upward arrow) and negative (blue  
704 downward arrow) biases for the meteorological and air quality variables in parentheses in the MB  
705 column. Note that NS in Fig. 3e-h and Appendix Table B4 counted the samples of SI provided by  
706 the simulations simultaneously with and without ARI. Also the 5th, 25th, 75th and 95th percentiles  
707 of SI are illustrated in box-and-whisker plots, and the dashed line in the box is the mean value (not  
708 median) and the circles are outliers.

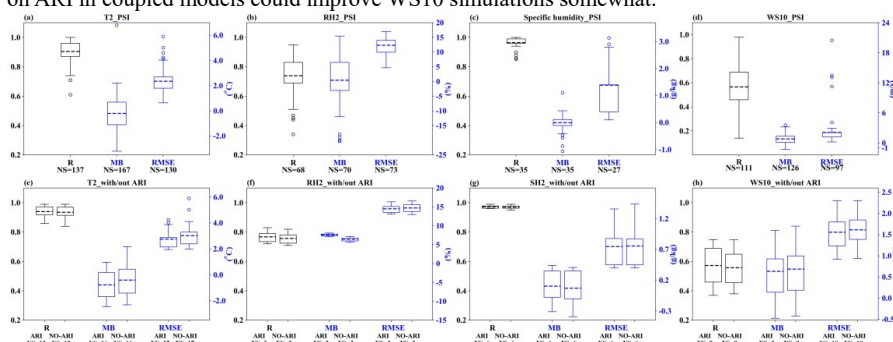
709 The evaluations for T2 (Fig. 3a) from PSI revealed that in Asia coupled models performed  
710 rather well for temperature (mean R = 0.90) with RMSE ranging from 0.64 to 5.90 °C, but 60 % of  
711 samples showed the tendency towards temperature underestimations (mean value of MB = -0.20 °C)  
712 with the largest average MB (-0.31 °C) occurring during winter months (70 samples). The  
713 underestimations of temperature had been reported not only from modeling studies by using WRF  
714 or coupled models, but also in Asia, Europe and North America (Brunner et al., 2015; Gao et al.,  
715 2019; García-Diez et al., 2013; Makar et al., 2015a; Yahya et al., 2015). The WRF simulations in  
716 China (Gao et al., 2019) and US (EPA, 2018) also showed wintertime cold biases of T2 but in Europe  
717 warm biases were reported (García-Diez et al., 2013). This temperature bias was probably related  
718 to the impacts of model resolutions (Kuik et al., 2016), urban canopies (Liao et al., 2014) and PBL  
719 schemes (Hu et al., 2013). With the ARI turned on in the coupled models, modeled temperatures



720 (limited papers with 12 samples) were improved somewhat and the mean correlation coefficient  
 721 increased from 0.93 to 0.95 and RMSE decreased slightly (Fig. 3e), but average MB of temperature  
 722 was decreased from -0.98 to -1.24 °C. In short, temperatures from PSI or simulations with/without  
 723 ARI turned on agreed well with observations but were mostly underestimated, and the negative bias  
 724 of T2 simulated by models with ARI turned on got worse and reasons behind it will be explained in  
 725 Section 6.

726 Figures 3b-c illustrate that RH2 was simulated reasonably well (mean R = 0.73) and the  
 727 modeled SH2 was also well correlated with observations (R varied between 0.85 and 1.00). RH2  
 728 and SH2 from more than half of samples had slightly positive and negative mean biases with average  
 729 MB values of 0.4 % and -0.01 g·kg<sup>-1</sup>, respectively. The overestimations of RH2 could be caused by  
 730 the negative bias of T2 (Cuchiara et al., 2014). Compared with results without ARI effects, statistics  
 731 of RH2 and SH2 from simulations with ARI showed better R and RMSE. However, the increased  
 732 positive mean biases (average MBs of RH2 and SH2 were from 6.4 % to 7.6 % and from 0.07 g·kg<sup>-1</sup>  
 733 to 0.11 g·kg<sup>-1</sup>, respectively) indicated that turning on ARI could cause further overprediction of  
 734 humidity variables. It should be noted that only 2 or 1 PSI supplying statistical analysis of modeled  
 735 RH2 and SH2 with/without ARI effects may not be enough to make these comparisons statistically  
 736 significant and further investigations are much needed. Overall, the modeled RH2 and SH2 were in  
 737 good agreement with observations with slight over- and under-estimations, respectively, and the  
 738 very limited studies showed that RH2 and SH2 simulated by models with ARI turned on had  
 739 marginally larger positive biases relative to the results without ARI.

740 Compared with the correlation coefficients of T2, RH2 and SH2, mean R (0.59) of WS10 was  
 741 smallest with a large fluctuation ranging from 0.14 to 0.98 (Fig. 3d). The meta-analysis also  
 742 indicated the most modeled WS10 tended to be overestimated (81 % of the samples) with the  
 743 average MB value of 0.79 m·s<sup>-1</sup>, and the mean RMSE value was 2.76 m·s<sup>-1</sup>. The general  
 744 overpredictions of WS10 by WRF (Mass and Ovens, 2011) and coupled models (Gao M. et al.,  
 745 2018a; Gao Y. et al., 2015) had been explained with possible reasons such as out-of-date  
 746 geographical data, coarse model resolutions and lacking of better representations of urban canopy  
 747 physics. The 5 PSI with ARI effects suggested that the correlation of wind speed was slightly  
 748 improved (mean R from 0.56 to 0.57) and the average RMSE and positive MB decreased by 0.003  
 749 m·s<sup>-1</sup> and 0.051 m·s<sup>-1</sup>, respectively (Fig. 3h). The collected SI indicated relatively poor performance  
 750 of modeled WS10 (most wind speeds were overestimated) compared to T2 and humidity, but turning  
 751 on ARI in coupled models could improve WS10 simulations somewhat.



752

753 Figure 3. The quantile distributions of R, MB and RMSE for different meteorological variables from coupled  
 754 models performance data (a-d) and comparisons of the statistical indices with/out ARI (e-h).

### 755 5.1.2 Comparisons of SI at different temporal scales for meteorology

756 To probe the model performance of simulated T2, RH2, SH2 and WS2 at different temporal  
 757 scales, the SI of these meteorological variables from PSI were grouped according to the simulation  
 758 time (yearly, seasonal, monthly and daily) and plotted in Fig. 4. Note that the seasonal results  
 759 contained SI values from simulations lasting more than one month and less than or equal to 3 months.  
 760 Here in Fig. 4, NP and NS were the number of PSI and samples with SI at different time scales,  
 761 respectively, and also their total values were the same as the ones listed in Appendix Table S2. The  
 762 correlation between simulated and observed T2 (Fig. 4a) at the seasonal (mean R= 0.97 with the  
 763 smallest sample size), yearly (0.91) and monthly (0.90) scales were stronger than that at the daily  
 764 scale (0.87), indicating that long-term simulations of T2 were well reproduced by coupled models.

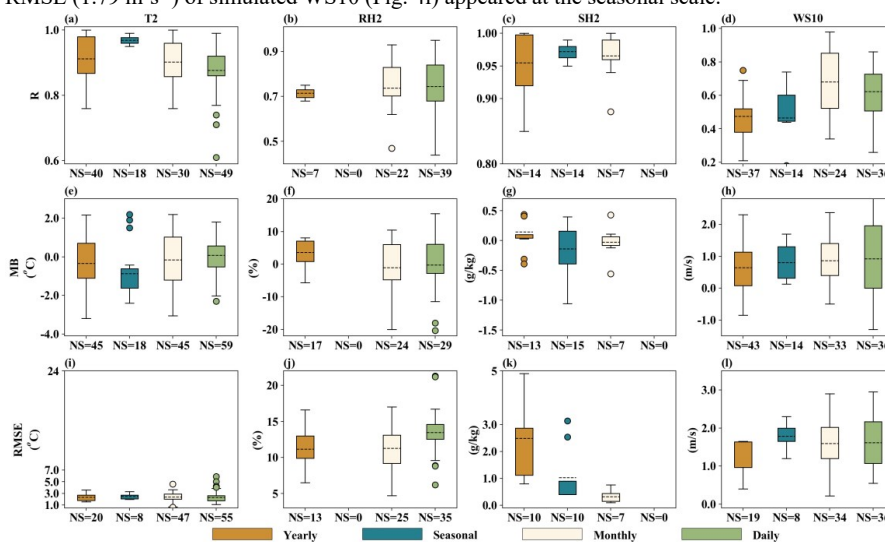


765 As shown in Fig. 4e, T2 underestimation mentioned above (Fig. 3a) appeared also in the seasonal,  
 766 monthly and yearly simulations (average MB = -0.87 °C, -0.15 °C and -0.34 °C, respectively), but  
 767 the daily T2 were overestimated (average MB = 0.07 °C). It should be noted that T2 at the monthly  
 768 scale was underpredicted mainly during winter months (16 samples). Regarding the mean RMSE,  
 769 its value (Fig. 4i) at the daily scale was the largest (0.97 °C) in comparison with that at the other  
 770 temporal scales.

771 Given that no SI was available for RH2 at the seasonal scale, results at other time scales were  
 772 discussed here. Figure 4b presented that simulated RH2 at the daily scale had the best correlation  
 773 coefficient (mean R = 0.74), followed by those at the monthly (0.73) and yearly (0.71) scales. Except  
 774 overestimation (average MB = 3.6 %) at the yearly scale (Fig. 4f), modeled RH2 were  
 775 underestimated at the monthly (average MB = -1.1 %) and daily (average MB = -0.2 %) scales,  
 776 respectively. Therefore, coupled models calculated RH2 reasonably well in short-term simulations.  
 777 However, at the daily scale, RMSE of modeled RH2 (Fig. 4j) was relatively large fluctuation ranging  
 778 from 6.2 % to 21.3 %.

779 Lacking of SI for SH2 at the daily scale, only those at other time scales were compared. Even  
 780 though NP and NS were very limited, the modeled SH2 (Fig. 4c) exhibited especially good  
 781 correlation with observations with the mean R values exceeding 0.95 at the yearly, seasonal and  
 782 monthly scales (0.99, 0.97 and 0.96, respectively) but had the largest mean RMSE (2.09 g·kg<sup>-1</sup>) at  
 783 the yearly scale (Fig. 4k). Also, both over- and under-estimations of modeled SH2 (Fig. 4g)  
 784 were reported at different time scales with average MB values as 0.15 g·kg<sup>-1</sup>, -0.02 g·kg<sup>-1</sup>, and -0.14 g·kg<sup>-1</sup>  
 785 for yearly, seasonal and monthly simulations, respectively. Generally, the long-term simulations of  
 786 SH2 agreed better with observations than the short-term ones.

787 As seen in Fig. 4d, the modeled WS10 at the monthly scale (mean R = 0.68) correlated with  
 788 observations better than that at the daily, yearly and seasonal scales (mean R = 0.62, 0.48 and 0.46,  
 789 respectively). The simulations at all temporal scales tended to overestimate WS10 comparing  
 790 against observations (Fig. 4h) and their average MB were 0.80 m·s<sup>-1</sup> (seasonal), 0.86 m·s<sup>-1</sup> (monthly),  
 791 0.64 m·s<sup>-1</sup> (yearly) and 0.62 m·s<sup>-1</sup> (daily), respectively. The short-term simulations of WS10 better  
 792 matched with observations compared to the long-term ones. At the same time, the largest mean  
 793 RMSE (1.79 m·s<sup>-1</sup>) of simulated WS10 (Fig. 4l) appeared at the seasonal scale.



794  
 795  
 796  
 797  
 798  
 799  
 800  
 801  
 802

Figure 4. The statistical indices of modeled meteorological variables at different temporal scales (Yearly, Seasonal, Monthly and Daily) from past studies in Asia.

### 5.1.3 Comparisons of SI for meteorology using different coupled models

Also, to examine how different coupled models (i.e., WRF-Chem, WRF-CMAQ, WRF-NAQPMS and GRAPES-CUACE) performed in Asia with respect to meteorological variables, the SI were extracted from PSI in term of these four coupled models and displayed in Fig. 5. The SI for T2, RH2, SH2, and WS10 from WRF-NAQPMS and GRAPES-CUACE simulations were missing or with rather limited samples so that the discussions here only focused on the WRF-Chem and



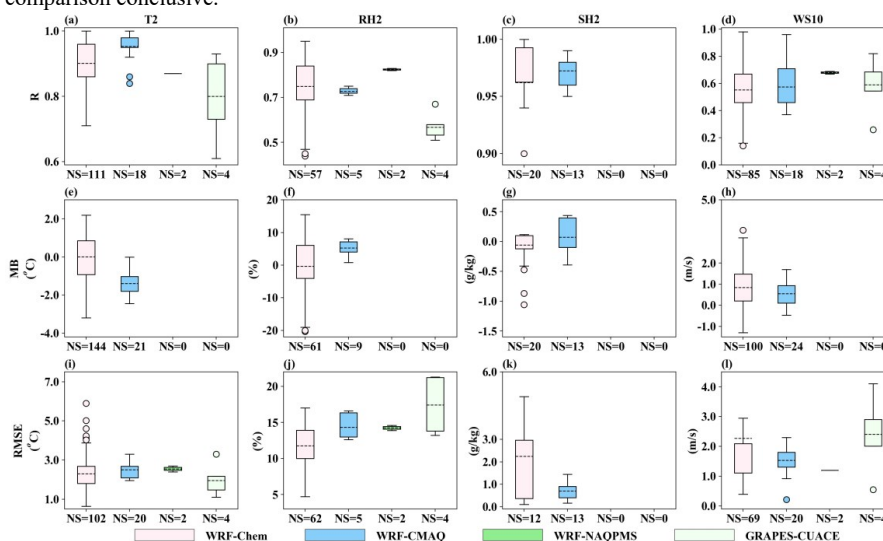
803 WRF-CMAQ simulations. Moreover, the SI sample size from studies involving WRF-Chem was  
 804 generally larger than that involving WRF-CMAQ, except for SH2.

805 As seen in Fig. 5a, the modeled T2 by both WRF-CMAQ and WRF-Chem was well correlated  
 806 with observations but WRF-CMAQ (mean R = 0.95) outperformed WRF-Chem (mean R = 0.90)  
 807 to some extent. On the other hand, WRF-CMAQ underestimated T2 (mean MB = -1.39 °C) but WRF-  
 808 Chem slightly overestimated it (mean MB = 0.09 °C) (Fig. 5e). The RMSE of modeled T2 by both  
 809 models was at the similar level with mean RMSE values of 2.51 °C and 2.31 °C by WRF-CMAQ  
 810 and WRF-Chem simulations, respectively (Fig. 5i).

811 Both WRF-Chem and WRF-CMAQ performed better for SH2 (mean R = 0.96 and 0.97,  
 812 respectively) than RH2 (mean R = 0.75 and 0.73, respectively) (Figures 5b and 5c), which might be  
 813 due to the influence of temperature on RH2 (Bei et al., 2017). Also the modeled RH2 (SH2) by  
 814 WRF-Chem correlated better (worsen) with observations than those by WRF-CMAQ. The mean  
 815 RMSE of modeled RH2 (Fig. 5j) by WRF-Chem (11.1 %) was lower than that by WRF-CMAQ  
 816 (14.3%) but the mean RMSE of modeled SH2 (Fig. 5k) by WRF-Chem (2.25 g·kg<sup>-1</sup>) higher than  
 817 that by WRF-CMAQ (0.71 g·kg<sup>-1</sup>). It was seen in Figures 5f and 5d that WRF-CMAQ overestimated  
 818 RH2 and SH2 (average MB were 5.30 % and 0.07 g·kg<sup>-1</sup>, respectively), and WRF-Chem  
 819 underpredicted RH2 (average MB = -0.32 %) and SH2 (average MB = -0.06 g·kg<sup>-1</sup>). Generally,  
 820 the modeled RH2 and SH2 were reproduced more reasonably by WRF-Chem than those by WRF-  
 821 CMAQ.

822 The modeled WS10 by both WRF-Chem and WRF-CMAQ (Fig. 5d) correlated with  
 823 observations on the same level with the mean R of 0.56. The mean RMSE of modeled WS10 by  
 824 WRF-Chem and WRF-CMAQ were 1.54 m·s<sup>-1</sup> and 2.28 m·s<sup>-1</sup>, respectively, as depicted in Fig. 5l.  
 825 Both models overpredicted WS10 to some extent with average MBs of 0.55 m·s<sup>-1</sup> (WRF-CMAQ)  
 826 and 0.84 m·s<sup>-1</sup> (WRF-Chem), respectively. These results demonstrated that overall WRF-CMAQ  
 827 and WRF-Chem had similar model performance of WS10.

828 In general, WRF-CMAQ performed better than WRF-Chem for T2 but worse for humidity  
 829 (RH2 and SH2), and both models' performance for WS10 was very similar. WRF-Chem  
 830 overestimated T2, RH2 and WS10 and underestimated SH2 slightly, while WRF-CMAQ  
 831 overpredicted humidity and WS10 but underpredicted T2. Compared to WRF-Chem and WRF-  
 832 CMAQ, the very few SI samples indicated that for the meteorological variables excluding SH2,  
 833 WRF-NAQPMS simulations matched with observations better than GRAPES-CUACE simulations  
 834 but more applications and statistical analysis of these two models are needed to make this kind of  
 835 comparison conclusive.



836  
 837  
 838

Figure 5. Bar chart plots summarizing the statistical indices of simulated meteorological variables using different two-way coupled models from past studies in Asia.

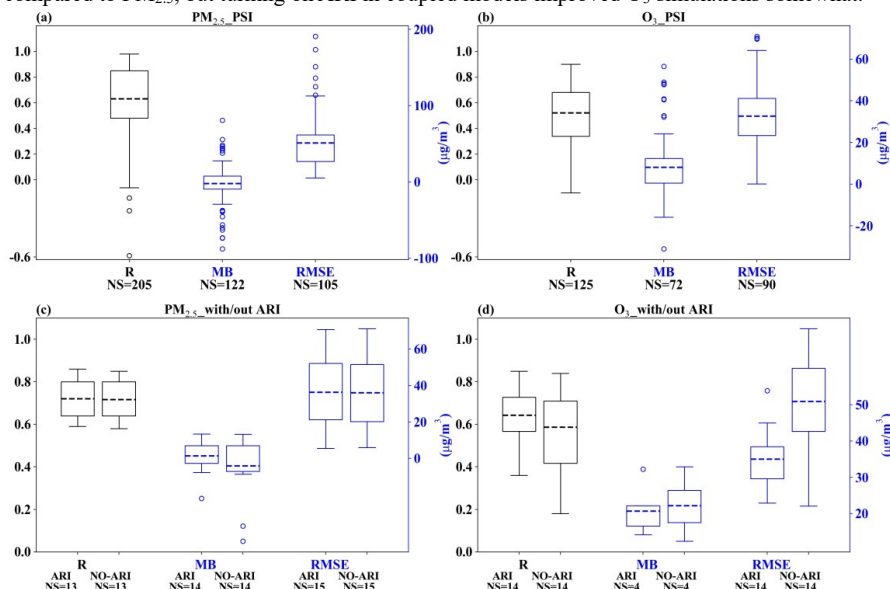


## 839 5.2 Model performance for air quality variables

### 840 5.2.1 Overall performance

841 The results of the overall statistical evaluation for the online air quality simulations are  
842 presented in Figure 6, and all labels and colors indicating SI were the same as those for  
843 meteorological variables. In Fig. 6a, the correlation between the simulated and observed  $PM_{2.5}$   
844 concentrations from PSI showed that in Asia coupled models performed relatively well for  $PM_{2.5}$   
845 (mean  $R = 0.63$ ), but RMSE was between  $-87.60$  and  $80.90$  and more than half of samples of  
846 simulated  $PM_{2.5}$  were underestimated (mean  $MB = -2.08 \mu\text{g}\cdot\text{m}^{-3}$ ). With the ARI turned on in the  
847 coupled models, modeled  $PM_{2.5}$  concentrations (limited papers with 15 samples) were improved  
848 somewhat and the mean  $R$  slightly increased from  $0.71$  to  $0.72$  and mean absolute  $MB$  decreased  
849 from  $4.10$  to  $1.33 \mu\text{g}\cdot\text{m}^{-3}$  (Fig. 6c), but RMSE of  $PM_{2.5}$  concentrations slightly increased from  $35.40$   
850 to  $36.20 \mu\text{g}\cdot\text{m}^{-3}$ . In short,  $PM_{2.5}$  with/without ARI agreed well with observations but were mostly  
851 underestimated, and  $PM_{2.5}$  bias simulated by models became overpredicted.

852 Compared with  $PM_{2.5}$ , mean  $R$  ( $0.59$ ) of  $O_3$  was relatively smaller (Fig. 6b). The statistical  
853 analysis also showed the most modeled  $O_3$  concentrations tended to be overestimated ( $76\%$  of the  
854 samples) with the average  $MB$  value of  $8.05 \mu\text{g}\cdot\text{m}^{-3}$ , and the mean RMSE value was  $32.65 \mu\text{g}\cdot\text{m}^{-3}$ .  
855 The 14 PSI with ARI effects suggested that the correlation of  $O_3$  was slightly improved (mean  $R$   
856 from  $0.58$  to  $0.64$ ) and the average RMSE and  $MB$  were decreased by  $15.93 \mu\text{g}\cdot\text{m}^{-3}$  and  $1.55 \mu\text{g}\cdot\text{m}^{-3}$   
857  $^3$ , respectively (Fig. 6d). The collected studies indicated relatively poor performance of modeled  $O_3$   
858 compared to  $PM_{2.5}$ , but turning on ARI in coupled models improved  $O_3$  simulations somewhat.



859

860 Figure 6. The variations of statistical indices for  $PM_{2.5}$  and  $O_3$  (a-b) and ARI simulations verse no-ARI  
861 simulations (c-d) using two-way coupled models in Asia from literatures.

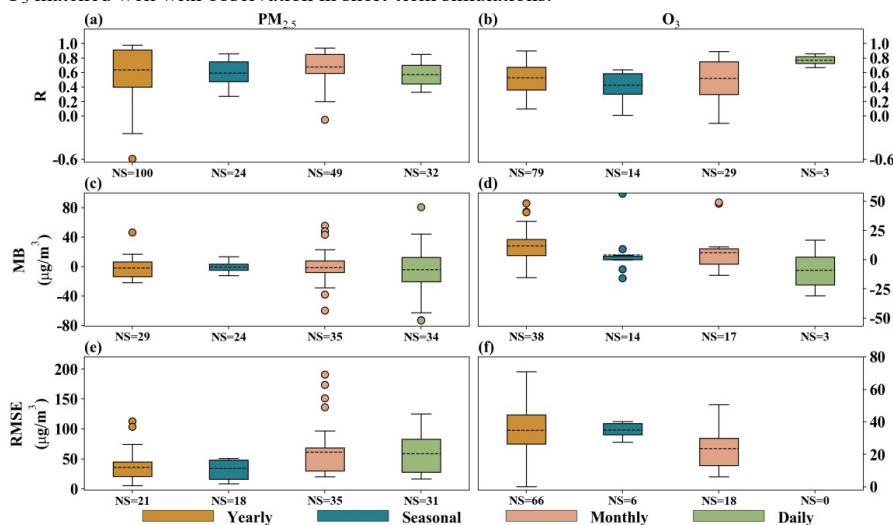
### 862 5.2.2 Comparisons of SI at different temporal scales for air quality

863 Figure 7 depicted the SI of simulated  $PM_{2.5}$  and  $O_3$  at yearly, seasonal, monthly and daily scales.  
864 The correlation between simulated and observed  $PM_{2.5}$  (Fig. 7a) at the monthly scale (mean  $R=0.68$ )  
865 was largest compared to those at the yearly ( $0.64$ ), seasonal ( $0.59$ ), daily ( $0.57$ ) scales. All the  
866 simulated  $PM_{2.5}$  were underestimated, with the average daily, monthly, seasonal, and yearly  $MB$  as  
867  $-4.13$ ,  $-1.46$ ,  $-0.28$ , and  $-1.89 \mu\text{g}\cdot\text{m}^{-3}$ , respectively (Fig. 7c). As displayed in Fig. 7e, the mean RMSE  
868 at the monthly scale was the largest ( $61.57 \mu\text{g}\cdot\text{m}^{-3}$ ).

869 Regarding to correlation between simulated and observed  $O_3$  (Fig. 7b), it was the best at the  
870 daily scale (mean  $R=0.77$ ). Modeled  $O_3$  were overestimated at the seasonal (average  $MB = +4.12$   
871  $\mu\text{g}\cdot\text{m}^{-3}$ ), monthly (average  $MB = +6.11 \mu\text{g}\cdot\text{m}^{-3}$ ) and yearly (average  $MB = +11.71 \mu\text{g}\cdot\text{m}^{-3}$ ) scales,  
872 but underestimated at the daily scale (average  $MB = -8.89 \mu\text{g}\cdot\text{m}^{-3}$ ) (Fig. 7d). Note that no RMSE for



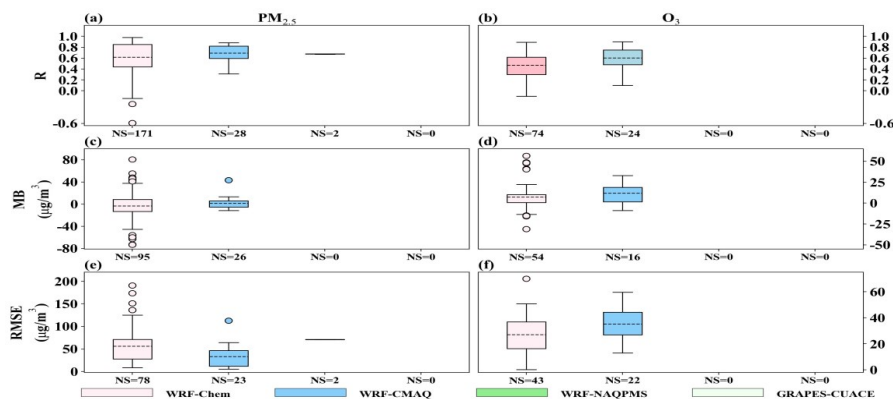
873 O<sub>3</sub> simulation was available at the daily scale, and the RMSE at the yearly scale (Fig. 7f) had  
 874 relatively large fluctuation ranging from 0.21 to 71 μg·m<sup>-3</sup>. Therefore, coupled models calculated  
 875 O<sub>3</sub> matched well with observation in short-term simulations.



876  
 877 Figure 7. The quantile distributions of simulated PM<sub>2.5</sub> and O<sub>3</sub> performance metrics at different temporal  
 878 scales from past studies in Asia.

### 879 5.2.3 Comparisons of SI for air quality using different coupled models

880 Figure 8 showed the SI for PM<sub>2.5</sub> and O<sub>3</sub> from different coupled models, and only WRF-Chem  
 881 and WRF-CMAQ simulations were discussed for the same reason as in Section 5.1.3. The modeled  
 882 PM<sub>2.5</sub> by WRF-CMAQ (mean R = 0.69) outperformed WRF-Chem (mean R = 0.62) to some extent  
 883 (Fig. 8a) and the RMSE of modeled PM<sub>2.5</sub> by WRF-CMAQ (33.24 μg·m<sup>-3</sup>) was smaller than that by  
 884 WRF-Chem (56.16 μg·m<sup>-3</sup>). With respect to MB, WRF-CMAQ overestimated PM<sub>2.5</sub> (mean MB =  
 885 +1.60 μg·m<sup>-3</sup>) but WRF-Chem slightly underestimated it (mean R = -3.12 μg·m<sup>-3</sup>) (Fig. 8c). Figure  
 886 8b showed that the modeled O<sub>3</sub> by WRF-CMAQ (0.60) correlated better with observations than  
 887 those by WRF-Chem (0.47), but the mean RMSE of modeled O<sub>3</sub> (Fig. 8f) by WRF-Chem (27.13  
 888 μg·m<sup>-3</sup>) was lower than that by WRF-CMAQ (35.19 μg·m<sup>-3</sup>). It was seen in Figures 8d that both  
 889 WRF-CMAQ and WRF-Chem overestimated O<sub>3</sub>, with mean MBs as 11.98 and 7.21 μg·m<sup>-3</sup>,  
 890 respectively. Generally, the modeled PM<sub>2.5</sub> and O<sub>3</sub> were reproduced more reasonably by WRF-  
 891 CMAQ than by WRF-Chem, even though there were much more samples available from WRF-  
 892 Chem simulations than WRF-CMAQ simulations.  
 893



894  
 895 Figure 8. The quantile distributions of R, MB and RMSE of PM<sub>2.5</sub> and O<sub>3</sub> presented by different two-  
 896 way coupled models.



## 897 6 Impacts of aerosol feedbacks in Asia

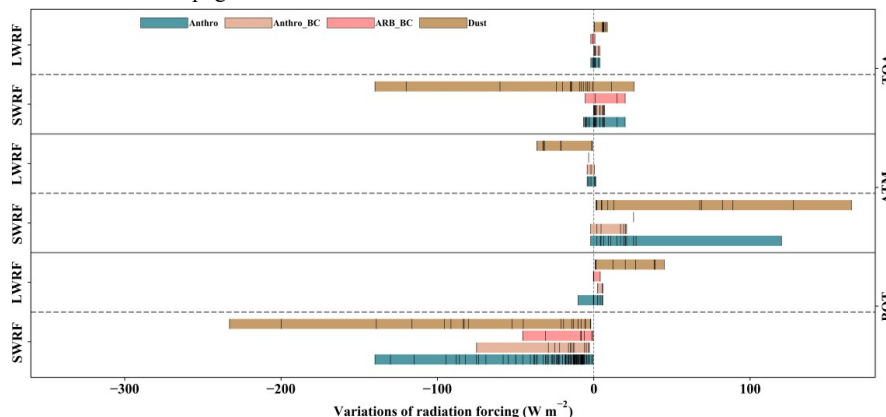
898 Aerosol feedbacks not only impact the performances of two-way coupled models but also the  
899 simulated meteorological and air quality variables to a certain extent. In this section, we collected  
900 and quantified the variations (Table C3.xlsx) of these variables induced by ARI or/and ACI from the  
901 modeling studies in Asia. Due to limited sample sizes in the collected papers, the target variables  
902 only include radiative forcing, surface meteorological parameters (T2, RH2, SH2 and WS10), PBLH,  
903 cloud, precipitation, and PM<sub>2.5</sub> and gaseous pollutants.

### 904 6.1 Impacts of aerosol feedbacks on meteorology

#### 905 6.1.1 Radiative forcing

906 With regard to radiative forcing, most studies with two-way coupled models in Asia had  
907 focused on the effects of dust aerosols (Dust), BC emitted from ARB (ARB\_BC) and anthropogenic  
908 sources (Anthro\_BC), and total anthropogenic aerosols (Anthro). Figure 9 presents the variations of  
909 simulated SWRF and LWRF at the bottom (BOT) and TOA and in the ATM due to aerosol feedbacks.  
910 In this figure, the color bars show the range of radiative forcing variations and the black tick marks  
911 inside the color bars represent these variations extracted from all the collected papers. It should be  
912 noted that in this figure all the radiative forcing variations were plotted regardless of temporal  
913 resolutions of data reporting and simulation durations. Apparently in Asia, most studies targeted the  
914 SWRF variations induced by anthropogenic aerosols at the BOT that exhibited the largest  
915 differences ranging from -140.00 to -0.45 W·m<sup>-2</sup>, with the most variations (88 % of samples)  
916 concentrated in the range of -50.00 to -0.45 W·m<sup>-2</sup>. The SWRF variations due to anthropogenic  
917 aerosols in the ATM and at the TOA were -2.00 to +120.00 W·m<sup>-2</sup> and -6.50 to 20.00 W·m<sup>-2</sup>,  
918 respectively. There were much less studies reported LWRF variations caused by anthropogenic  
919 aerosols, which ranged from -10.00 to +5.78 W·m<sup>-2</sup>, -1.91 to +3.94 W·m<sup>-2</sup>, and -4.26 to +1.21 W·m<sup>-2</sup>  
920 at the BOT and TOA, and in the ATM, respectively.

921 Considering BC from anthropogenic sources and ARB, they both led to positive SWRF at the  
922 TOA (with mean values of 2.69 and 7.55 W·m<sup>-2</sup>, respectively) and in the ATM (with mean values  
923 of 11.70 and 25.45 W·m<sup>-2</sup>, respectively) but negative SWRF at the BOT (with mean values of -18.43  
924 and -14.39 W·m<sup>-2</sup>, respectively). The responses of LWRF to Anthro\_BC and ARB\_BC at the BOT  
925 (in the ATM) on average were 4.01 and 0.72 W·m<sup>-2</sup> (-1.89 and -3.24 W·m<sup>-2</sup>), respectively, and weak  
926 at the TOA (+0.92 and -0.53 W·m<sup>-2</sup>, respectively). The SWRF variations induced by dust were in  
927 the range of -233.00 to -1.94 W·m<sup>-2</sup> and -140.00 to +25.70 W·m<sup>-2</sup>, and +1.44 to +164.80 W·m<sup>-2</sup>  
928 at the BOT and TOA, and in the ATM, respectively. The LWRF variations caused by dust were the  
929 largest (with mean values of 22.83 W·m<sup>-2</sup> and +5.20 W·m<sup>-2</sup>, and -22.12 W·m<sup>-2</sup> at the BOT and TOA,  
930 and in the ATM, respectively), comparing to the ones caused by anthropogenic aerosols and BC  
931 aerosols from anthropogenic sources and ARB.



932 Figure 9. Variations of simulated SWRF and LWRF at the BOT and TOA, and in the atmosphere  
933 induced by aerosol feedbacks in Asia.

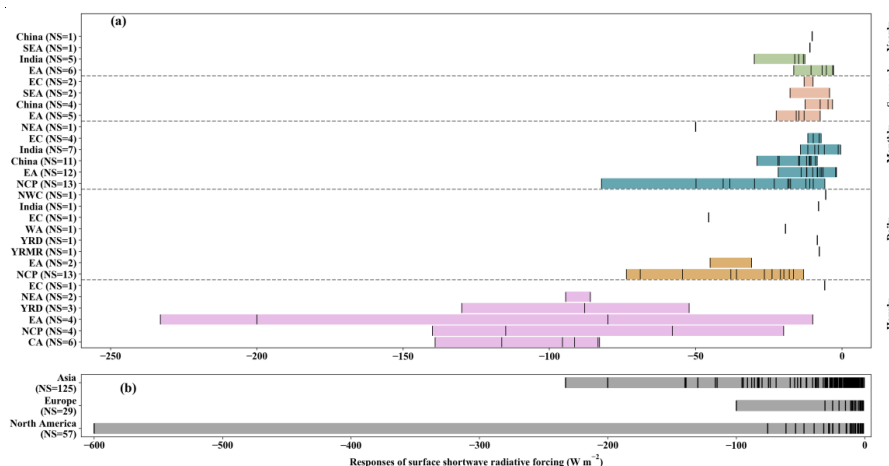
934 As shown in Fig. 9, SWRF variations at the BOT caused by total aerosols (sum of Anthro,  
935 Anthro\_BC, ARB\_BC and Dust) had been widely assessed in Asia. Therefore, we further analyzed  
936 their spatiotemporal distributions and inter-regional differences, which are displayed in Fig. 10.  
937



938 Figure 10a presents the SWRF variations over different areas of Asia (the acronyms used in Fig. 10  
 939 are listed in Appendix Table B1) at different time scales. In Asia, almost 41 % of the selected papers  
 940 investigated SWRF towards its monthly variations, 36 % towards its hourly and daily variations,  
 941 and 23 % towards its seasonal and yearly variations. Most studies reported aerosol-induced SWRF  
 942 variations were primarily conducted in NCP, EA, China, and India. At the hourly scale, the range of  
 943 SWRF decreases was from  $-350.00$  to  $-5.90 \text{ W}\cdot\text{m}^{-2}$  (mean value of  $-106.92 \text{ W}\cdot\text{m}^{-2}$ ) during typical  
 944 pollution episodes, and significant variations occurred in EA. The daily and monthly mean SWRF  
 945 reductions varied from  $-73.71$  to  $-5.58 \text{ W}\cdot\text{m}^{-2}$  and  $-82.20$  to  $-0.45 \text{ W}\cdot\text{m}^{-2}$ , respectively, with relative  
 946 large perturbations in NCP. At the seasonal and yearly scales, the SWRF changes ranged from  $-$   
 947  $22.54$  to  $-3.30 \text{ W}\cdot\text{m}^{-2}$  and  $-30.00$  to  $-2.90 \text{ W}\cdot\text{m}^{-2}$  with mean value of  $-11.28$  and  $-11.82 \text{ W}\cdot\text{m}^{-2}$ ,  
 948 respectively, with EA as the most researched area.

949 To identify the differences of aerosol-induced SWRF variations between high- (Asia) and low-  
 950 polluted regions (Europe and North America), their inter-regional comparisons are depicted in Fig.  
 951 10b. This figure does not include information about temporal resolutions of data reporting and  
 952 durations of model simulations with ARI or/and ACI, but intends to delineate the range of SWRF  
 953 changes due to aerosol feedbacks. The SWRF variations fluctuated from  $-233.00$  to  $-0.45 \text{ W}\cdot\text{m}^{-2}$ ,  $-$   
 954  $100.00$  to  $-1.00 \text{ W}\cdot\text{m}^{-2}$ , and  $-600.00$  to  $-1.00 \text{ W}\cdot\text{m}^{-2}$  in Asia, Europe, and North America, respectively.  
 955 It should be pointed out that the two extreme values were caused by dust ( $-233.00 \text{ W}\cdot\text{m}^{-2}$ ) in Asia  
 956 and wildfire ( $-600.00 \text{ W}\cdot\text{m}^{-2}$ ) in North America. Overall, the median value of SWRF reductions due  
 957 to ARI or/and ACI in Asia ( $-15.92 \text{ W}\cdot\text{m}^{-2}$ ) was larger than those in North America ( $-10.50 \text{ W}\cdot\text{m}^{-2}$ )  
 958 and Europe ( $-7.00 \text{ W}\cdot\text{m}^{-2}$ ).

959



961  
 962 Figure 10. Responses of SWRF to aerosol feedbacks in different areas/periods in Asia (a) and the  
 963 inter-regional comparisons of SWRF variations among Asia, Europe and North America (b).  
 964

### 965 6.1.2 Temperature, wind speed, humidity and PBLH

966 The impact of aerosols on radiation can influence energy balance, which eventually alter other  
 967 meteorological variables. The summary of aerosol-induced variations of T2, WS10, RH2, SH2 and  
 968 PBLH in different regions of Asia as well as at different temporal scales are provided in Table 3. In  
 969 this table, the minimum and maximum values were collected from the corresponding papers and the  
 970 mean values were calculated with adding all the variations from these papers and then divided by  
 971 the number of samples.

972 Overall, aerosol effects led to decreases of T2, WS10 and PBLH with average changes of  $-$   
 973  $0.65 \text{ }^\circ\text{C}$ ,  $-0.13 \text{ m}\cdot\text{s}^{-1}$  and  $-60.70 \text{ m}$ , respectively, and increases of humidity (mean  $\Delta\text{RH2} = 2.56 \%$ )  
 974 in most regions of Asia. On average, the hourly aerosol-induced changes of surface meteorological  
 975 variables (T2, WS10 and RH2) and PBLH were the largest among the different time scales. At the  
 976 hourly time scale, the mean variations of T2, WS10, RH2 and PBLH due to ARI or/and ACI were  $-$   
 977  $1.85 \text{ }^\circ\text{C}$ ,  $-0.32 \text{ m}\cdot\text{s}^{-1}$ ,  $4.60 \%$  and  $-165.84 \text{ m}$ , respectively, and their absolute maximum values in EC,  
 978 YRD, NCP and NCP, respectively. Compared to variations at the hourly time scale, smaller daily  
 variations of T2, WS10, RH2 and PBLH were caused by aerosol effects, and their mean values were



979 -0.63 °C, -0.15 m·s<sup>-1</sup>, +2.89 % and -34.61 m, respectively. The largest daily variations of T2, WS10,  
 980 RH2 and PBLH occurred in NCP, EC, EC and SEC, respectively. For other time scales (monthly,  
 981 seasonal and yearly), the respective mean variations of T2, RH2 and PBLH induced by aerosol  
 982 effects were comparable. However, the WS10 perturbations at the monthly time scale were about  
 983 two to three times higher than those at the seasonal and yearly time scales. High variations at the  
 984 monthly, seasonal and yearly time scales were reported in NCP (T2, RH2 and PBLH), EA (T2,  
 985 WS10 and PBLH) and PRD (T2 and PBLH), respectively. In addition, comparing to T2 and PBLH,  
 986 the aerosol-induced variations of WS10 and humidity were less revealed.

987  
 988 Table 3. Summary of variations of T2, WS10, RH2, SH2 and PBLH caused by aerosol feedbacks in  
 989 different regions of Asia and at different temporal scales.

Region	Time scale	$\Delta T2$ [mean] (°C)	$\Delta WS10$ [mean] (m·s <sup>-1</sup> )	$\Delta RH2/SH2$ [mean]	$\Delta PBLH$ [mean] (m)
EC	hours	-8.00 to -0.20 [-2.68]			-300.00 to -50.00 [-175.00]
EA	hours	-3.00 to -2.00 [-2.50]			
YRD	hours	-1.40 to -1.00 [-1.15]	-0.80 to -0.10 [-0.41]		-276.00 to -29.90 [-105.42]
NCP	hours	-2.80 to -0.20 [-1.05]	-0.30 to -0.10 [-0.23]	1.00 % to 12.00 % [4.60 %]	-287.20 to -147.00 [-217.10]
	Hourly mean	-1.85	-0.32	4.60%	-165.84
NCP	days	-2.00 to -0.10 [-0.88]	-0.4 to -0.01 [-0.17]	0.51 % to 4.10 % [2.52 %]	-111.40 to -10.00 [-49.07]
EC	days	-0.94 to -0.65 [-0.79]	-0.52 to -0.37 [-0.45]	1.92 % to 9.75 % [5.84 %]	
India	days	-1.60 to 0.10 [-0.75]			
SEC	days	-1.38 to -0.18 [-0.70]	-0.07 to 0.05 [-0.023]	-0.37 % to 6.57 % [2.63 %]	-84.1 to -27.55 [-53.62]
NEA	days	-0.52	-0.08		-46.39
MRYR	days	-0.16	-0.01	0.56 %	-16.46
India	days				-6.90
	Daily mean	-0.63	-0.15	2.89 %	-34.61
India	months	-0.45			
NCP	months	-1.30 to -0.06 [-0.43]		1.30 % to 4.70 % [2.53 %]	-109.00 to -5.48 [-36.01]
NEA	months	-0.30	-0.10		-50.00
PRD	months	-0.60 to 0.13 [-0.16]			
EA	months	-0.45 to -0.03 [-0.13]			-35.70 to -13.00 [-24.35]
China	months	-0.89 to 0.60 [-0.12]			-66.60 to -2.30 [-25.67]
EC	months	-0.30 to -0.05 [-0.11]			-13.10 to -6.20 [-9.65]
	Monthly mean	-0.24	-0.10	2.53 %	-29.13
EA	seasons	-0.58 to -0.30 [-0.40]	-0.05 to -0.02 [-0.035]		-64.62 to -30.70 [-43.27]
SEA	seasons	-0.39 to -0.03 [-0.21]	-0.06 to -0.01 [-0.035]		-48.33 to -6.71 [-27.52]
	Seasonal mean	-0.31	-0.035		-34.61
PRD	years	-0.27			-45.00
TP	years	-0.24			
SEA	years	-0.21	-0.03		-27.25
EA	years		-0.03	0.13 g·kg <sup>-1</sup>	-46.47 to -45.00 [-45.74]
EC	years		-0.014	0.21 %	
	Yearly mean	-0.24	-0.025	0.21 %	-39.33

990

### 991 6.1.3 Cloud and precipitation

992 In the included publications, only a few papers focusing on the effects of aerosol feedbacks on  
 993 cloud properties (cloud fraction, LWP, ice water path (IWP), CDNC and cloud effective radius) and  
 994 precipitation characteristics (amount, spatial distribution, peak occurrence and onset time) using  
 995 two-way coupled models in Asia, as shown in Table 4. In this table, the abbreviations representing  
 996 aerosol emission sources (Dust, ARB\_BC, Anthro\_BC, and Anthro) and regions in Asia are defined  
 997 in Appendix Table B1. The plus and minus signs indicate increase and decrease, respectively.



998 The variations of cloud properties and precipitation characteristics induced by ARI or/and ACI  
 999 are rather complex and not uniform in different parts of Asia and time periods. BC from both ARB  
 1000 and anthropogenic sources reduced cloud fraction through ARI and both ARI and ACI in several  
 1001 areas in China. ARI or/and ACI induced by anthropogenic aerosols could increase or decrease cloud  
 1002 fraction and affect cloud fraction differently in various atmospheric layers and time periods.  
 1003 Considering EA and subareas in China, anthropogenic aerosols tended to increase LWP through ARI  
 1004 and ACI as well as ACI alone but decrease LWP in some areas of SC (ARI and ACI) at noon and in  
 1005 afternoon during summertime and NC (ACI) in winter. ARI and ACI induced by anthropogenic BC  
 1006 aerosols had negative effects on LWP except at daytime in CC. Dust aerosols increased both LWP  
 1007 and IWP through ACI in EA, which was reported only by one study. The increase (decrease) of  
 1008 CDNC caused by the ARI and ACI effects of anthropogenic (anthropogenic BC) aerosols in EC  
 1009 during summertime was reported. Through ACI, anthropogenic aerosols affected CDNC positively  
 1010 in EA and China. Compared to anthropogenic aerosols, dust aerosols could have much larger  
 1011 positive impacts on CDNC via ACI in springtime over EA. The ACI effects of anthropogenic  
 1012 aerosols reduced cloud effective radius over China (January) and EA (July).

1013 Among all the variables describing cloud properties and precipitation characteristics, the  
 1014 variations of precipitation amount were studied the most using two-way coupled models in Asia.  
 1015 How turning on ARI or/and ACI in coupled models can change precipitation amount is not  
 1016 unidirectional and depends on many factors, including different aerosol sources, areas, emission  
 1017 levels, atmospheric humidity, precipitation types, seasons, and time of a day. Under the high (low)  
 1018 emission levels as well as at slightly different humidity levels of  $RH > 85\%$  ( $RH < 80\%$ ) with  
 1019 increasing emissions, the ACI effects of anthropogenic aerosols increased (decreased) precipitation  
 1020 in the MRYR area of China. In PRD (SK), wintertime (summertime) precipitation was enhanced  
 1021 (enhanced and inhibited) by the ACI effects of anthropogenic aerosols but inhibited (enhanced and  
 1022 inhibited) by ARI. In locations upwind (downwind) of Beijing, rainfall amount was raised (lowered)  
 1023 by the ARI effects of anthropogenic aerosols but lowered (raised) by ACI. Both ARI and ACI  
 1024 induced by anthropogenic aerosols had positive impacts on total, convective, and stratiform rain in  
 1025 India during the summer season and the increase of convective rain was larger than those of  
 1026 stratiform. Summertime precipitation amounts could be enhanced or inhibited at various subareas  
 1027 inside simulation domains over India, China, and Korea and during day- or night-time due to ARI  
 1028 and ACI of anthropogenic aerosols. Over China, dust-induced ACI decreased (increased) springtime  
 1029 precipitation in CC (western part of NC), and over India, dust aerosols from local sources and ME  
 1030 had positive impacts on total, convective, and stratiform rain through ARI and ACI. Simulations in  
 1031 India also revealed that precipitation could be increased in some subareas but decreased in another  
 1032 and absorptive (non-absorptive) dust enhanced (inhibited) summertime precipitation via ARI and  
 1033 ACI. The ARI (ACI) effects of BC from ARB caused precipitation reduction (increase) in SEC but  
 1034 CAs emitted from ARB (ARB CAs) caused rainfall enhancement in Myanmar. During pre-  
 1035 monsoon (monsoon) season, ARI induced by anthropogenic BC could lead to +42 % (-5 to -8 %)   
 1036 variations of precipitation in NEI (SI). Considering both ARI and ACI effects, BC from ARB and  
 1037 sea salt aerosols enhanced or inhibited precipitation in different parts of India and BC from  
 1038 anthropogenic sources enhanced (inhibited) nighttime (daytime) rainfall in CC (NC and SC) at the  
 1039 rate of +1 to +4  $\text{mm}\cdot\text{day}^{-1}$  (-2 to -6  $\text{mm}\cdot\text{day}^{-1}$ ) during summer season. With respect to spatial  
 1040 variations, 6.5 % larger rainfall area in PRD was caused by ARI and ACI effects under 50 % reduced  
 1041 anthropogenic emissions. ACI induced by anthropogenic aerosols tended to delay the peak  
 1042 occurrence time and onset time of precipitation by one to nine hours in China and South Korea.

1043  
 1044 Table4. Summary of changes of cloud properties and precipitation characteristics due to aerosol  
 1045 feedbacks in Asia.

Variables	Variations (aerosol effects)	Simulation time period	Regions	References
Cloud properties	-7 % low-level cloud (ARB_BC ARI)	Apr., 2013	SEC	Huang et al., 2019
	+0.03 to +0.08 below 850 hPa and at 750 hPa (Anthro ARI & ACI), esp. at early morning and nighttime	Aug., 2008	EC	Gao and Zhang, 2018
	Max -0.06 between 750 hPa and 850 hPa (Anthro ARI & ACI), esp. in afternoon and evening	Aug., 2008	CC	Gao and Zhang, 2018
	-0.02 to -0.06 below 750 hPa (Anthro_BC ARI & ACI), esp. in afternoon	Aug., 2008	SC & NC	Gao and Zhang, 2018
	-0.04 to -0.06 between 750 hPa and 850 hPa (Anthro_BC ARI & ACI), esp. in afternoon	Aug., 2008	CC	Gao and Zhang, 2018
	-6.7 % to +3.8 % (Anthro ARI)	Jun. 6-9 & Jun. 11-14, 2015	SK	Park et al., 2018



		+22.7 % (Anthro ACI)	Jun. 6-9 & Jun. 11-14, 2015	SK	Park et al., 2018
		-0.03 % low-, -0.54 % middle- and -0.58 % high-level cloud (Anthro ACI)	2008 to 2012	PRD	Liu Z. et al., 2018
		+5 to +50 g·m <sup>-2</sup> (Anthro ARI & ACI)	Aug., 2008	EC	Gao and Zhang, 2018
		+10 to +20 g·m <sup>-2</sup> (Anthro_BC ARI & ACI) at daytime	Aug., 2008	CC	Gao and Zhang, 2018
		-5 to -40 g·m <sup>-2</sup> (Anthro ARI & ACI) at noon and in afternoon	Aug., 2008	Part of SC	Gao and Zhang, 2018
		-2 to -20 g·m <sup>-2</sup> (Anthro_BC ARI & ACI)	Aug., 2008	SC	Gao and Zhang, 2018
		-2 to -30 g·m <sup>-2</sup> (Anthro_BC ARI & ACI)	Aug., 2008	NC	Gao and Zhang, 2018
	LWP	Max+18 g·m <sup>-2</sup> (Dust ACI)	Mar.-May., 2010	EA	Wang et al., 2018
		+40 to +60 g·m <sup>-2</sup> (Anthro ACI)	Jan., 2008	SC	Gao et al., 2012
		+40 g·m <sup>-2</sup> (Anthro ACI)	Jan., 2008	CC	Gao et al., 2012
		Less than +5 g·m <sup>-2</sup> or -5 g·m <sup>-2</sup> (Anthro ACI)	Jan., 2008	NC	Gao et al., 2012
		+30 to +50 g·m <sup>-2</sup> (Anthro ACI)	Jul., 2008	EA	Gao et al., 2012
	IWP	+5 to +10 g·m <sup>-2</sup> (Dust ACI)	Mar. 17-Apr. 30, 2012	EA	Su and Fung, 2018a
		+20 to +160 cm <sup>-3</sup> (Anthro ARI & ACI)	Aug., 2008	EC	Gao and Zhang, 2018
		-5 to -60 cm <sup>-3</sup> (Anthro_BC ARI & ACI)	Aug., 2008	EC	Gao and Zhang, 2018
		Max +10500 cm <sup>-3</sup> (Dust ACI)	Mar.-May., 2010	EA	Wang et al., 2018
	CDNC	+650 cm <sup>-3</sup> (Anthro ACI)	Jan., 2008	EC	Gao et al., 2012
		+400 cm <sup>-3</sup> (Anthro ACI)	Jan., 2008	CC & SWC	Gao et al., 2012
		Less than +200 cm <sup>-3</sup> (Anthro ACI)	Jan., 2008	NC	Gao et al., 2012
		+250 to +400 cm <sup>-3</sup> (Anthro ACI)	Jul., 2008	EA	Gao et al., 2012
	Cloud effective radius	More than -4 μm (Anthro ACI)	Jan., 2008	SWC, CC & SEC	Gao et al., 2012
		More than -2 μm (Anthro ACI)	Jan., 2008	NC	Gao et al., 2012
		-3 μm (Anthro ACI)	Jul., 2008	EA	Gao et al., 2012
		Enhancement/inhibition of precip. due to high/low Anthro emissions (ACI), ACI inhibited (enhanced) precip. at RH < 80 % (> 85 %) with increasing Anthro emissions	Jun. 18-19, 2018	MRYR	Bai et al., 2020
		-4.72 mm (Anthro ARI) and +33.7 mm (Anthro ACI)	Dec. 14-16, 2013	PRD	Liu Z. et al., 2020
		+2 to +5 % (ARB CAs ARI)	Mar.-Apr., 2013	Myanmar	Singh et al., 2020
		-1.09 mm·day <sup>-1</sup> (ARB_BC ARI)	Apr., 2013	SEC	Huang et al., 2019
		+0.49 mm·day <sup>-1</sup> (ARB_BC ARI)	Apr., 2013	SEC	Huang et al., 2019
		-0 to -4 mm·day <sup>-1</sup> (Anthro ARI & ACI)	Jun.-Sep., 2010	Indus basin & eastern IGP	Kedia et al., 2019b
		+1 to +3 mm·day <sup>-1</sup> non-convective rain (Anthro ARI & ACI)	Jun.-Sep., 2010	WG of India	Kedia et al., 2019b
		+5 mm·day <sup>-1</sup> non-convective rain (Anthro ARI & ACI)	Jun.-Sep., 2010	NEI	Kedia et al., 2019b
		Increase of total rain (Dust ARI & ACI)	Jun.-Sep., 2010	NI, CI, WG, NEI & central IGP	Kedia et al., 2019b
		Decrease of total rain (Dust ARI & ACI)	Jun.-Sep., 2010	NWI & SPI	Kedia et al., 2019b
		Decrease of total rain (ARB_BC ARI & ACI)	Jun.-Sep., 2010	WG, SPI, NWI, EI & NEI	Kedia et al., 2019b
		Increase of total rain (ARB_BC ARI & ACI)	Jun.-Sep., 2010	CI, Central IGP & EPI	Kedia et al., 2019b
		Decrease of total rain (Sea salt ARI & ACI)	Jun.-Sep., 2010	EPI, WPI, CPI & SPI	Kedia et al., 2019b
		Increase of total rain (Sea salt ARI & ACI)	Jun.-Sep., 2010	NCI & central IGP	Kedia et al., 2019b
		-20 to -200mm (Anthro ARI & ACI)	Aug., 2008	SC & NC	Gao and Zhang, 2018
		+20 to +100 mm (Anthro_BC ARI & ACI)	Aug., 2008	CC	Gao and Zhang, 2018
		+1 to +4 mm·day <sup>-1</sup> nighttime precip. (ARI & ACI of Anthro or Anthro_BC)	Aug., 2008	CC	Gao and Zhang, 2018
		-2 to -6 mm·day <sup>-1</sup> daytime precip. (ARI & ACI of Anthro or Anthro_BC)	Aug., 2008	NC	Gao and Zhang, 2018
		-2 to -4 mm·day <sup>-1</sup> daytime precip. (Anthro ARI & ACI)	Aug., 2008	SC	Gao and Zhang, 2018
		-2 to -6 mm·day <sup>-1</sup> daytime precip. (Anthro_BC ARI & ACI)	Aug., 2008	SC	Gao and Zhang, 2018



	-54.6 to +24.1 mm (Anthro ARI)	Jun. 6-9, 2015	SK	Park et al., 2018
	-23.8 to +24.0 mm (Anthro ACI)	Jun. 6-9, 2015	SK	Park et al., 2018
	-63.2 to +27.1 mm (Anthro ARI & ACI)	Jun. 6-9, 2015	SK	Park et al., 2018
	Min -7.0 mm (Anthro ARI)	Jun. 11-14, 2015	SK	Park et al., 2018
	Min -36.6 mm (Anthro ACI)	Jun. 11-14, 2015	SK	Park et al., 2018
	+42 % (Anthro_BC ARI) during pre-monsoon season	Mar.-May., 2010	NEI	Soni et al., 2018
	-5 to -8 % (Anthro_BC ARI) during monsoon season	Jun.-Sep., 2010	SI	Soni et al., 2018
	+1 mm·day <sup>-1</sup> precip. (Dust ACI)	Mar. 17-Apr. 30, 2012	Western part of NC	Su and Fung, 2018b
	-1 mm·day <sup>-1</sup> precip. (Dust ACI)	Mar. 17-Apr. 30, 2012	CC	Su and Fung, 2018b
	+0.95 mm·day <sup>-1</sup> precip. (absorptive Dust ARI & ACI)	Jun.-Aug., 2008	India	Jin et al., 2016a
	-0.4 mm·day <sup>-1</sup> precip. (non-absorptive Dust ARI & ACI)	Jun.-Aug., 2008	India	Jin et al., 2016a
	+0.44 mm·day <sup>-1</sup> total precip. (Dust ARI & ACI over whole study domain)	Jun.-Aug., 2008	India	Jin et al., 2016b
	+0.34 mm·day <sup>-1</sup> total precip. (Dust ARI & ACI from ME)	Jun.-Aug., 2008	India	Jin et al., 2016b
	+0.31 mm·day <sup>-1</sup> total precip. (Anthro ARI & ACI over whole study domain)	Jun.-Aug., 2008	India	Jin et al., 2016b
	+0.32 mm·day <sup>-1</sup> convective precip. (Dust ARI & ACI over whole study domain)	Jun.-Aug., 2008	India	Jin et al., 2016b
	+0.24 mm·day <sup>-1</sup> convective precip. (ARI & ACI of Dust from ME)	Jun.-Aug., 2008	India	Jin et al., 2016b
	+0.20 mm·day <sup>-1</sup> convective precip. (Anthro ARI & ACI over whole study domain)	Jun.-Aug., 2008	India	Jin et al., 2016b
	+0.12 mm·day <sup>-1</sup> stratiform precip. (Dust ARI & ACI over whole study domain)	Jun.-Aug., 2008	India	Jin et al., 2016b
	+0.10 mm·day <sup>-1</sup> stratiform precip. (ARI & ACI of Dust from ME)	Jun.-Aug., 2008	India	Jin et al., 2016b
	+0.11 mm·day <sup>-1</sup> stratiform precip. (Anthro ARI & ACI over whole study domain)	Jun.-Aug., 2008	India	Jin et al., 2016b
	-48.29 %/+24.87 % precip. in downwind/upwind regions (Anthro ARI)	Jun. 27-28, 2008	Beijing	Zhong et al. 2015
	+33.26 % /-4.64 % precip. in downwind/upwind regions (Anthro ACI)	Jun. 27-28, 2008	Beijing	Zhong et al. 2015
	+0.44 mm·day <sup>-1</sup> precip. (Dust ARI & ACI)	Jun. 1-Aug. 31, 2008	India	Jin et al., 2015
Spatial variation	+6.5 % precip. area (ARI & ACI) with 50% Anthro emissions	Jun. 9-12, 2017	YRD	Liu C. et al., 2019
	1 to 2h delay (Anthro ACI)	Jun. 18-19, 2018	MRYR	Bai et al., 2020
Peak occurrence time	1h delay (ARI & ACI) with 50% Anthro emissions	Jun. 9-12, 2017	YRD	Liu C. et al., 2019
	9h delay (Anthro ACI)	Jun. 7, 2015	Gosan, SK	Park et al., 2018
	4h delay (Anthro ACI)	Jun. 7, 2015	Jinju, SK	Park et al., 2018
Onset time	9h delay (Anthro ACI)	Jun. 7, 2015	Gosan, SK	Park et al., 2018
	2h delay (Anthro ACI)	Jun. 7, 2015	Jinju, SK	Park et al., 2018

1046

1047

## 6.2 Impacts of aerosol feedbacks on air quality

1048

1049

1050

1051

1052

1053

1054

1055

1056

1057

1058

1059

1060

Aerosol effects not only gave rise to changes in meteorological variables but also air quality. Table 5 (the minimum, maximum and mean values were defined in the same way as in Table 3) summarizes the variations of atmospheric pollutant concentrations induced by aerosol effects in different regions of Asia and at different time scales. In Asia, most modeling studies with coupled models targeted the impacts of aerosol feedbacks on surface PM<sub>2.5</sub> and O<sub>3</sub> concentrations, with only few focusing on other gaseous pollutants.

Simulation results showed that turning on aerosol feedbacks in coupled models generally made PM<sub>2.5</sub> concentrations increased in different regions of Asia at various time scales, which stemmed from decrease (increase) of shortwave radiation, T<sub>2</sub>, and WS10 (RH<sub>2</sub>) as well as PBLH. Some studies did show negative impacts of aerosol effects on hourly, daily, and seasonal PM<sub>2.5</sub> at some areas that could be attributed to ACI effects, changes in transport and dispersion patterns, reductions in humidity levels and secondary aerosol formations (Zhang B. et al., 2015; Zhan et al., 2017; Yang et al., 2017; Wang K. et al., 2018). Similar to the perturbations of surface meteorological variables



1061 due to aerosol effects, the hourly  $PM_{2.5}$  variations and the range were the largest compared to those  
 1062 at other time scales. The largest  $PM_{2.5}$  increases were reported in NCP, SEC, EA, SEA and PRD at  
 1063 the hourly, daily, monthly, seasonal and yearly time scales with average values of  $23.48 \mu\text{g}\cdot\text{m}^{-3}$ ,  
 1064  $14.73 \mu\text{g}\cdot\text{m}^{-3}$ ,  $16.50 \mu\text{g}\cdot\text{m}^{-3}$ ,  $1.12 \mu\text{g}\cdot\text{m}^{-3}$  and  $2.90 \mu\text{g}\cdot\text{m}^{-3}$ , respectively.

1065 In addition to  $PM_{2.5}$ , gaseous pollutants ( $O_3$ ,  $NO_2$ ,  $SO_2$ ,  $CO$  and  $NH_3$ ) are impacted by ARI  
 1066 or/and ACI effects as well. As shown in Table 5, general reductions of ozone concentrations were  
 1067 reported in Asia across all the modeling domains and time scales based on coupled models'  
 1068 simulations. However, the influences of aerosol feedbacks on atmospheric dynamics and stability,  
 1069 and photochemistry (photolysis rate and ozone formation regimes) could make ozone concentrations  
 1070 increase somewhat in summer months or during wet season (Jung et al., 2019; Nguyen et al., 2019b;  
 1071 Xing et al., 2017). The largest hourly, daily, monthly, seasonal, and annual variations of  $O_3$  occurred  
 1072 in YRD ( $-32.80 \mu\text{g}\cdot\text{m}^{-3}$ ), EC ( $-5.97 \mu\text{g}\cdot\text{m}^{-3}$ ), China ( $-23.90 \mu\text{g}\cdot\text{m}^{-3}$ ), EA ( $-4.48 \mu\text{g}\cdot\text{m}^{-3}$ ) and EA ( $-$   
 1073  $2.76 \mu\text{g}\cdot\text{m}^{-3}$ ), respectively. Along with reduced  $O_3$  due to ARI or/and ACI,  $NO_2$  concentrations were  
 1074 enhanced with average changes of  $+12.30 \mu\text{g}\cdot\text{m}^{-3}$  (YRD) at the hourly scale and  $+0.66 \mu\text{g}\cdot\text{m}^{-3}$  (EA)  
 1075 at both the seasonal and yearly scales, which could be attributed to slower photochemical reactions,  
 1076 strengthened atmospheric stability and  $O_3$  titration (Nguyen et al., 2019b). Regarding other gaseous  
 1077 pollutants, limited studies pointed out daily and annual  $SO_2$  concentrations increased in NEA and  
 1078 EA due to lower PBLH induced by the ARI effects of anthropogenic aerosols (Jung et al., 2019;  
 1079 Nguyen et al., 2019b). The seasonal  $SO_2$  reduction (increase) was rather large (small), which related  
 1080 to higher (lower) PBLH induced by the ACI (ARI) effects of dust (anthropogenic) aerosols in the  
 1081 NCP area (whole domain) of EA (Wang et al., 2018; Nguyen et al., 2019b). There was only one  
 1082 study depicted increased  $CO$  ( $NH_3$ ) concentration in EC (NEA) due to both the ARI and ACI (ARI)  
 1083 effects of anthropogenic aerosols but these results may not be conclusive.

1084  
 1085 Table 5. Compilation of aerosol-induced variations of  $PM_{2.5}$  and gaseous pollutants in different  
 1086 regions of Asia and at different temporal scales.

Region	Time scale	$\Delta PM_{2.5}$ [mean] ( $\mu\text{g}\cdot\text{m}^{-3}$ )	$\Delta O_3$ [mean] ( $\mu\text{g}\cdot\text{m}^{-3}$ )	$\Delta NO_2$ [mean] ( $\mu\text{g}\cdot\text{m}^{-3}$ )	$\Delta SO_2$ [mean] ( $\mu\text{g}\cdot\text{m}^{-3}$ )	$\Delta CO$ [mean] ( $\mu\text{g}\cdot\text{m}^{-3}$ )	$\Delta NH_3$ [mean] ( $\mu\text{g}\cdot\text{m}^{-3}$ )
NCP	hours	-3.50 to 90.00 [23.48]					
YRD	hours	7.00 to 30.50 [15.17]	-32.80 to -0.20 [-11.25]	12.30			
	Hourly mean	19.32	-11.25	12.30			
SEC	days	-1.91 to 32.49 [14.73]					
NCP	days	-5.00 to 56.00 [14.51]					
EC	days	2.87 to 18.60 [10.74]	-5.97 to -1.45 [-3.71]				
NEA	days	1.75			0.97		0.11
	Daily mean	10.43	-3.71		0.97		0.11
India	months	3.00 to 30.00 [16.50]					
EC	months	1.00 to 40.00 [16.33]	-2.40 to -1.00 [-1.70]			4.00 to 6.00 [5.00]	
China	months	1.60 to 33.20 [14.38]	-23.90 to 4.92 [-3.42]				
EA	months	3.60 to 10.20 [5.79]					
	Monthly mean	13.25	-2.56			5.00	
SEA	seasons	0.15 to 2.09 [1.12]	-1.92 to 0.26 [-0.83]				
EA	seasons	-8.00 to 2.70 [-0.14]	-4.48 to -1.00 [-2.99]	0.43 to 0.88 [0.66]	-4.29 to 0.72 [-0.42]		
	Seasonal mean	0.49	-1.91	0.66	-0.42		
PRD	years	2.90					
EA	years	1.82	-2.76	0.66	0.54		
NCP	years	0.10 to 5.10 [1.70]					
SEA	years	1.21	-0.80				
	Yearly mean	1.91	-1.78	0.66	0.54		

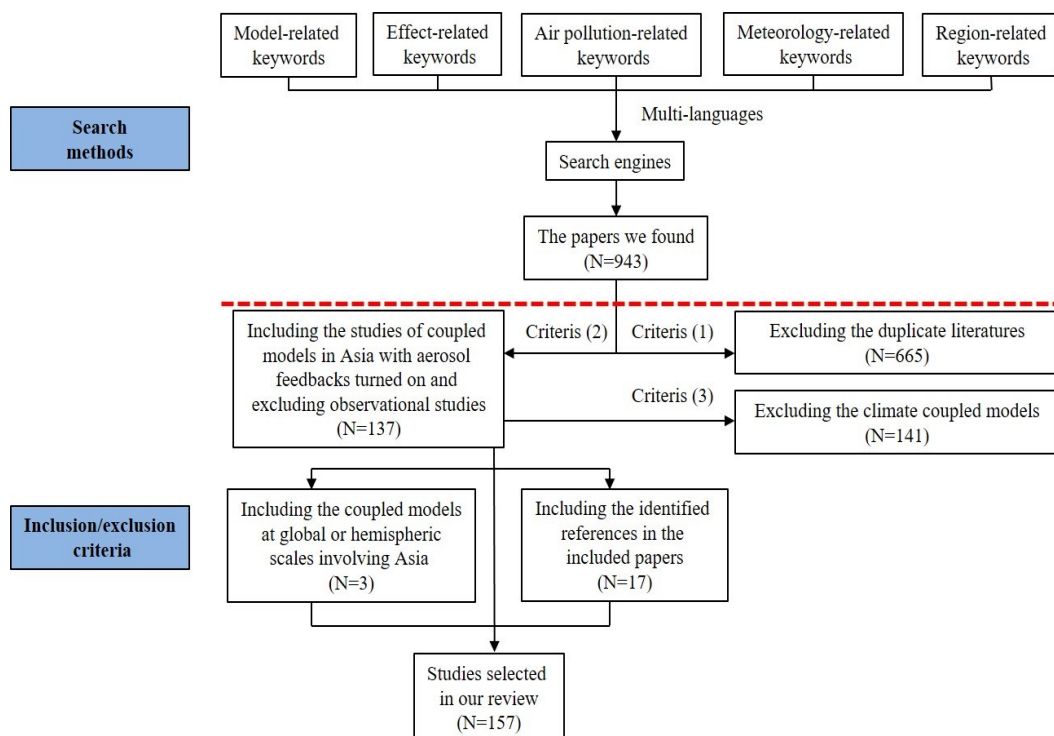
1087





1124 many pressing issues facing the modeling community. The latest advances in the measurements and  
 1125 research of cloud properties, precipitation characteristics, and physiochemical characteristics of  
 1126 aerosols (e.g., origin, morphology, size distribution, optical property, hygroscopicity, mixing state,  
 1127 and chemical composition) that play pivotal roles in CCN or IN activation mechanisms can guide  
 1128 the improvements and enhancements in two-way coupled models, especially to abate the  
 1129 uncertainties in simulated ACI effects. At the same time, computational costs should be considered  
 1130 with any new/enhanced parameterization schemes concerning ACI related processes, since running  
 1131 two-way coupled models is more expensive than running models without turning on feedbacks.  
 1132 Further inter-comparisons of multiple coupled models need to be conducted in Asia and other  
 1133 regions to comprehensively assess the model performances with/without aerosol feedbacks and how  
 1134 ARI or/and ACI affect meteorology and air quality. Besides the four two-way coupled models  
 1135 mentioned in this paper, more models capable of simulating aerosol feedbacks (such as WRF-  
 1136 CHIMERE and WRF-GEOS-Chem) have become available and should be included in future inter-  
 1137 comparisons. Future assessments of the ARI or/and ACI effects should pay extra attention to their  
 1138 impacts on dry and wet depositions simulated by two-way coupled models. So far, the majority of  
 1139 two-way coupled models' simulations and evaluations focuses on episodic air pollution events  
 1140 occurring in certain areas, therefore their long-term applications and evaluations are necessary and  
 1141 their real-time forecasting capabilities should be explored as well.

1142 **Appendix A**



1144  
 1145 **Figure A1** Flowchart of literature search and identification  
 1146

1147 **Appendix B**

1148 **Table B1** Lists of abbreviations and acronyms

Acronym	Description
ACI	Aerosol-cloud interactions
AOD	Aerosol optical depth
ARB	Agriculture residue burning



---

ARB_BC	BC emitted from agriculture residue burning
ARB_CAs	Carbonaceous aerosols emitted from agriculture residue burning
ARI	Aerosol-radiation interactions
ATM	In the atmosphere
BC	Black carbon
BOT	At the surface
BrC	Brown carbon
CA	Central Asia
CAMx	Comprehensive Air quality Model with extensions
CAs	Carbonaceous aerosols
CCN	Cloud condensation nuclei
CDNC	Cloud droplet number concentration
CC	Central China
CHIMERE	A multi-scale chemistry-transport model for atmospheric composition analysis and forecast
CMAQ	Community Multiscale Air Quality model
CO	Carbon monoxide
DRF	Direct radiative forcing
EA	East Asia
EC	East China
GRAPES-CUACE	Global-regional assimilation and prediction system coupled with the Chinese Unified Atmospheric Chemistry Environment forecasting system
H <sub>2</sub> O <sub>2</sub>	Hydrogen peroxide
HNO <sub>3</sub>	Nitric acid
HO <sub>2</sub>	Hydroperoxyl
·OH	Hydroxyl radical
IN	Ice nuclei
INPs	Ice nucleation parameterizations
IPCC	Intergovernmental Panel on Climate Change
IPR	Ice particle radius
IWP	Ice water path
LWP	Liquid water path
LWRF	Longwave radiative forcing
MB	Mean bias
ME	Middle East
MICS-Asia	Model Inter-Comparison Study for Asia
MRYR	middle reaches of the Yangtze River
N <sub>2</sub> O <sub>5</sub>	Nitrogen pentoxide
NAQPMS	Nested Air Quality Prediction Modeling System
NCP	North China Plain
NEA	Northeast Asia
NO <sub>2</sub>	Nitrogen dioxide
NO <sub>3</sub>	Nitrate
NC	North China
NU-WRF	National aeronautics and space administration Unified Weather Research and Forecasting model
NWC	Northwest China
O <sub>3</sub>	Ozone
OA	Organic aerosols
OC	Organic carbon
PBL	Planetary boundary layer
PBLH	Planetary boundary layer height
PM <sub>2.5</sub>	Fine particulate matter
PRD	Pearl River Delta
PSI	Papers with statistical indices
R	Correlation coefficient
RH2	Relative humidity at 2 meters above the surface
RMSE	Root mean square error
RRTM	The Rapid Radiative Transfer Model
RRTMG	The Rapid Radiative Transfer Model for General Circulation Models
SEA	Southeast Asia
SEC	Southeast China
SH2	Specific humidity at 2 meters above the surface
SI	Statistical indices
SO <sub>2</sub>	Sulfur dioxide
SO <sub>4</sub> <sup>2-</sup>	Sulfate
SC	South China
SWC	Southwest China
SWRF	Shortwave radiative forcing
T2	Air temperature at 2 meters above the surface
TOA	At the top of atmosphere
TP	Tibetan Plateau
WA	West Asia
WRF	Weather Research and Forecasting model
WRF-Chem	Weather Research and Forecasting model coupled with Chemistry
WRF-CHIMERE	Weather Research and Forecasting model coupled with a multi-scale Chemistry-Transport Model (CTM) for air quality forecasting and simulation
WRF-CMAQ	Weather Research and Forecasting model coupled with Community Multiscale Air Quality model
WRF-NAQPMS	Weather Research and Forecasting model coupled with the Nested Air Quality Prediction Modeling System
WS10	Wind speed at 10 meters above the surface
YRD	Yangtze River Delta

---



1151 Table B2 The compiled number of publications (NP) and number of samples (NS) for papers that  
 1152 providing the SI of meteorological variables.

No.*	Meteorological variables															
	T2				RH2				SH2				WS10			
	NS				NS				NS				NS			
	NP	R	MB	RMSE	NP	R	MB	RMSE	NP	R	MB	RMSE	NP	R	MB	RMSE
4	1	5	5 (4†, 1)	5	1	5	5 (1†, 4)	5								
5																
7	1	4	4 (3†, 1)													
13	1		1 (1)													
15	1	1										1	2			
16	1	1														
20	1	2	2 (1†, 1)	2	1	2	2 (1†, 1)	2				1	1	1 (1†)		1
21	1	0	2 (2)	2								1		2 (1†, 1)		2
22	1	1	1 (1)	1	1	1	1 (1†)	1				1	1	1 (1)		1
23	1	1	1 (1)				1 (1)					1	1	1 (1)		
24	1	1	1 (1)				1 (1)					1	1	1 (1)		
25	1	1	1 (1)				1 (1)					1	1	1 (1)		
28	1		1 (1)	1	1		1 (1)	1				1		1 (1)		1
29	1	9	9 (6†, 3)	9		8		9				1	9	9 (9†)		9
33	1	6	6 (4†, 2)	6								1	2	2 (2)		2
34	1	2	2 (2)	2								1	1	1 (1)		1
35	1	2		2	1	1		1				1	1	1 (1)		1
38	1		4 (4)	4	1		4 (3†, 1)	4								
50	1		8 (8)	8												
56	1	1	1 (1)	1	1	1	1 (1)	1				1	1	1 (1)		1
57	1	1										1	1			
61	1	4	4 (4)	4	1	4	4 (4†)	4				1	4	4 (4†)		4
62	1		5 (5)	5								1		5 (4†, 1)		5
63	1	1														
71	1	1														
72	1	4	4 (3†, 1)	4	1	4	4 (3†, 1)	4								
73	1	1	1 (1)	1					1	1	1 (1†)	1	1	1 (1†)		1
75	1	4	4 (4†)									0	1	4 (1†, 3)		4
77	1	4	4 (2†, 2)						1	4	3 (3†)	4	1	4 (4†)		4
79	1		8 (6†, 2)	8												
80	1	8	8 (8†)	8	1	8	8 (8)	8								
85	1		4 (1†, 3)	4	1		4 (2†, 2)	4								
87	1		3 (2†, 1)	3												
88	1	3	3 (1†, 2)	3	1	3	3 (2†, 1)	3								
90	1	4	4 (1†, 3)						1	4	4 (4†)					
91	1	1	1 (1)	1					1	1	1 (1)	1	1	1 (1)		1
94	1	6	6 (4†, 2)	6	1	6	6 (2†, 4)	6								
96	1	16	16 (11†, 5)													
97	1	1	1 (1)	1	1	1	1 (1†)	1								
106	1	6	6 (6)						1	6	5 (2†, 3)					
109	1	2	2 (2)	2	1	3	3 (3†)	3								
112	1		2 (2)	2					1		2 (2)	2	1	2 (2)		2
116	1	2	2 (1†, 1)	0	1	2	2 (1†, 1)									
121	1	1	1 (1)	1												
122	1		2 (2)	2	1		2 (2†)	2								
125	1	4	4 (4)	4	1	4	4 (4†)	4								
126	1	4	4 (4)	4												
127	1		2 (2)	2												
128	1	8	8 (8)	8												
129	1	1	1 (1)	1	1	1	1 (1†)	1								
133	1		1 (1)	0	1		4 (4†)									
143	1	4		4	1	4										
147	1	2		2	1	2		2								
151	1	7	7 (7)	7					1	7	7 (3†, 4)	7	1	7 (7†)		7
Total	53	137	167 (67†, 100)	130	30	68	70 (42†, 28)	73	9	35	35 (21†, 14)	27	40	111	126 (104†, 22)	97

1153 Note that the No.\* is consistent with the No. in Table 1, and † and ‡ mark over- and underestimations of variables, respectively, along with  
 1154 their number of samples.

1155

1156 Table B3 The compiled number of publications (NP) and number of samples (NS) for papers that  
 1157 providing the SI of air quality variables.

No.*	Air quality variables							
	PM <sub>2.5</sub>				O <sub>3</sub>			
	NS				NS			
	NP	R	MB	RMSE	NP	R	MB	RMSE
4	1	5	5 (5)	5				
5	1		1 (1)	1				
11	1	60						
15	1	1						
21	1		2 (1†, 1)					
22	1	1	1 (1)	1				
23	1	1	1 (1)	1	1	1 (1)		
24	1	1	1 (1)	1				
25	1	1	1 (1)	1	1	1 (1)		
29	1	9	9 (6†, 3)	9				
33	1	4	4 (4)	4	1	4	4 (3†, 1)	4
34	1	2	2 (1†, 1)	2				
35	1				1	1		1
50	1		4 (1†, 3)	4				
56	1	1	1 (1)	1				
57	1	1						
59	1	6	6 (6)	6	1	6	6 (6)	6
61	1	12	12 (12†)	12				
67	1	10	2 (2)	10				
71	1	1						
73	1	2	2 (1†, 1)		1	4	4 (4)	
77	1	4						
85	1	3	3 (3)					
86	1	4	4 (2†, 2)	4				



88	1	3	3 (1↑, 2↓)	3					
90	1	8	8 (2↑, 6↓)		1	14	14 (14↑)		
91	1	4	4 (1↑, 3↓)	4	1	6	6 (4↑, 2↓)	6	
94	1	4	4 (3↑, 1↓)	4					
97	1	1	1 (1↓)	1					
100	1	1			1	1			
106	1	6	6 (2↑, 4↓)		1	8	8 (4↑, 4↓)		
112	1				1				
121					1				5
122	1	4	4 (1↑, 3↓)						
125	1	4	4 (2↑, 2↓)	4	1	4	4 (4↑)	4	
126	1	4	4 (2↑, 2↓)	4	1	4	4 (4↑)	4	
127	1		1 (1↑)	1					
128	1	8	8 (3↑, 5↓)	8					
129	1	3	3 (2↑, 1↓)	3	1	2	2 (1↑, 1↓)	2	
133					1	4	4 (3↑, 1↓)	4	
136	1	5	5 (5↓)						
146	1	1			1	20		20	
147	1	2		2					
149	1	6		6					
150					1	21		21	
151	1	12	6 (6↑)	6	1	24	12 (7↑, 5↓)	12	
Total	42	205	122 (55↑, 67↓)	105	21	125	72 (55↑, 17↓)	90	

1158 Note that the No.\* is consistent with the No. in Table 1, and ↑ and ↓ mark over- and underestimations of variables, respectively, along with  
 1159 their number of samples.

1160  
 1161  
 1162  
 1163  
 1164

1165 Table B4 The compiled number of publications (NP) and number of samples (NS) for papers that  
 1166 simultaneously providing the SI of meteorological variables simulated by coupled models with and  
 1167 without ARI turned on.

No.*	Meteorological variables															
	T2			RH2			SH2			WS10						
	NP	NS		NP	NS		NP	NS		NP	NS					
	R	MB	RMSE		R	MB	RMSE		R	MB	RMSE		R	MB	RMSE	
32	1	3	3 (2↑, 1↓)	3												
78	1		4 (3↑, 1↓)	4												
124	1	2	2 (2↓)	2	1	2	2 (2↑)	2				1	2	2 (2↓)	2	
125	1	2	2 (2↓)	2					1	2	2 (1↑, 1↓)	2	1	2	2 (2↑)	2
126	1		1 (1↓)	1								1		1 (1↑)	1	
127	1	4	4 (4↓)	4					1	4	4 (3↑, 1↓)	4	1	4	4 (4↑)	4
146	1	1		1	1	1		1				1	1		1	
Total	7	12	16 (5↑, 11↓)	17	2	3	2 (2↑)	3	2	6	6 (4↑, 2↓)	6	5	9	9 (7↑, 2↓)	10

1168 Note that the No.\* is consistent with the No. in Table 1, and ↑ and ↓ mark over- and underestimations of variables, respectively, along with  
 1169 their number of samples.

1170  
 1171  
 1172  
 1173

Table B5 The compiled number of publications (NP) and number of samples (NS) for papers that  
 simultaneously providing the SI of air quality variables simulated by coupled models with and without  
 ARI turned on.

No.*	Air quality variables							
	PM <sub>2.5</sub>				O <sub>3</sub>			
	NP	NS			NP	NS		
	R	MB	RMSE		R	MB	RMSE	
49	1		2 (1↑, 1↓)	2	1	10		10
60	1	4	4 (4↑)	4				
124	1	2	2 (1↑, 1↓)	2	1	2	2 (2↑)	2
125	1	2	2 (1↑, 1↓)	2	1	2	2 (2↑)	2
127	1	4	4 (2↑, 2↓)	4				
146	1	1		1				
Total	5	13	14 (9↑, 5↓)	15	3	14	4 (4↑)	14

1174 Note that the No.\* is consistent with the No. in Table 1, and ↑ and ↓ mark over- and underestimations of variables, respectively, along with  
 1175 their number of samples.

1176  
 1177  
 1178

#### Data availability

The related dataset can be downloaded from <https://doi.org/10.5281/zenodo.5571076> (Gao et al., 2021), and this dataset includes basic information (Table C1.xlsx), performance metrics (Table C2.xlsx), and quantitative effects of aerosol feedbacks on meteorological and air quality variables (Table C3.xlsx) extracted from collected studies of applications of two-way coupled meteorology



1182 and air quality models in Asia.

1183

#### 1184 **Author contribution**

1185 Chao Gao, Aijun Xiu, Xuelei Zhang and Qingqing Tong carried out the data collection, related  
1186 analysis, figure plotting, and manuscript writing; Hongmei Zhao, Shichun Zhang, Guangyi Yang  
1187 and Mengduo Zhang involved with the original research plan and made suggestions to the  
1188 manuscript writing.

1189

#### 1190 **Competing interest**

1191 The authors declare that they have no conflict of interest.

1192

#### 1193 **Acknowledgement**

1194 This study was financially sponsored by National Key Research and Development Program of  
1195 China (No. 2017YFC0212304) and National Natural Science Foundation of China (No. 41571063  
1196 and No. 41771071).

#### 1197 **Reference**

- 1198 Albrecht, B.A., 1989. Aerosols, cloud microphysics, and fractional cloudiness. *Science*. 245, 1227-  
1199 1230. <https://doi.org/10.1126/science.245.4923.1227>.
- 1200 An, Z., Huang, R.-J., Zhang, R., Tie, X., Li, G., Cao, J., Zhou, W., Shi, Z., Han, Y., Gu, Z., 2019.  
1201 Severe haze in northern China: A synergy of anthropogenic emissions and atmospheric  
1202 processes. *Proc. Natl. Acad. Sci.* 116, 8657-8666. <https://doi.org/10.1073/pnas.1900125116>.
- 1203 Andreae, M.O., Rosenfeld, D., 2008. Aerosol-cloud-precipitation interactions. Part 1. The nature  
1204 and sources of cloud-active aerosols. *Earth-Science Rev.* 89, 13-41.  
1205 <https://doi.org/10.1016/j.earscirev.2008.03.001>.
- 1206 Appel, K.W., Napelenok, S.L., Foley, K.M., Pye, H.O.T., Hogrefe, C., Luecken, D.J., Bash, J.O.,  
1207 Roselle, S.J., Pleim, J.E., Foroutan, H., Hutzell, W.T., Pouliot, G.A., Sarwar, G., Fahey, K.M.,  
1208 Gantt, B., Gilliam, R.C., Heath, N.K., Kang, D., Mathur, R., Schwede, D.B., Spero, T.L., Wong,  
1209 D.C., Young, J.O., 2017. Description and evaluation of the Community Multiscale Air Quality  
1210 (CMAQ) modeling system version 5.1. *Geosci. Model Dev.* 10, 1703-1732.  
1211 <https://doi.org/10.5194/gmd-10-1703-2017>.
- 1212 Archer-Nicholls, S., Lowe, D., Lacey, F., Kumar, R., Xiao, Q., Liu, Y., Carter, E., Baumgartner, J.,  
1213 Wiedinmyer, C., 2019. Radiative Effects of Residential Sector Emissions in China: Sensitivity  
1214 to Uncertainty in Black Carbon Emissions. *J. Geophys. Res. Atmos.* 124, 5029-5044.  
1215 <https://doi.org/10.1029/2018JD030120>.
- 1216 Ashrafi, K., Motlagh, M.S., Neyestani, S.E., 2017. Dust storms modeling and their impacts on air  
1217 quality and radiation budget over Iran using WRF-Chem. *Air Qual. Atmos. Heal.* 10, 1059-  
1218 1076. <https://doi.org/10.1007/s11869-017-0494-8>.
- 1219 Bai, Y., Qi, H., Zhao, T., Zhou, Y., Liu, L., Xiong, J., Zhou, Z., Cui, C., 2020. Simulation of the  
1220 responses of rainstorm in the Yangtze River Middle Reaches to changes in anthropogenic  
1221 aerosol emissions. *Atmos. Environ.* 220, 117081.  
1222 <https://doi.org/10.1016/j.atmosenv.2019.117081>.
- 1223 Baklanov, A., Schlünzen, K., Suppan, P., Baldasano, J., Brunner, D., Aksoyoglu, S., Carmichael, G.,  
1224 Douros, J., Flemming, J., Forkel, R., 2014. Online coupled regional meteorology chemistry  
1225 models in Europe: current status and prospects. *Atmos. Chem. Phys.* 14, 317-398.  
1226 <https://doi.org/10.5194/acp-14-317-2014>.
- 1227 Baró, R., Jiménez-Guerrero, P., Balzarini, A., Curci, G., Forkel, R., Grell, G., Hirtl, M., Honzak, L.,  
1228 Langer, M., Pérez, J.L., 2015. Sensitivity analysis of the microphysics scheme in WRF-Chem  
1229 contributions to AQMEII phase 2. *Atmos. Environ.* 115, 620-629.  
1230 <https://doi.org/10.1016/j.atmosenv.2015.01.047>.
- 1231 Bauer, P., Thorpe, A., Brunet, G., 2015. The quiet revolution of numerical weather prediction.  
1232 *Nature* 525, 47-55. <https://doi.org/10.1038/nature14956>.
- 1233 Bei, N., Wu, J., Elser, M., Tian, F., Cao, J., El-Haddad, I., Li, X., Huang, R., Li, Z., Long, X., 2017.



- 1234 Impacts of meteorological uncertainties on the haze formation in Beijing-Tianjin-Hebei (BTH)  
1235 during wintertime: a case study. *Atmos. Chem. Phys.* 17, 14579. <https://doi.org/10.5194/acp->  
1236 17-14579-2017.
- 1237 Beig, G., Chate, D.M., Ghude, S.D., Mahajan, A.S., Srinivas, R., Ali, K., Sahu, S.K., Parkhi, N.,  
1238 Surendran, D., Trimbake, H.R., 2013. Quantifying the effect of air quality control measures  
1239 during the 2010 Commonwealth Games at Delhi, India. *Atmos. Environ.* 80, 455-463.  
1240 <https://doi.org/10.1016/j.atmosenv.2013.08.012>.
- 1241 Bellouin, N., Jones, A., Haywood, J., Christopher, S.A., 2008. Updated estimate of aerosol direct  
1242 radiative forcing from satellite observations and comparison against the Hadley Centre climate  
1243 model. *J. Geophys. Res. Atmos.* 113. <https://doi.org/10.1029/2007JD009385>.
- 1244 Benas, N., Meirink, J.F., Karlsson, K.-G., Stengel, M., Stammes, P., 2020. Satellite observations of  
1245 aerosols and clouds over southern China from 2006 to 2015: analysis of changes and possible  
1246 interaction mechanisms. *Atmos. Chem. Phys.* 20, 457-474. <https://doi.org/10.5194/acp-20->  
1247 457-2020.
- 1248 Bennartz, R., Fan, J., Rausch, J., Leung, L.R., Heidinger, A.K., 2011. Pollution from China increases  
1249 cloud droplet number, suppresses rain over the East China Sea. *Geophys. Res. Lett.* 38.  
1250 <https://doi.org/10.1029/2011GL047235>.
- 1251 Bharali, C., Nair, V.S., Chutia, L., Babu, S.S., 2019. Modeling of the effects of wintertime aerosols  
1252 on boundary layer properties over the Indo Gangetic Plain. *J. Geophys. Res. Atmos.* 124, 4141-  
1253 4157. <https://doi.org/10.1029/2018JD029758>.
- 1254 Bhattacharya, A., Chakraborty, A., Venugopal, V., 2017. Role of aerosols in modulating cloud  
1255 properties during active-break cycle of Indian summer monsoon. *Clim. Dyn.* 49, 2131-2145.  
1256 <https://doi.org/10.1007/s00382-016-3437-4>.
- 1257 Bollasina, M.A., Ming, Y., Ramaswamy, V., 2011. Anthropogenic aerosols and the weakening of the  
1258 South Asian summer monsoon. *Science* (80-. ). 334, 502-505.  
1259 <https://doi.org/10.1126/science.1204994>.
- 1260 Boucher, O., Randall, D., Artaxo, P., Bretherton, C., Feingold, G., Forster, P., Kerminen, V.M.,  
1261 Kondo, Y., Liao, H., Lohmann, U., 2013. Clouds and aerosols. *Climate change 2013: The*  
1262 *physical science basis. Contribution of working group I to the fifth assessment report of the*  
1263 *intergovernmental panel on climate change. Cambridge Univ. Press. Cambridge, United*  
1264 *Kingdom New York, NY, USA 571-657. https://doi.org/10.13140/2.1.1081.8883.*
- 1265 Bran, S.H., Jose, S., Srivastava, R., 2018. Investigation of optical and radiative properties of aerosols  
1266 during an intense dust storm: A regional climate modeling approach. *J. Atmos. Solar-Terrestrial*  
1267 *Phys.* 168, 21-31. <https://doi.org/10.1016/j.jastp.2018.01.003>.
- 1268 Briant, R., Tuccella, P., Deroubaix, A., Khvorostyanov, D., Menut, L., Mailler, S., Turquety, S., 2017.  
1269 Aerosol-radiation interaction modelling using online coupling between the WRF 3.7.1  
1270 meteorological model and the CHIMERE 2016 chemistry-transport model, through the  
1271 OASIS3-MCT coupler. *Geosci. Model Dev.* 10, 927-944. <https://doi.org/10.5194/gmd-10-927->  
1272 2017.
- 1273 Brunekreef, B., Holgate, S.T., 2002. Air pollution and health. *Lancet* 360, 1233-1242.  
1274 [https://doi.org/10.1016/S0140-6736\(02\)11274-8](https://doi.org/10.1016/S0140-6736(02)11274-8).
- 1275 Brunner, D., Savage, N., Jorba, O., Eder, B., Giordano, L., Badia, A., Balzarini, A., Baro, R.,  
1276 Bianconi, R., Chemel, C., 2015. Comparative analysis of meteorological performance of  
1277 coupled chemistry-meteorology models in the context of AQMEII phase 2. *Atmos. Environ.*  
1278 115, 470-498. <https://doi.org/10.1016/j.atmosenv.2014.12.032>.
- 1279 Byun, D., Schere, K.L., 2006. Review of the governing equations, computational algorithms, and  
1280 other components of the Models-3 Community Multiscale Air Quality (CMAQ) modeling  
1281 system. *Appl. Mech. Rev.* 59, 51-77. <https://doi.org/10.1115/1.2128636>.
- 1282 Campbell, P., Zhang, Y., Wang, K., Leung, R., Fan, J., Zheng, B., Zhang, Q., He, K., 2017.  
1283 Evaluation of a multi-scale WRF-CAM5 simulation during the 2010 East Asian Summer  
1284 Monsoon. *Atmos. Environ.* 169, 204-217. <https://doi.org/10.1016/j.atmosenv.2017.09.008>.
- 1285 Campbell, P., Zhang, Y., Yahya, K., Wang, K., Hogrefe, C., Pouliot, G., Knote, C., Hodzic, A., San  
1286 Jose, R., Perez, J.L., 2015. A multi-model assessment for the 2006 and 2010 simulations under  
1287 the Air Quality Model Evaluation International Initiative (AQMEII) phase 2 over North  
1288 America: Part I. Indicators of the sensitivity of O<sub>3</sub> and PM<sub>2.5</sub> formation regimes. *Atmos.*  
1289 *Environ.* 115, 569-586. <https://doi.org/10.1016/j.atmosenv.2014.12.026>.
- 1290 Casazza, M., Lega, M., Liu, G., Ulgiati, S., Endreny, T.A., 2018. Aerosol pollution, including eroded



- 1291 soils, intensifies cloud growth, precipitation, and soil erosion: A review. *J. Clean. Prod.* 189,  
1292 135-144. <https://doi.org/10.1016/j.jclepro.2018.04.004>.
- 1293 Chang, S., 2018. Characteristics of aerosols and cloud condensation nuclei (CCN) over China  
1294 investigated by the two-way coupled WRF-CMAQ air quality model.
- 1295 Chapman, E.G., Jr, W.I.G., Easter, R.C., Barnard, J.C., Ghan, S.J., Pekour, M.S., Fast, J.D., 2009.  
1296 and Physics Coupling aerosol-cloud-radiative processes in the WRF-Chem model :  
1297 Investigating the radiative impact of elevated point sources 945-964.  
1298 <https://doi.org/10.5194/acp-9-945-2009>.
- 1299 Chen, D.-S., Ma, X., Xie, X., Wei, P., Wen, W., Xu, T., Yang, N., Gao, Q., Shi, H., Guo, X., 2015.  
1300 Modelling the effect of aerosol feedbacks on the regional meteorology factors over China.  
1301 *Aerosol. Air. Qual. Res* 15, 1559-1579. <https://doi.org/10.4209/aaqr.2014.11.0272>.
- 1302 Chen, J., Li, C., Ristovski, Z., Milic, A., Gu, Y., Islam, M.S., Wang, S., Hao, J., Zhang, H., He, C.,  
1303 2017. A review of biomass burning: Emissions and impacts on air quality, health and climate  
1304 in China. *Sci. Total Environ.* 579, 1000-1034. <https://doi.org/10.1016/j.scitotenv.2016.11.025>.
- 1305 Chen, L., Gao, Y., Zhang, M., Fu, J.S., Zhu, J., Liao, H., Li, J., Huang, K., Ge, B., Wang, X., 2019a.  
1306 MICS-Asia III: Multi-model comparison and evaluation of aerosol over East Asia. *Atmos.*  
1307 *Chem. Phys.* 19, 11911-11937. <https://doi.org/10.5194/acp-19-11911-2019>.
- 1308 Chen, L., Zhu, J., Liao, H., Gao, Y., Qiu, Y., Zhang, M., Liu, Z., Li, N., Wang, Y., 2019b. Assessing  
1309 the formation and evolution mechanisms of severe haze pollution in the Beijing-Tianjin-Hebei  
1310 region using process analysis. *Atmos. Chem. Phys.* 19, 10845-10864.  
1311 <https://doi.org/10.5194/acp-19-10845-2019>.
- 1312 Chen, S., Huang, J., Kang, L., Wang, H., Ma, X., He, Y., Yuan, T., Yang, B., Huang, Z., Zhang, G.,  
1313 2017a. Emission, transport, and radiative effects of mineral dust from the Taklimakan and Gobi  
1314 deserts: comparison of measurements and model results. *Atmos. Chem. Phys.* 17,  
1315 <https://doi.org/10.5194/acp-17-2401-2017>.
- 1316 Chen, S., Huang, J., Qian, Y., Zhao, C., Kang, L., Yang, B., Wang, Y., Liu, Y., Yuan, T., Wang, T.,  
1317 2017b. An overview of mineral dust modeling over East Asia. *J. Meteorol. Res.* 31, 633-653.  
1318 <https://doi.org/10.1007/s13351-017-6142-2>.
- 1319 Chen, S., Huang, J., Zhao, C., Qian, Y., Leung, L.R., Yang, B., 2013. Modeling the transport and  
1320 radiative forcing of Taklimakan dust over the Tibetan Plateau: A case study in the summer of  
1321 2006. *J. Geophys. Res. Atmos.* 118, 797-812. <https://doi.org/10.1002/jgrd.50122>.
- 1322 Chen, S., Zhao, C., Qian, Y., Leung, L.R., Huang, J., Huang, Z., Bi, J., Zhang, W., Shi, J., Yang, L.,  
1323 2014. Regional modeling of dust mass balance and radiative forcing over East Asia using  
1324 WRF-Chem. *Aeolian Res.* 15, 15-30. <https://doi.org/10.1016/j.aeolia.2014.02.001>.
- 1325 Chen, Y., Zhang, Y., Fan, J., Leung, L.-Y.R., Zhang, Q., He, K., 2015. Application of an online-  
1326 coupled regional climate model, WRF-CAM5, over East Asia for examination of ice nucleation  
1327 schemes: Part I. Comprehensive model evaluation and trend analysis for 2006 and 2011.  
1328 *Climate* 3, 627-667. <https://doi.org/10.3390/cli3030627>.
- 1329 Choobari, O.A., Zawar-Reza, P., Sturman, A., 2014. The global distribution of mineral dust and its  
1330 impacts on the climate system: A review. *Atmos. Res.* 138, 152-165.  
1331 <https://doi.org/10.1016/j.atmosres.2013.11.007>.
- 1332 Chung, C.E., 2012. Aerosol direct radiative forcing: a review, *Atmospheric Aerosols-Regional*  
1333 *Characteristics-Chemistry and Physics*; Abdul-Razzak, H., Ed. <https://doi.org/10.5772/50248>.
- 1334 Conibear, L., Butt, E.W., Knote, C., Arnold, S.R., Spracklen, D. V., 2018a. Stringent Emission  
1335 Control Policies Can Provide Large Improvements in Air Quality and Public Health in India.  
1336 *GeoHealth* 2, 196-211. <https://doi.org/10.1029/2018gh000139>.
- 1337 Conibear, L., Butt, E.W., Knote, C., Arnold, S.R., Spracklen, D. V., 2018b. Residential energy use  
1338 emissions dominate health impacts from exposure to ambient particulate matter in India. *Nat.*  
1339 *Commun.* 9, 1-9. <https://doi.org/10.1038/s41467-018-02986-7>.
- 1340 Conti, G.O., Heibati, B., Kloog, I., Fiore, M., Ferrante, M., 2017. A review of AirQ Models and their  
1341 applications for forecasting the air pollution health outcomes. *Environ. Sci. Pollut. Res.* 24,  
1342 6426-6445. <https://doi.org/10.1007/s11356-016-8180-1>.
- 1343 Craig, A., Valcke, S., Coquart, L., 2017. Development and performance of a new version of the  
1344 OASIS coupler, OASIS3-MCT\_3. 0. *Geosci. Model Dev.* 10, 3297.  
1345 <https://doi.org/10.5194/gmd-10-3297-2017>.
- 1346 Cuchiara, G.C., Li, X., Carvalho, J., Rappenglück, B., 2014. Intercomparison of planetary boundary  
1347 layer parameterization and its impacts on surface ozone concentration in the WRF/Chem model



- 1348 for a case study in Houston/Texas. *Atmos. Environ.* 96, 175-185.  
1349 <https://doi.org/10.1016/j.atmosenv.2014.07.013>.
- 1350 Dahutia, P., Pathak, B., Bhuyan, P.K., 2019. Vertical distribution of aerosols and clouds over north-  
1351 eastern South Asia: Aerosol-cloud interactions. *Atmos. Environ.* 215, 116882.  
1352 <https://doi.org/10.1016/j.atmosenv.2019.116882>.
- 1353 Ding, A.J., Huang, X., Nie, W., Sun, J.N., Kerminen, V., Petäjä, T., Su, H., Cheng, Y.F., Yang, X.,  
1354 Wang, M.H., 2016. Enhanced haze pollution by black carbon in megacities in China. *Geophys.*  
1355 *Res. Lett.* 43, 2873-2879. <https://doi.org/10.1002/2016GL067745>.
- 1356 Ding, Q.J., Sun, J., Huang, X., Ding, A., Zou, J., Yang, X., Fu, C., 2019. Impacts of black carbon on  
1357 the formation of advection-radiation fog during a haze pollution episode in eastern China.  
1358 *Atmos. Chem. Phys.* 19, 7759-7774. <https://doi.org/10.5194/acp-19-7759-2019>.
- 1359 Dipu, S., Prabha, T. V, Pandithurai, G., Dudhia, J., Pfister, G., Rajesh, K., Goswami, B.N., 2013.  
1360 Impact of elevated aerosol layer on the cloud macrophysical properties prior to monsoon onset.  
1361 *Atmos. Environ.* 70, 454-467. <https://doi.org/10.1016/j.atmosenv.2012.12.036>.
- 1362 Donat, M.G., Lowry, A.L., Alexander, L. V, O’Gorman, P.A., Maher, N., 2016. More extreme  
1363 precipitation in the world’s dry and wet regions. *Nat. Clim. Chang.* 6, 508-513.  
1364 <https://doi.org/10.1038/nclimate2941>.
- 1365 Dong, X., Fu, J.S., Huang, K., Zhu, Q., Tipton, M., 2019. Regional Climate Effects of Biomass  
1366 Burning and Dust in East Asia: Evidence From Modeling and Observation. *Geophys. Res. Lett.*  
1367 46, 11490-11499. <https://doi.org/10.1029/2019GL083894>.
- 1368 Eck, T.F., Holben, B.N., Reid, J.S., Xian, P., Giles, D.M., Sinyuk, A., Smirnov, A., Schafer, J.S.,  
1369 Slutsker, I., Kim, J., 2018. Observations of the interaction and transport of fine mode aerosols  
1370 with cloud and/or fog in Northeast Asia from Aerosol Robotic Network and satellite remote  
1371 sensing. *J. Geophys. Res. Atmos.* 123, 5560-5587. <https://doi.org/10.1029/2018JD028313>.
- 1372 El-Harbawi, M., 2013. Air quality modelling, simulation, and computational methods: a review.  
1373 *Environ. Rev.* 21, 149-179. <https://doi.org/10.1139/er-2012-0056>.
- 1374 ENVIRON, U.G., 2008. Comprehensive Air Quality Model with Extensions (CAMx). Version 4.50.  
1375 Env. Int. Corp. Novato.
- 1376 EPA, 2018. Meteorological Model Performance for Annual 2016 Simulation WRF v3.8. United  
1377 States Environ. Prot. Agency.
- 1378 Fan, J., Rosenfeld, D., Yang, Y., Zhao, C., Leung, L.R., Li, Z., 2015. Substantial contribution of  
1379 anthropogenic air pollution to catastrophic floods in Southwest China. *Geophys. Res. Lett.* 42,  
1380 6066-6075. <https://doi.org/10.1002/2015GL064479>.
- 1381 Fan, J., Rosenfeld, D., Zhang, Y., Giangrande, S.E., Li, Z., Machado, L.A.T., Martin, S.T., Yang, Y.,  
1382 Wang, J., Artaxo, P., 2018. Substantial convection and precipitation enhancements by ultrafine  
1383 aerosol particles. *Science* (80-. ). 359, 411-418. <https://doi.org/10.1126/science.aan8461>.
- 1384 Fan, J., Wang, Y., Rosenfeld, D., Liu, X., 2016. Review of aerosol-cloud interactions: Mechanisms,  
1385 significance, and challenges. *J. Atmos. Sci.* 73, 4221-4252. <https://doi.org/10.1175/JAS-D-16-0037.1>.
- 1387 Fast, J.D., Gustafson Jr, W.I., Easter, R.C., Zaveri, R.A., Barnard, J.C., Chapman, E.G., Grell, G.A.,  
1388 Peckham, S.E., 2006. Evolution of ozone, particulates, and aerosol direct radiative forcing in  
1389 the vicinity of Houston using a fully coupled meteorology-chemistry-aerosol model. *J.*  
1390 *Geophys. Res. Atmos.* 111. <https://doi.org/10.1029/2005JD006721>.
- 1391 Feingold, G., Eberhard, W.L., Veron, D.E., Previdi, M., 2003. First measurements of the Twomey  
1392 indirect effect using ground-based remote sensors. *Geophys. Res. Lett.* 30.  
1393 <https://doi.org/10.1029/2002GL016633>.
- 1394 Feng, Y., Kotamarthi, V.R., Coulter, R., Zhao, C., Cadeddu, M., 2016. Radiative and thermodynamic  
1395 responses to aerosol extinction profiles during the pre-monsoon month over South Asia. *Atmos.*  
1396 *Chem. Phys.* 16. <https://doi.org/10.5194/acp-16-247-2016>.
- 1397 Forke, R., Brunner, D., Baklanov, A., Balzarini, A., Hirtl, M., Honzak, L., Jiménez-Guerrero, P.,  
1398 Jorba, O., Pérez, J.L., San José, R., 2016. A multi-model case study on aerosol feedbacks in  
1399 online coupled chemistry-meteorology models within the cost action ES1004 EuMetChem, in:  
1400 *Air Pollution Modeling and Its Application XXIV*. Springer, pp. 23-28.  
1401 [https://doi.org/10.1007/978-3-319-24478-5\\_4](https://doi.org/10.1007/978-3-319-24478-5_4).
- 1402 Gao, C., Zhang, X., Xiu, A., Huang, L., Zhao, H., Wang, K., Tong, Q., 2019. Spatiotemporal  
1403 distribution of biogenic volatile organic compounds emissions in China. *Acta Sci.*  
1404 *Circumstantiae* 39, 4140-4151. <https://doi.org/10.13671/j.hjkxxb.2019.0243>.



- 1405 Gao, J., Zhu, B., Xiao, H., Kang, H., Pan, C., Wang, D., Wang, H., 2018. Effects of black carbon  
1406 and boundary layer interaction on surface ozone in Nanjing, China. *Atmos. Chem. Phys.* 18,  
1407 <https://doi.org/10.5194/acp-18-7081-2018>.
- 1408 Gao, M., Carmichael, G.R., Saide, P.E., Lu, Z., Yu, M., Streets, D.G., Wang, Z., 2016a. Response of  
1409 winter fine particulate matter concentrations to emission and meteorology changes in North  
1410 China. *Atmos. Chem. Phys.* 16, 11837. <https://doi.org/10.5194/acp-16-11837-2016>.
- 1411 Gao, M., Carmichael, G.R., Wang, Y., Saide, P.E., Liu, Z., Xin, J., Shan, Y., Wang, Z., 2017a.  
1412 Chemical and Meteorological Feedbacks in the Formation of Intense Haze Events, in: *Air  
1413 Pollution in Eastern Asia: An Integrated Perspective*. Springer, pp. 437-452.  
1414 [https://doi.org/10.1007/978-3-319-59489-7\\_21](https://doi.org/10.1007/978-3-319-59489-7_21).
- 1415 Gao, M., Carmichael, G.R., Wang, Y., Saide, P.E., Yu, M., Xin, J., Liu, Z., Wang, Z., 2016b.  
1416 Modeling study of the 2010 regional haze event in the North China Plain. *Atmos. Chem. Phys.*  
1417 16, 1673. <https://doi.org/10.5194/acp-16-1673-2016>.
- 1418 Gao, M., Guttikunda, S.K., Carmichael, G.R., Wang, Y., Liu, Z., Stanier, C.O., Saide, P.E., Yu, M.,  
1419 2015. Health impacts and economic losses assessment of the 2013 severe haze event in Beijing  
1420 area. *Sci. Total Environ.* 511, 553-561. <https://doi.org/10.1016/j.scitotenv.2015.01.005>.
- 1421 Gao, M., Han, Z., Liu, Z., Li, M., Xin, J., Tao, Z., Li, J., Kang, J.E., Huang, K., Dong, X., Zhuang,  
1422 B., Li, S., Ge, B., Wu, Q., Cheng, Y., Wang, Y., Lee, H.J., Kim, C.H., Fu, J.S., Wang, T., Chin,  
1423 M., Woo, J.H., Zhang, Q., Wang, Z., Carmichael, G.R., 2018a. Air quality and climate change,  
1424 Topic 3 of the Model Inter-Comparison Study for Asia Phase III (MICS-Asia III)- Part 1:  
1425 Overview and model evaluation. *Atmos. Chem. Phys.* 18, 4859-4884.  
1426 <https://doi.org/10.5194/acp-18-4859-2018>.
- 1427 Gao, M., Ji, D., Liang, F., Liu, Y., 2018b. Attribution of aerosol direct radiative forcing in China and  
1428 India to emitting sectors. *Atmos. Environ.* 190, 35-42.  
1429 <https://doi.org/10.1016/j.atmosenv.2018.07.011>.
- 1430 Gao, M., Liu, Z., Wang, Y., Lu, X., Ji, D., Wang, L., Li, M., Wang, Z., Zhang, Q., Carmichael, G.R.,  
1431 2017b. Distinguishing the roles of meteorology, emission control measures, regional transport,  
1432 and co-benefits of reduced aerosol feedbacks in "APEC Blue." *Atmos. Environ.* 167, 476-486.  
1433 <https://doi.org/10.1016/j.atmosenv.2017.08.054>.
- 1434 Gao, M., Saide, P.E., Xin, J., Wang, Yuesi, Liu, Z., Wang, Yuxuan, Wang, Z., Pagowski, M.,  
1435 Guttikunda, S.K., Carmichael, G.R., 2017c. Estimates of health impacts and radiative forcing  
1436 in winter haze in eastern China through constraints of surface PM<sub>2.5</sub> predictions. *Environ. Sci.  
1437 Technol.* 51, 2178-2185. <https://doi.org/10.1021/acs.est.6b03745>.
- 1438 Gao, Y., Zhang, M., 2018. Changes in the diurnal variations of clouds and precipitation induced by  
1439 anthropogenic aerosols over East China in August 2008. *Atmos. Pollut. Res.* 9, 513-525.  
1440 <https://doi.org/10.1016/j.apr.2017.11.013>.
- 1441 Gao, Y., Zhang, M., Liu, X., Wang, L., 2016. Change in diurnal variations of meteorological  
1442 variables induced by anthropogenic aerosols over the North China Plain in summer 2008. *Theor.  
1443 Appl. Climatol.* 124, 103-118. <https://doi.org/10.1007/s00704-015-1403-4>.
- 1444 Gao, Y., Zhang, M., Liu, X., Zhao, C., 2012. Model Analysis of the Anthropogenic Aerosol Effect  
1445 on Clouds over East Asia. *Atmos. Ocean. Sci. Lett.* 5, 1-7.  
1446 <https://doi.org/10.1080/16742834.2012.11446968>.
- 1447 Gao, Y., Zhang, M., Liu, Z., Wang, L., Wang, P., Xia, X., Tao, M., Zhu, L., 2015. Modeling the  
1448 feedback between aerosol and meteorological variables in the atmospheric boundary layer  
1449 during a severe fog-haze event over the North China Plain. *Atmos. Chem. Phys.* 15,  
1450 <https://doi.org/10.5194/acp-15-4279-2015>.
- 1451 Gao, Y., Zhao, C., Liu, X., Zhang, M., Leung, L.R., 2014. WRF-Chem simulations of aerosols and  
1452 anthropogenic aerosol radiative forcing in East Asia. *Atmos. Environ.* 92, 250-266.  
1453 <https://doi.org/10.1016/j.atmosenv.2014.04.038>.
- 1454 García-Díez, M., Fernández, J., Fita, L., Yagüe, C., 2013. Seasonal dependence of WRF model  
1455 biases and sensitivity to PBL schemes over Europe. *Q. J. R. Meteorol. Soc.* 139, 501-514.  
1456 <https://doi.org/10.1002/qj.1976>.
- 1457 Ge, C., Wang, J., Reid, J.S., 2014. Mesoscale modeling of smoke transport over the Southeast Asian  
1458 Maritime Continent: coupling of smoke direct radiative effect below and above the low-level  
1459 clouds. *Atmos. Chem. Phys.* 14, 159. <https://doi.org/10.5194/acp-14-159-2014>.
- 1460 Ghude, S.D., Chate, D.M., Jena, C., Beig, G., Kumar, R., Barth, M.C., Pfister, G.G., Fadnavis, S.,  
1461 Pithani, P., 2016. Premature mortality in India due to PM<sub>2.5</sub> and ozone exposure. *Geophys. Res.*



- 1462 Lett. 43, 4650–4658. <https://doi.org/10.1002/2016GL068949>.
- 1463 Gong, S.L., Zhang, X.Y., Zhao, T.L., McKendry, I.G., Jaffe, D.A., Lu, N.M., 2003. Characterization  
1464 of soil dust aerosol in China and its transport and distribution during 2001 ACE-Asia: 2. Model  
1465 simulation and validation. *J. Geophys. Res. Atmos.* 108.  
1466 <https://doi.org/10.1029/2002JD002633>.
- 1467 Goren, T., Rosenfeld, D., 2014. Decomposing aerosol cloud radiative effects into cloud cover, liquid  
1468 water path and Twomey components in marine stratocumulus. *Atmos. Res.* 138, 378–393.  
1469 <https://doi.org/10.1016/j.atmosres.2013.12.008>.
- 1470 Govardhan, G., Nanjundiah, R.S., Satheesh, S.K., Krishnamoorthy, K., Kotamarthi, V.R., 2015.  
1471 Performance of WRF-Chem over Indian region: Comparison with measurements. *J. Earth Syst.*  
1472 *Sci.* 124, 875–896. <https://doi.org/10.1007/s12040-015-0576-7>.
- 1473 Govardhan, G.R., Nanjundiah, R.S., Satheesh, S.K., Moorthy, K.K., Takemura, T., 2016. Inter-  
1474 comparison and performance evaluation of chemistry transport models over Indian region.  
1475 *Atmos. Environ.* 125, 486–504. <https://doi.org/10.1016/j.atmosenv.2015.10.065>.
- 1476 Gray, L.J., Beer, J., Geller, M., Haigh, J.D., Lockwood, M., Matthes, K., Cubasch, U., Fleitmann,  
1477 D., Harrison, G., Hood, L., 2010. Solar influences on climate. *Rev. Geophys.* 48.  
1478 <https://doi.org/10.1029/2009RG000282>.
- 1479 Grell, G., Freitas, S.R., Stuefer, M., Fast, J., 2011. Inclusion of biomass burning in WRF-Chem:  
1480 impact of wildfires on weather forecasts. *Atmos. Chem. Phys.* 11, 5289–5303.  
1481 <https://doi.org/10.5194/acp-11-5289-2011>.
- 1482 Grell, G.A., Peckham, S.E., Schmitz, R., McKeen, S.A., Frost, G., Skamarock, W.C., Eder, B., 2005.  
1483 Fully coupled “online” chemistry within the WRF model. *Atmos. Environ.* 39, 6957–6975.  
1484 <https://doi.org/10.1016/j.atmosenv.2005.04.027>.
- 1485 Groß, S., Esselborn, M., Weinzierl, B., Wirth, M., Fix, A., Petzold, A., 2013. Aerosol classification  
1486 by airborne high spectral resolution lidar observations. *Atmos. Chem. Phys.* 13, 2487.  
1487 <https://doi.org/10.5194/acp-13-2487-2013>.
- 1488 Guo, J., Deng, M., Fan, J., Li, Z., Chen, Q., Zhai, P., Dai, Z., Li, X., 2014. Precipitation and air  
1489 pollution at mountain and plain stations in northern China: Insights gained from observations  
1490 and modeling. *J. Geophys. Res. Atmos.* 119, 4793–4807.  
1491 <https://doi.org/10.1002/2013JD021161>.
- 1492 Guo, J., Liu, H., Li, Z., Rosenfeld, D., Jiang, M., Xu, W., Jiang, J.H., 2018. Aerosol-induced changes  
1493 in the vertical structure of precipitation: a perspective of TRMM precipitation radar 13329–  
1494 13343. <https://doi.org/10.5194/acp-18-13329-2018>.
- 1495 Gurjar, B.R., Ravindra, K., Nagpure, A.S., 2016. Air pollution trends over Indian megacities and  
1496 their local-to-global implications. *Atmos. Environ.* 142, 475–495.  
1497 <https://doi.org/10.1016/j.atmosenv.2016.06.030>.
- 1498 Haywood, J., Boucher, O., 2000. Estimates of the direct and indirect radiative forcing due to  
1499 tropospheric aerosols: A review. *Rev. Geophys.* 38, 513–543.  
1500 <https://doi.org/10.1029/1999RG000078>.
- 1501 He, J., Zhang, Y., Wang, K., Chen, Y., Leung, L.R., Fan, J., Li, M., Zheng, B., Zhang, Q., Duan, F.,  
1502 2017. Multi-year application of WRF-CAM5 over East Asia-Part I: Comprehensive evaluation  
1503 and formation regimes of O<sub>3</sub> and PM<sub>2.5</sub>. *Atmos. Environ.* 165, 122–142.  
1504 <https://doi.org/10.1016/j.atmosenv.2017.06.015>.
- 1505 Hodshire, A.L., Akherati, A., Alvarado, M.J., Brown-Steiner, B., Jathar, S.H., Jimenez, J.L.,  
1506 Kreidenweis, S.M., Lonsdale, C.R., Onasch, T.B., Ortega, A.M., 2019. Aging effects on  
1507 biomass burning aerosol mass and composition: A critical review of field and laboratory studies.  
1508 *Environ. Sci. Technol.* 53, 10007–10022. <https://doi.org/10.1021/acs.est.9b02588>.
- 1509 Hong, C., Zhang, Q., Zhang, Y., Davis, S.J., Tong, D., Zheng, Y., Liu, Z., Guan, D., He, K.,  
1510 Schellnhuber, H.J., 2019. Impacts of climate change on future air quality and human health in  
1511 China. *Proc. Natl. Acad. Sci.* 116, 17193–17200. <https://doi.org/10.1073/pnas.1812881116>.
- 1512 Hong, C., Zhang, Q., Zhang, Y., Tang, Y., Tong, D., He, K., 2017. Multi-year downscaling  
1513 application of two-way coupled WRF v3.4 and CMAQ v5.0.2 over east Asia for regional  
1514 climate and air quality modeling: model evaluation and aerosol direct effects. *Geosci. Model*  
1515 *Dev.* 10. <https://doi.org/10.5194/gmd-10-2447-2017>.
- 1516 Hu, X., Klein, P.M., Xue, M., 2013. Evaluation of the updated YSU planetary boundary layer  
1517 scheme within WRF for wind resource and air quality assessments. *J. Geophys. Res. Atmos.*  
1518 118, 10–490. <https://doi.org/10.1002/jgrd.50823>.



- 1519 Huang, J., Wang, T., Wang, W., Li, Z., Yan, H., 2014. Climate effects of dust aerosols over East  
1520 Asian arid and semiarid regions. *J. Geophys. Res. Atmos.* 119, 11-398.  
1521 <https://doi.org/10.1002/2014JD021796>.
- 1522 Huang, L., Lin, W., Li, F., Wang, Y., Jiang, B., 2019. Climate impacts of the biomass burning in  
1523 Indochina on atmospheric conditions over southern China. *Aerosol Air Qual. Res.* 19, 2707-  
1524 2720. <https://doi.org/10.4209/aaqr.2019.01.0028>.
- 1525 Huang, X., Ding, A., Liu, L., Liu, Q., Ding, K., Niu, X., Nie, W., Xu, Z., Chi, X., Wang, M., 2016.  
1526 Effects of aerosol-radiation interaction on precipitation during biomass-burning season in East  
1527 China. *Atmos. Chem. Phys.* 16. <https://doi.org/10.5194/acp-16-10063-2016>.
- 1528 Huang, X., Song, Y., Zhao, C., Cai, X., Zhang, H., Zhu, T., 2015. Direct radiative effect by  
1529 multicomponent aerosol over China. *J. Clim.* 28, 3472-3495. <https://doi.org/10.1175/JCLI-D-14-00365.1>.
- 1531 Illingworth, A.J., Barker, H.W., Beljaars, A., Ceccaldi, M., Chepfer, H., Clerbaux, N., Cole, J.,  
1532 Delanoë, J., Domenech, C., Donovan, D.P., 2015. The EarthCARE satellite: The next step  
1533 forward in global measurements of clouds, aerosols, precipitation, and radiation. *Bull. Am.*  
1534 *Meteorol. Soc.* 96, 1311-1332. <https://doi.org/10.1175/BAMS-D-12-00227.1>.
- 1535 Im, U., Bianconi, R., Solazzo, E., Kioutsioukis, I., Badia, A., Balzarini, A., Baró, R., Bellasio, R.,  
1536 Brunner, D., Chemel, C., 2015a. Evaluation of operational online-coupled regional air quality  
1537 models over Europe and North America in the context of AQMEII phase 2. Part II: Particulate  
1538 matter. *Atmos. Environ.* 115, 421-441. <https://doi.org/10.1016/j.atmosenv.2014.08.072>.
- 1539 Im, U., Bianconi, R., Solazzo, E., Kioutsioukis, I., Badia, A., Balzarini, A., Baró, R., Bellasio, R.,  
1540 Brunner, D., Chemel, C., 2015b. Evaluation of operational on-line-coupled regional air quality  
1541 models over Europe and North America in the context of AQMEII phase 2. Part I: Ozone.  
1542 *Atmos. Environ.* 115, 404-420. <https://doi.org/10.1016/j.atmosenv.2014.09.042>.
- 1543 IPCC, 2014. Climate change 2014: Synthesis Report. Contribution of Working Groups I, II and III  
1544 to the fifth assessment report of the Intergovernmental Panel on Climate Change.
- 1545 IPCC, 2007. Climate change 2007: Synthesis Report. Contribution of Working Groups I, II and III  
1546 to the Fifth Assessment Report of the Intergovernmental Panel on Climate Change.
- 1547 Jacobson, M.Z., 2001. Strong radiative heating due to the mixing state of black carbon in  
1548 atmospheric aerosols 409, 695-697. <https://doi.org/10.1038/35055518>.
- 1549 Jena, C., Ghude, S.D., Pfister, G.G., Chate, D.M., Kumar, R., Beig, G., Surendran, D.E., Fadnavis,  
1550 S., Lal, D.M., 2015. Influence of springtime biomass burning in South Asia on regional ozone  
1551 (O<sub>3</sub>): A model based case study. *Atmos. Environ.* 100, 37-47.  
1552 <https://doi.org/10.1016/j.atmosenv.2014.10.027>.
- 1553 Jeong, J.I., Park, R.J., 2017. Winter monsoon variability and its impact on aerosol concentrations in  
1554 East Asia. *Environ. Pollut.* 221, 285-292. <https://doi.org/10.1016/j.envpol.2016.11.075>.
- 1555 Jia, X., Guo, X., 2012. Impacts of Anthropogenic Atmospheric Pollutant on Formation and  
1556 Development of a Winter Heavy Fog Event. *Chinese J. Atmos. Sci.* 36, 995-1008.  
1557 <https://doi.org/10.1007/s11783-011-0280-z>.
- 1558 Jia, X., Quan, J., Zheng, Z., Liu, X., Liu, Q., He, H., Liu, Y., 2019. Impacts of Anthropogenic  
1559 Aerosols on Fog in North China Plain. *J. Geophys. Res. Atmos.* 124, 252-265.  
1560 <https://doi.org/10.1029/2018JD029437>.
- 1561 Jiang, B., Huang, B., Lin, W., Xu, S., 2016. Investigation of the effects of anthropogenic pollution  
1562 on typhoon precipitation and microphysical processes using WRF-Chem. *J. Atmos. Sci.* 73,  
1563 1593-1610. <https://doi.org/10.1175/JAS-D-15-0202.1>.
- 1564 Jiang, B., Lin, W., Li, F., Chen, B., 2019a. Simulation of the effects of sea-salt aerosols on cloud ice  
1565 and precipitation of a tropical cyclone. *Atmos. Sci. Lett.* 20, e936.  
1566 <https://doi.org/10.1002/asl.936>.
- 1567 Jiang, B., Lin, W., Li, F., Chen, J., 2019b. Sea-salt aerosol effects on the simulated microphysics  
1568 and precipitation in a tropical cyclone. *J. Meteorol. Res.* 33, 115-125.  
1569 <https://doi.org/10.1007/s13351-019-8108-z>.
- 1570 Jimenez, P.A., Hacker, J.P., Dudhia, J., Haupt, S.E., Ruiz-Arias, J.A., Gueymard, C.A., Thompson,  
1571 G., Eidhammer, T., Deng, A., 2016. WRF-Solar: Description and clear-sky assessment of an  
1572 augmented NWP model for solar power prediction. *Bull. Am. Meteorol. Soc.* 97, 1249-1264.  
1573 <https://doi.org/10.1175/BAMS-D-14-00279.1>.
- 1574 Jin, Q., Wei, J., Yang, Z.-L., Pu, B., Huang, J., 2015. Consistent response of Indian summer monsoon  
1575 to Middle East dust in observations and simulations. *Atmos. Chem. Phys.* 15, 9897-9915.



- 1576 <https://doi.org/10.5194/acp-15-9897-2015>.
- 1577 Jin, Q., Yang, Z.-L., Wei, J., 2016a. Seasonal responses of Indian summer monsoon to dust aerosols  
1578 in the Middle East, India, and China. *J. Clim.* 29, 6329-6349. [https://doi.org/10.1175/JCLI-D-](https://doi.org/10.1175/JCLI-D-15-0622.1)  
1579 15-0622.1.
- 1580 Jin, Q., Yang, Z.-L., Wei, J., 2016b. High sensitivity of Indian summer monsoon to Middle East dust  
1581 absorptive properties. *Sci. Rep.* 6, 1-8. <https://doi.org/10.1038/srep30690>.
- 1582 Jung, J., Souri, A.H., Wong, D.C., Lee, S., Jeon, W., Kim, J., Choi, Y., 2019. The Impact of the  
1583 Direct Effect of Aerosols on Meteorology and Air Quality Using Aerosol Optical Depth  
1584 Assimilation During the KORUS-AQ Campaign. *J. Geophys. Res. Atmos.* 124, 8303-8319.  
1585 <https://doi.org/10.1029/2019JD030641>.
- 1586 Kajino, M., Ueda, H., Han, Z., Kudo, R., Inomata, Y., Kaku, H., 2017. Synergy between air pollution  
1587 and urban meteorological changes through aerosol-radiation-diffusion feedback—A case study  
1588 of Beijing in January 2013. *Atmos. Environ.* 171, 98-110.  
1589 <https://doi.org/10.1016/j.atmosenv.2017.10.018>.
- 1590 Kant, S., Panda, J., Gautam, R., 2019. A seasonal analysis of aerosol-cloud-radiation interaction  
1591 over Indian region during 2000-2017. *Atmos. Environ.* 201, 212-222.  
1592 <https://doi.org/10.1016/j.atmosenv.2018.12.044>.
- 1593 Kedia, S., Cherian, R., Islam, S., Das, S.K., Kaginalkar, A., 2016. Regional simulation of aerosol  
1594 radiative effects and their influence on rainfall over India using WRFChem model. *Atmos. Res.*  
1595 182, 232-242. <https://doi.org/10.1016/j.atmosres.2016.07.008>.
- 1596 Kedia, S., Kumar, S., Islam, S., Hazra, A., Kumar, N., 2019a. Aerosols impact on the convective  
1597 and non-convective rain distribution over the Indian region: Results from WRF-Chem  
1598 simulation. *Atmos. Environ.* 202, 64-74. <https://doi.org/10.1016/j.atmosenv.2019.01.020>.
- 1599 Kedia, S., Vellore, R.K., Islam, S., Kaginalkar, A., 2019b. A study of Himalayan extreme rainfall  
1600 events using WRF-Chem. *Meteorol. Atmos. Phys.* 131, 1133-1143.  
1601 <https://doi.org/10.1007/s00703-018-0626-1>.
- 1602 Kim, B., Schwartz, S.E., Miller, M.A., Min, Q., 2003. Effective radius of cloud droplets by ground-  
1603 based remote sensing: Relationship to aerosol. *J. Geophys. Res. Atmos.* 108.  
1604 <https://doi.org/10.1029/2003JD003721>.
- 1605 Koch, D., Del Genio, A.D., 2010. Black carbon semi-direct effects on cloud cover: review and  
1606 synthesis. *Atmos. Chem. Phys.* 10. <https://doi.org/10.5194/acp-10-7685-2010>.
- 1607 Kong, X., Forkel, R., Sokhi, R.S., Suppan, P., Baklanov, A., Gauss, M., Brunner, D., Barò, R.,  
1608 Balzarini, A., Chemel, C., Curci, G., Jiménez-Guerrero, P., Hirtl, M., Honzak, L., Im, U., Pérez,  
1609 J.L., Pirovano, G., San Jose, R., Schlünzen, K.H., Tsegas, G., Tuccella, P., Werhahn, J., Žabkar,  
1610 R., Galmarini, S., 2015. Analysis of meteorology-chemistry interactions during air pollution  
1611 episodes using online coupled models within AQMEII phase-2. *Atmos. Environ.* 115, 527-540.  
1612 <https://doi.org/10.1016/j.atmosenv.2014.09.020>.
- 1613 Kuik, F., Lauer, A., Churkina, G., Denier van der Gon, H., Fenner, D., Mar, K., Butler, T., 2016. Air  
1614 quality modelling in the Berlin-Brandenburg region using WRF-Chem v3. 7.1: sensitivity to  
1615 resolution of model grid and input data. *Geosci. Model Dev.* 4339-4363.  
1616 <https://doi.org/10.5194/gmd-9-4339-2016>.
- 1617 Kumar, P., Sokolik, I.N., Nenes, A., 2009. Parameterization of cloud droplet formation for global  
1618 and regional models: including adsorption activation from insoluble CCN. *Atmos. Chem. Phys.*  
1619 9. <https://doi.org/10.5194/acp-9-2517-2009>.
- 1620 Kumar, R., Barth, M.C., Pfister, G.G., Naja, M., Brasseur, G.P., 2014. WRF-Chem simulations of a  
1621 typical pre-monsoon dust storm in northern India: influences on aerosol optical properties and  
1622 radiation budget. *Atmos. Chem. Phys.* 14, 2431-2446. [https://doi.org/10.5194/acp-14-2431-](https://doi.org/10.5194/acp-14-2431-2014)  
1623 2014.
- 1624 Kumar, R., Naja, M., Pfister, G.G., Barth, M.C., Brasseur, G.P., 2012a. Simulations over South Asia  
1625 using the Weather Research and Forecasting model with Chemistry (WRF-Chem): set-up and  
1626 meteorological evaluation. *Geosci. Model Dev.* 5, 321-343. [https://doi.org/10.5194/gmd-5-](https://doi.org/10.5194/gmd-5-321-2012)  
1627 321-2012.
- 1628 Kumar, R., Naja, M., Pfister, G.G., Barth, M.C., Wiedinmyer, C., Brasseur, G.P., 2012b. Simulations  
1629 over South Asia using the Weather Research and Forecasting model with Chemistry (WRF-  
1630 Chem): chemistry evaluation and initial results. *Geosci. Model Dev.* 5, 619-648.  
1631 <https://doi.org/10.5194/gmd-5-619-2012>.
- 1632 Kuniyal, J.C., Guleria, R.P., 2019. The current state of aerosol-radiation interactions: a mini review.



- 1633 J. Aerosol Sci. 130, 45-54. <https://doi.org/10.1016/j.jaerosci.2018.12.010>.
- 1634 Lau, W.K.M., Kim, K.-M., Shi, J.-J., Matsui, T., Chin, M., Tan, Q., Peters-Lidard, C., Tao, W.-K.,  
1635 2017. Impacts of aerosol-monsoon interaction on rainfall and circulation over Northern India  
1636 and the Himalaya Foothills. *Clim. Dyn.* 49, 1945-1960. [https://doi.org/10.1007/s00382-016-  
3430-y](https://doi.org/10.1007/s00382-016-<br/>1637 3430-y).
- 1638 Lee, Y.C., Yang, X., Wenig, M., 2010. Transport of dusts from East Asian and non-East Asian  
1639 sources to Hong Kong during dust storm related events 1996-2007. *Atmos. Environ.* 44, 3728-  
1640 3738. <https://doi.org/10.1016/j.atmosenv.2010.03.034>.
- 1641 Lelieveld, J., Bourtsoukidis, E., Brühl, C., Fischer, H., Fuchs, H., Harder, H., Hofzumahaus, A.,  
1642 Holland, F., Marno, D., Neumaier, M., 2018. The South Asian monsoon-pollution pump and  
1643 purifier. *Science* (80-. ). 361, 270-273. <https://doi.org/10.1126/science.aar2501>.
- 1644 Lelieveld, J., Evans, J.S., Fnais, M., Giannadaki, D., Pozzer, A., 2015. The contribution of outdoor  
1645 air pollution sources to premature mortality on a global scale. *Nature* 525, 367.  
1646 <https://doi.org/10.1038/nature15371>.
- 1647 Li, J., Nagashima, T., Kong, L., Ge, B., Yamaji, K., Fu, J.S., Wang, X., Fan, Q., Itahashi, S., Hyo-  
1648 Jung, L., 2019. Model evaluation and intercomparison of surface-level ozone and relevant  
1649 species in East Asia in the context of MICS-Asia Phase III-Part I: Overview. *Atmos. Chem.  
1650 Phys.* 19, 12993-13015. <https://doi.org/10.5194/acp-19-12993-2019>.
- 1651 Li, J., Chen, X., Wang, Z., Du, H., Yang, W., Sun, Y., Hu, B., Li, Jianjun, Wang, W., Wang, T., 2018.  
1652 Radiative and heterogeneous chemical effects of aerosols on ozone and inorganic aerosols over  
1653 East Asia. *Sci. Total Environ.* 622, 1327-1342. <https://doi.org/10.1016/j.scitotenv.2017.12.041>.
- 1654 Li, L., Hong, L., 2014. Role of the Radiative Effect of Black Carbon in Simulated PM<sub>2.5</sub>  
1655 Concentrations during a Haze Event in China. *Atmos. Ocean. Sci. Lett.* 7, 434-440.  
1656 <https://doi.org/10.3878/j.issn.1674-2834.14.0023>.
- 1657 Li, L., Sokolik, I.N., 2018. The Dust Direct Radiative Impact and Its Sensitivity to the Land Surface  
1658 State and Key Minerals in the WRF-Chem-DuMo Model: A Case Study of Dust Storms in  
1659 Central Asia. *J. Geophys. Res. Atmos.* 123, 4564-4582. <https://doi.org/10.1029/2017JD027667>.
- 1660 Li, M., Wang, T., Xie, M., Li, S., Zhuang, B., Chen, P., Huang, X., Han, Y., 2018. Agricultural fire  
1661 impacts on ozone photochemistry over the Yangtze River Delta region, East China. *J. Geophys.  
1662 Res. Atmos.* <https://doi.org/10.1029/2018JD028582>.
- 1663 Li, M., Wang, T., Xie, M., Li, S., Zhuang, B., Huang, X., Chen, P., Zhao, M., Liu, J., 2019. Formation  
1664 and evolution mechanisms for two extreme haze episodes in the Yangtze River Delta region of  
1665 China during winter 2016. *J. Geophys. Res. Atmos.* 124, 3607-3623.  
1666 <https://doi.org/10.1029/2019JD030535>.
- 1667 Li, M., Zhang, Q., Kurokawa, J., Woo, J.-H., 2017. MIX: a mosaic Asian anthropogenic emission  
1668 inventory under the international collaboration framework of the MICS-Asia and HTAP. *Atmos.  
1669 Chem. Phys.* 17, 935-963. <https://doi.org/10.5194/acp-17-935-2017>.
- 1670 Li, M.M., Wang, T., Han, Y., Xie, M., Li, S., Zhuang, B., Chen, P., 2017a. Modeling of a severe dust  
1671 event and its impacts on ozone photochemistry over the downstream Nanjing megacity of  
1672 eastern China. *Atmos. Environ.* 160, 107-123. <https://doi.org/10.1016/j.atmosenv.2017.04.010>.
- 1673 Li, M.M., Wang, T., Xie, M., Zhuang, B., Li, S., Han, Y., Chen, P., 2017b. Impacts of aerosol-  
1674 radiation feedback on local air quality during a severe haze episode in Nanjing megacity,  
1675 eastern China. *Tellus, Ser. B Chem. Phys. Meteorol.* 69, 1-16.  
1676 <https://doi.org/10.1080/16000889.2017.1339548>.
- 1677 Li, Z., Guo, J., Ding, A., Liao, H., Liu, J., Sun, Y., Wang, T., Xue, H., Zhang, H., Zhu, B., 2017.  
1678 Aerosol and boundary-layer interactions and impact on air quality. *Natl. Sci. Rev.* 4, 810-833.  
1679 <https://doi.org/10.1093/nsr/nwx117>.
- 1680 Li, Z., Lau, W.K.M., Ramanathan, V., Wu, G., Ding, Y., Manoj, M.G., Liu, J., Qian, Y., Li, J., Zhou,  
1681 T., Fan, J., Rosenfeld, D., Ming, Y., Wang, Y., Huang, J., Wang, B., Xu, X., Lee, S.S., Cribb,  
1682 M., Zhang, F., Yang, X., Zhao, C., Takemura, T., Wang, K., Xia, X., Yin, Y., Zhang, H., Guo,  
1683 J., Zhai, P.M., Sugimoto, N., Babu, S.S., Brasseur, G.P., 2016. Aerosol and monsoon climate  
1684 interactions over Asia. *Rev. Geophys.* 54, 866-929. <https://doi.org/10.1002/2015RG000500>.
- 1685 Li, Z., Niu, F., Fan, J., Liu, Y., Rosenfeld, D., Ding, Y., 2011. Long-term impacts of aerosols on the  
1686 vertical development of clouds and precipitation. *Nat. Geosci.* 4, 888-894.  
1687 <https://doi.org/10.1038/ngeo1313>.
- 1688 Li, Z., Wang, Y., Guo, J., Zhao, C., Cribb, M.C., Dong, X., Fan, J., Gong, D., Huang, J., Jiang, M.,  
1689 2019. East Asian study of tropospheric aerosols and their impact on regional clouds,



- 1690 precipitation, and climate (EAST-AIRCPC). *J. Geophys. Res. Atmos.* 124, 13026-13054.  
1691 <https://doi.org/10.1029/2019JD030758>.
- 1692 Liao, J., Wang, T., Wang, X., Xie, M., Jiang, Z., Huang, X., Zhu, J., 2014. Impacts of different urban  
1693 canopy schemes in WRF/Chem on regional climate and air quality in Yangtze River Delta,  
1694 China. *Atmos. Res.* 145, 226-243. <https://doi.org/10.1016/j.atmosres.2014.04.005>.
- 1695 Lin, C.-Y., Zhao, C., Liu, X., Lin, N.-H., Chen, W.-N., 2014. Modelling of long-range transport of  
1696 Southeast Asia biomass-burning aerosols to Taiwan and their radiative forcings over East Asia.  
1697 *Tellus B Chem. Phys. Meteorol.* 66, 23733. <https://doi.org/10.3402/tellusb.v66.23733>.
- 1698 Lin, N.-H., Sayer, A.M., Wang, S.-H., Loftus, A.M., Hsiao, T.-C., Sheu, G.-R., Hsu, N.C., Tsay, S.-  
1699 C., Chantara, S., 2014. Interactions between biomass-burning aerosols and clouds over  
1700 Southeast Asia: Current status, challenges, and perspectives. *Environ. Pollut.* 195, 292-307.  
1701 <https://doi.org/10.1016/j.envpol.2014.06.036>.
- 1702 Liu, C., Wang, T., Chen, P., Li, M., Zhao, M., Zhao, K., Wang, M., Yang, X., 2019. Effects of  
1703 Aerosols on the Precipitation of Convective Clouds: A Case Study in the Yangtze River Delta  
1704 of China. *J. Geophys. Res. Atmos.* 124, 7868-7885. <https://doi.org/10.1029/2018JD029924>.
- 1705 Liu, G., Shao, H., Coakley Jr, J.A., Curry, J.A., Haggerty, J.A., Tschudi, M.A., 2003. Retrieval of  
1706 cloud droplet size from visible and microwave radiometric measurements during INDOEX:  
1707 Implication to aerosols' indirect radiative effect. *J. Geophys. Res. Atmos.* 108, AAC-2.  
1708 <https://doi.org/10.1029/2001JD001395>.
- 1709 Liu, L., Bai, Y., Lin, C., Yang, H., 2018. Evaluation of Regional Air Quality Numerical Forecasting  
1710 System in Central China and Its Application for Aerosol Radiative Effect. *Meteorol. Mon.* 44,  
1711 1179-1190. <https://doi.org/10.7519/j.issn.1000-0526.2018.09.006>.
- 1712 Liu, L., Huang, X., Ding, A., Fu, C., 2016. Dust-induced radiative feedbacks in north China : A dust  
1713 storm episode modeling study using WRF-Chem. *Atmos. Environ.* 129, 43-54.  
1714 <https://doi.org/10.1016/j.atmosenv.2016.01.019>.
- 1715 Liu, Q., Jia, X., Quan, J., Li, J., Li, X., Wu, Y., Chen, D., Wang, Z., Liu, Y., 2018. New positive  
1716 feedback mechanism between boundary layer meteorology and secondary aerosol formation  
1717 during severe haze events. *Sci. Rep.* 8, 1-8. <https://doi.org/10.1038/s41598-018-24366-3>.
- 1718 Liu, X., Zhang, Y., Zhang, Q., He, K., 2016. Application of online-coupled WRF/Chem-MADRID  
1719 in East Asia : Model evaluation and climatic effects of anthropogenic aerosols. *Atmos. Environ.*  
1720 124, 321-336. <https://doi.org/10.1016/j.atmosenv.2015.03.052>.
- 1721 Liu, Z., Yi, M., Zhao, C., Lau, N.C., Guo, J., Bollasina, M., Yim, S.H.L., 2020. Contribution of local  
1722 and remote anthropogenic aerosols to a record-breaking torrential rainfall event in Guangdong  
1723 Province, China. *Atmos. Chem. Phys.* 20, 223-241. <https://doi.org/10.5194/acp-20-223-2020>.
- 1724 Liu, Z., Yim, S.H.L., Wang, C., Lau, N.C., 2018. The Impact of the Aerosol Direct Radiative Forcing  
1725 on Deep Convection and Air Quality in the Pearl River Delta Region. *Geophys. Res. Lett.* 45,  
1726 4410-4418. <https://doi.org/10.1029/2018GL077517>.
- 1727 Lohmann, U., Diehl, K., 2006. Sensitivity studies of the importance of dust ice nuclei for the indirect  
1728 aerosol effect on stratiform mixed-phase clouds. *J. Atmos. Sci.* 63, 968-982.  
1729 <https://doi.org/10.1175/JAS3662.1>.
- 1730 Lohmann, U., Feichter, J., 2005. Global indirect aerosol effects: a review. *Atmos. Chem. Phys.* 5,  
1731 715-737. <https://doi.org/10.5194/acp-5-715-2005>.
- 1732 Ma, X., Chen, D., Wen, W., Sheng, L., Hu, J., Tong, H., Wei, P., 2016. Effect of Particle Pollution  
1733 on Regional Meteorological Factors in China. *J. Beijing Univ. Technol.* 285-295.  
1734 <https://doi.org/10.11936/bjtxb2015040075>.
- 1735 Ma, X., Wen, W., 2017. Modelling the Effect of Black Carbon and Sulfate Aerosol on the Regional  
1736 Meteorology Factors, in: IOP Conf. Ser. Earth Environ. Sci. p. 12002.  
1737 <https://doi.org/10.1088/1755-1315/78/1/012002>.
- 1738 Mailler, S., Menut, L., Khvorostyanov, D., Valari, M., Couvidat, F., Siour, G., Turquety, S., Briant,  
1739 R., Tuccella, P., Bessagnet, B., 2017. CHIMERE-2017: from urban to hemispheric chemistry-  
1740 transport modeling. *Geosci. Model Dev.* 10, 2397-2423. <https://doi.org/10.5194/gmd-10-2397-2017>.
- 1741 Makar, P.A., Gong, W., Hogrefe, C., Zhang, Y., Curci, G., Žabkar, R., Milbrandt, J., Im, U., Balzarini,  
1742 A., Baró, R., Bianconi, R., Cheung, P., Forkel, R., Gravel, S., Hirtl, M., Honzak, L., Hou, A.,  
1743 Jiménez-Guerrero, P., Langer, M., Moran, M.D., Pabla, B., Pérez, J.L., Pirovano, G., San José,  
1744 R., Tuccella, P., Werhahn, J., Zhang, J., Galmarini, S., 2015a. Feedbacks between air pollution  
1745 and weather, part 2: Effects on chemistry. *Atmos. Environ.* 115, 499-526.



- 1747 <https://doi.org/10.1016/j.atmosenv.2014.10.021>.
- 1748 Makar, P.A., Gong, W., Milbrandt, J., Hogrefe, C., Zhang, Y., Curci, G., Žabkar, R., Im, U., Balzarini,  
1749 A., Baró, R., Bianconi, R., Cheung, P., Forkel, R., Gravel, S., Hirtl, M., Honzak, L., Hou, A.,  
1750 Jiménez-Guerrero, P., Langer, M., Moran, M.D., Pabla, B., Pérez, J.L., Pirovano, G., San José,  
1751 R., Tuccella, P., Werhahn, J., Zhang, J., Galmarini, S., 2015b. Feedbacks between air pollution  
1752 and weather, Part 1: Effects on weather. *Atmos. Environ.* 115, 442-469.  
1753 <https://doi.org/10.1016/j.atmosenv.2014.12.003>.
- 1754 Manisalidis, I., Stavropoulou, E., Stavropoulos, A., Bezirtzoglou, E., 2020. Environmental and  
1755 health impacts of air pollution: A review. *Front. public Heal.* 8.  
1756 <https://doi.org/10.3389/fpubh.2020.00014>.
- 1757 Martin, D.E., Leight, W.G., 1949. Objective temperature estimates from mean circulation patterns.  
1758 *Mon. Weather Rev.* 77, 275-283. [https://doi.org/10.1175/1520-0493\(1949\)077<0275:OTEFMC>2.0.CO;2](https://doi.org/10.1175/1520-0493(1949)077<0275:OTEFMC>2.0.CO;2).
- 1760 Mass, C., Ovens, D., 2011. Fixing WRF's high speed wind bias: A new subgrid scale drag  
1761 parameterization and the role of detailed verification, in: 24th Conference on Weather and  
1762 Forecasting and 20th Conference on Numerical Weather Prediction, Preprints, 91st American  
1763 Meteorological Society Annual Meeting.
- 1764 McCormick, R.A., Ludwig, J.H., 1967. Climate modification by atmospheric aerosols. *Science*  
1765 (80-. ). 156, 1358-1359. <https://doi.org/10.1126/science.156.3780.1358>.
- 1766 Miao, Y., Guo, J., Liu, S., Zhao, C., Li, X., Zhang, G., Wei, W., Ma, Y., 2018. Impacts of synoptic  
1767 condition and planetary boundary layer structure on the trans-boundary aerosol transport from  
1768 Beijing-Tianjin-Hebei region to northeast China. *Atmos. Environ.* 181, 1-11.  
1769 <https://doi.org/10.1016/j.atmosenv.2018.03.005>.
- 1770 Miao, Y., Liu, S., Zheng, Y., Wang, S., 2016. Modeling the feedback between aerosol and boundary  
1771 layer processes: a case study in Beijing, China. *Environ. Sci. Pollut. Res.* 23, 3342-3357.  
1772 <https://doi.org/10.1007/s11356-015-5562-8>.
- 1773 Nguyen, G.T.H., Shimadera, H., Sekiguchi, A., Matsuo, T., Kondo, A., 2019a. Investigation of  
1774 aerosol direct effects on meteorology and air quality in East Asia by using an online coupled  
1775 modeling system. *Atmos. Environ.* 207, 182-196.  
1776 <https://doi.org/10.1016/j.atmosenv.2019.03.017>.
- 1777 Nguyen, G.T.H., Shimadera, H., Uranishi, K., Matsuo, T., Kondo, A., Thepanondh, S., 2019b.  
1778 Numerical assessment of PM<sub>2.5</sub> and O<sub>3</sub> air quality in continental Southeast Asia: Baseline  
1779 simulation and aerosol direct effects investigation. *Atmos. Environ.* 219, 117054.  
1780 <https://doi.org/10.1016/j.atmosenv.2019.117054>.
- 1781 North, G.R., Pyle, J.A., Zhang, F., 2014. *Encyclopedia of atmospheric sciences*. Elsevier.
- 1782 Park, S.-Y., Lee, H.-J., Kang, J.-E., Lee, T., Kim, C.-H., 2018. Aerosol radiative effects on mesoscale  
1783 cloud-precipitation variables over Northeast Asia during the MAPS-Seoul 2015 campaign.  
1784 *Atmos. Environ.* 172, 109-123. <https://doi.org/10.1016/j.atmosenv.2017.10.044>.
- 1785 Penner, J.E., Dong, X., Chen, Y., 2004. Observational evidence of a change in radiative forcing due  
1786 to the indirect aerosol effect. *Nature* 427, 231-234. <https://doi.org/10.1038/nature02234>.
- 1787 Qiu, Y., Liao, H., Zhang, R., Hu, J., 2017. Simulated impacts of direct radiative effects of scattering  
1788 and absorbing aerosols on surface layer aerosol concentrations in China during a heavily  
1789 polluted event in february 2014. *J. Geophys. Res.* 122, 5955-5975.  
1790 <https://doi.org/10.1002/2016JD026309>.
- 1791 Quaas, J., Boucher, O., Bellouin, N., Kinne, S., 2008. Satellite-based estimate of the direct and  
1792 indirect aerosol climate forcing. *J. Geophys. Res. Atmos.* 113.  
1793 <https://doi.org/10.1029/2007JD008962>.
- 1794 Reid, J.S., Koppmann, R., Eck, T.F., Eleuterio, D.P., 2005. A review of biomass burning emissions  
1795 part II: intensive physical properties of biomass burning particles. *Atmos. Chem. Phys.* 5, 799-  
1796 825. <https://doi.org/10.5194/acp-5-799-2005>.
- 1797 Rohde, R.A., Muller, R.A., 2015. Air pollution in China: mapping of concentrations and sources.  
1798 *PLoS One* 10, e0135749. <https://doi.org/10.1371/journal.pone.0135749>.
- 1799 Rosenfeld, D., 2000. Suppression of rain and snow by urban and industrial air pollution. *Science*  
1800 (80-. ). 287, 1793-1796. <https://doi.org/10.1126/science.287.5459.1793>.
- 1801 Rosenfeld, D., Andreae, M.O., Asmi, A., Chin, M., de Leeuw, G., Donovan, D.P., Kahn, R., Kinne,  
1802 S., Kivekäs, N., Kulmala, M., 2014. Global observations of aerosol-cloud-precipitation-climate  
1803 interactions. *Rev. Geophys.* 52, 750-808. <https://doi.org/10.1002/2013RG000441>.



- 1804 Rosenfeld, D., Lohmann, U., Raga, G.B., O'Dowd, C.D., Kulmala, M., Fuzzi, S., Reissell, A.,  
1805 Andreae, M.O., 2008. Flood or drought: How do aerosols affect precipitation? *Science* (80-. ).  
1806 321, 1309-1313. <https://doi.org/10.1126/science.1160606>.
- 1807 Rosenfeld, D., Zhu, Y., Wang, M., Zheng, Y., Goren, T., Yu, S., 2019. Aerosol-driven droplet  
1808 concentrations dominate coverage and water of oceanic low-level clouds. *Science* (80-. ). 363.  
1809 <https://doi.org/10.1126/science.aav0566>.
- 1810 Saleh, R., Robinson, E.S., Tkacik, D.S., Ahern, A.T., Liu, S., Aiken, A.C., Sullivan, R.C., Presto,  
1811 A.A., Dubey, M.K., Yokelson, R.J., 2014. Brownness of organics in aerosols from biomass  
1812 burning linked to their black carbon content. *Nat. Geosci.* 7, 647-650.  
1813 <https://doi.org/10.1038/ngeo2220>.
- 1814 Sanchez-Romero, A., Sanchez-Lorenzo, A., Calbó, J., González, J.A., Azorin-Molina, C., 2014. The  
1815 signal of aerosol-induced changes in sunshine duration records: A review of the evidence. *J.*  
1816 *Geophys. Res. Atmos.* 119, 4657-4673. <https://doi.org/10.1002/2013JD021393>.
- 1817 Sarangi, C., Tripathi, S.N., Tripathi, S., Barth, M.C., 2015. Aerosol-cloud associations over Gangetic  
1818 Basin during a typical monsoon depression event using WRF-Chem simulation. *J. Geophys.*  
1819 *Res. Atmos.* 120, 10-974. <https://doi.org/10.1002/2015JD023634>.
- 1820 Satheesh, S.K., Moorthy, K.K., 2005. Radiative effects of natural aerosols: A review. *Atmos.*  
1821 *Environ.* 39, 2089-2110. <https://doi.org/10.1016/j.atmosenv.2004.12.029>.
- 1822 Sato, Y., Suzuki, K., 2019. How do aerosols affect cloudiness? *Science* (80-. ). 363, 580-581.  
1823 <https://doi.org/10.1126/science.aaw3720>.
- 1824 Saylor, R.D., Baker, B.D., Lee, P., Tong, D., Pan, L., Hicks, B.B., 2019. The particle dry deposition  
1825 component of total deposition from air quality models: right, wrong or uncertain? *Tellus B*  
1826 *Chem. Phys. Meteorol.* 71, 1550324. <https://doi.org/10.1080/16000889.2018.1550324>.
- 1827 Seaman, N.L., 2000. Meteorological modeling for air-quality assessments. *Atmos. Environ.* 34,  
1828 2231-2259. [https://doi.org/10.1016/S1352-2310\(99\)00466-5](https://doi.org/10.1016/S1352-2310(99)00466-5).
- 1829 Seethala, C., Pandithurai, G., Fast, J.D., Polade, S.D., Reddy, M.S., Peckham, S.E., 2011. Evaluating  
1830 WRF-Chem multi-scale model in simulating aerosol radiative properties over the tropics-a case  
1831 study over India. *Mapan* 26, 269-284. <https://doi.org/10.1007/s12647-011-0025-2>.
- 1832 Sekiguchi, A., Shimadera, H., Kondo, A., 2018. Impact of aerosol direct effect on wintertime PM<sub>2.5</sub>  
1833 simulated by an online coupled meteorology-air quality model over east asia. *Aerosol Air Qual.*  
1834 *Res.* 18, 1068-1079. <https://doi.org/10.4209/aaqr.2016.06.0282>.
- 1835 Sekiguchi, M., Nakajima, T., Suzuki, K., Kawamoto, K., Higurashi, A., Rosenfeld, D., Sano, I.,  
1836 Mukai, S., 2003. A study of the direct and indirect effects of aerosols using global satellite data  
1837 sets of aerosol and cloud parameters. *J. Geophys. Res. Atmos.* 108.  
1838 <https://doi.org/10.1029/2002JD003359>.
- 1839 Shahid, M.Z., Shahid, I., Chishtie, F., Shahzad, M.I., Bulbul, G., 2019. Analysis of a dense haze  
1840 event over North-eastern Pakistan using WRF-Chem model and remote sensing. *J. Atmos.*  
1841 *Solar-Terrestrial Phys.* 182, 229-241. <https://doi.org/10.1016/j.jastp.2018.12.007>.
- 1842 Shao, Y., Dong, C.H., 2006. A review on East Asian dust storm climate, modelling and monitoring.  
1843 *Glob. Planet. Change* 52, 1-22. <https://doi.org/10.1016/j.gloplacha.2006.02.011>.
- 1844 Shen, H., Shi, Huawei, Shi, Huading, Ma, X., 2015. Simulation Study of Influence of Aerosol  
1845 Pollution on Regional Meteorological Factors in Beijing-Tianjin-Hebei Region. *J. Anhui Agric.*  
1846 *Sci.* 43, 207-210. <https://doi.org/10.13989/j.cnki.0517-6611.2015.25.217>.
- 1847 Shen, X., Jiang, X., Liu, D., Zu, F., Fan, S., 2017. Simulations of Anthropogenic Aerosols Effects  
1848 on the Intensity and Precipitation of Typhoon Fitow (1323) Using WRF-Chem Model. *Chinese*  
1849 *J. Atmos. Sci.* 41, 960-974. <https://doi.org/10.3878/j.issn.1006-9895.1703.16216>.
- 1850 Singh, P., Sarawade, P., Adhikary, B., 2020. Carbonaceous Aerosol from Open Burning and its  
1851 Impact on Regional Weather in South Asia. *Aerosol Air Qual. Res.* 20, 419-431.  
1852 <https://doi.org/10.4209/aaqr.2019.03.0146>.
- 1853 Soni, P., Tripathi, S.N., Srivastava, R., 2018. Radiative effects of black carbon aerosols on Indian  
1854 monsoon: a study using WRF-Chem model. *Theor. Appl. Climatol.* 132, 115-134.  
1855 <https://doi.org/10.1007/s00704-017-2057-1>.
- 1856 Srinivas, R., Panicker, A.S., Parkhi, N.S., Peshin, S.K., Beig, G., 2016. Sensitivity of online coupled  
1857 model to extreme pollution event over a mega city Delhi. *Atmos. Pollut. Res.* 7, 25-30.  
1858 <https://doi.org/10.1016/j.apr.2015.07.001>.
- 1859 Stephens, G.L., Li, J., Wild, M., Clayson, C.A., Loeb, N., Kato, S., L'ecuyer, T., Stackhouse, P.W.,  
1860 Lebsock, M., Andrews, T., 2012. An update on Earth's energy balance in light of the latest



- 1861 global observations. *Nat. Geosci.* 5, 691-696. <https://doi.org/10.1038/ngeo1580>.
- 1862 Su, L., Fung, J.C.H., 2018a. Investigating the role of dust in ice nucleation within clouds and further  
1863 effects on the regional weather system over East Asia--Part 2: modification of the weather  
1864 system. *Atmos. Chem. Phys.* 18. <https://doi.org/10.5194/acp-18-11529-2018>.
- 1865 Su, L., Fung, J.C.H., 2018b. Investigating the role of dust in ice nucleation within clouds and further  
1866 effects on the regional weather system over East Asia--Part 1: model development and  
1867 validation. *Atmos. Chem. Phys.* 18. <https://doi.org/10.5194/acp-18-8707-2018>.
- 1868 Sud, Y.C., Walker, G.K., 1990. A review of recent research on improvement of physical  
1869 parameterizations in the GLA GCM.
- 1870 Sun, K., Liu, H., Wang, X., Peng, Z., Xiong, Z., 2017. The aerosol radiative effect on a severe haze  
1871 episode in the Yangtze River Delta. *J. Meteorol. Res.* 31, 865-873.  
1872 <https://doi.org/10.1007/s13351-017-7007-4>.
- 1873 Takemura, T., Nakajima, T., Higurashi, A., Ohta, S., Sugimoto, N., 2003. Aerosol distributions and  
1874 radiative forcing over the Asian Pacific region simulated by Spectral Radiation-Transport  
1875 Model for Aerosol Species (SPRINTARS). *J. Geophys. Res. Atmos.* 108.  
1876 <https://doi.org/10.1029/2002JD003210>.
- 1877 Tang, Y., Han, Y., Ma, X., Liu, Z., 2018. Elevated heat pump effects of dust aerosol over  
1878 Northwestern China during summer. *Atmos. Res.* 203, 95-104.  
1879 <https://doi.org/10.1016/j.atmosres.2017.12.004>.
- 1880 Thompson, G., Eidhammer, T., 2014. A study of aerosol impacts on clouds and precipitation  
1881 development in a large winter cyclone. *J. Atmos. Sci.* 71, 3636-3658.  
1882 <https://doi.org/10.1175/JAS-D-13-0305.1>.
- 1883 Tremback, C., Tripoli, G., Arritt, R., Cotton, W.R., Pielke, R.A., 1986. The regional atmospheric  
1884 modeling system, in: Proceedings of an International Conference on Development Applications  
1885 of Computer Techniques Environmental Studies. Computational Mechanics Publication,  
1886 Rewood Burn Ltd, pp. 601-607.
- 1887 Tsay, S.-C., Hsu, N.C., Lau, W.K.-M., Li, C., Gabriel, P.M., Ji, Q., Holben, B.N., Welton, E.J.,  
1888 Nguyen, A.X., Janjai, S., 2013. From BASE-ASIA toward 7-SEAS: A satellite-surface  
1889 perspective of boreal spring biomass-burning aerosols and clouds in Southeast Asia. *Atmos.*  
1890 *Environ.* 78, 20-34. <https://doi.org/10.1016/j.atmosenv.2012.12.013>.
- 1891 Twomey, S., 1977. The influence of pollution on the shortwave albedo of clouds. *J. Atmos. Sci.* 34,  
1892 1149-1152. [https://doi.org/10.1175/1520-0469\(1977\)034<1149:TIOPOT>2.0.CO;2](https://doi.org/10.1175/1520-0469(1977)034<1149:TIOPOT>2.0.CO;2).
- 1893 Uno, I., Wang, Z., Chiba, M., Chun, Y.S., Gong, S.L., Hara, Y., Jung, E., Lee, S., Liu, M., Mikami,  
1894 M., 2006. Dust model intercomparison (DMIP) study over Asia: Overview. *J. Geophys. Res.*  
1895 *Atmos.* 111. <https://doi.org/10.1029/2005JD006575>.
- 1896 Wang, D., Jiang, B., Lin, W., Gu, F., 2019. Effects of aerosol-radiation feedback and topography  
1897 during an air pollution event over the North China Plain during December 2017. *Atmos. Pollut.*  
1898 *Res.* 10, 587-596. <https://doi.org/10.1016/j.apr.2018.10.006>.
- 1899 Wang, H., Niu, T., 2013. Sensitivity studies of aerosol data assimilation and direct radiative  
1900 feedbacks in modeling dust aerosols. *Atmos. Environ.* 64, 208-218.  
1901 <https://doi.org/10.1016/j.atmosenv.2012.09.066>.
- 1902 Wang, H., Peng, Y., Zhang, X., Liu, H., Zhang, M., Che, H., Cheng, Y., Zheng, Y., 2018.  
1903 Contributions to the explosive growth of PM<sub>2.5</sub> mass due to aerosol-radiation feedback and  
1904 decrease in turbulent diffusion during a red alert heavy haze in Beijing-Tianjin-Hebei, China.  
1905 *Atmos. Chem. Phys.* 18, 17717-17733. <https://doi.org/10.5194/acp-18-17717-2018>.
- 1906 Wang, H., Shi, G., Zhu, J., Chen, B., Che, H., Zhao, T., 2013. Case study of longwave contribution  
1907 to dust radiative effects over East Asia. *Chinese Sci. Bull.* 58, 3673-3681.  
1908 <https://doi.org/10.1007/s11434-013-5752-z>.
- 1909 Wang, H., Shi, G.Y., Zhang, X.Y., Gong, S.L., Tan, S.C., Chen, B., Che, H.Z., Li, T., 2015a.  
1910 Mesoscale modelling study of the interactions between aerosols and PBL meteorology during  
1911 a haze episode in China Jing-Jin-Ji and its near surrounding region-Part 2: Aerosols' radiative  
1912 feedback effects. *Atmos. Chem. Phys.* 15, 3277-3287. <https://doi.org/10.5194/acp-15-3277-2015>.
- 1913  
1914 Wang, H., Xue, M., Zhang, X.Y., Liu, H.L., Zhou, C.H., Tan, S.C., Che, H.Z., Chen, B., Li, T., 2015b.  
1915 Mesoscale modeling study of the interactions between aerosols and PBL meteorology during  
1916 a haze episode in Jing-Jin-Ji (China) and its nearby surrounding region-Part 1: Aerosol  
1917 distributions and meteorological features. *Atmos. Chem. Phys.* 15, 3257-3275.



- 1918 <https://doi.org/10.5194/acp-15-3257-2015>.
- 1919 Wang, H., Zhang, X., Gong, S., Chen, Y., Shi, G., Li, W., 2010. Radiative feedback of dust aerosols  
1920 on the East Asian dust storms. *J. Geophys. Res. Atmos.* 115.  
1921 <https://doi.org/10.1029/2009JD013430>.
- 1922 Wang, J., Allen, D.J., Pickering, K.E., Li, Z., He, H., 2016. Impact of aerosol direct effect on East  
1923 Asian air quality during the EAST-AIRE campaign. *J. Geophys. Res. Atmos.* 121, 6534-6554.  
1924 <https://doi.org/10.1002/2016JD025108>.
- 1925 Wang, J., Wang, S., Jiang, J., Ding, A., Zheng, M., Zhao, B., Wong, D.C., Zhou, W., Zheng, G.,  
1926 Wang, L., Pleim, J.E., Hao, J., 2014. Impact of aerosol-meteorology interactions on fine  
1927 particle pollution during China's severe haze episode in January 2013. *Environ. Res. Lett.* 9.  
1928 <https://doi.org/10.1088/1748-9326/9/9/094002>.
- 1929 Wang, J., Xing, J., Mathur, R., Pleim, J.E., Wang, S., Hogrefe, C., Gan, C.-M., Wong, D.C., Hao, J.,  
1930 2017. Historical trends in PM<sub>2.5</sub>-related premature mortality during 1990-2010 across the  
1931 northern hemisphere. *Environ. Health Perspect.* 125, 400-408. <https://doi.org/10.1289/EHP298>.
- 1932 Wang, K., Yahya, K., Zhang, Y., Hogrefe, C., Pouliot, G., Knote, C., Hodzic, A., San Jose, R., Perez,  
1933 J.L., Jiménez-Guerrero, P., 2015. A multi-model assessment for the 2006 and 2010 simulations  
1934 under the Air Quality Model Evaluation International Initiative (AQMEII) Phase 2 over North  
1935 America: Part II. Evaluation of column variable predictions using satellite data. *Atmos.*  
1936 *Environ.* 115, 587-603. <https://doi.org/10.1016/j.atmosenv.2014.07.044>.
- 1937 Wang, K., Zhang, Y., Zhang, X., Fan, J., Leung, L.R., Zheng, B., Zhang, Q., He, K., 2018. Fine-  
1938 scale application of WRF-CAM5 during a dust storm episode over East Asia: Sensitivity to  
1939 grid resolutions and aerosol activation parameterizations. *Atmos. Environ.* 176, 1-20.  
1940 <https://doi.org/10.1016/j.atmosenv.2017.12.014>.
- 1941 Wang, L., Fu, J.S., Wei, W., Wei, Z., Meng, C., Ma, S., Wang, J., 2018. How aerosol direct effects  
1942 influence the source contributions to PM<sub>2.5</sub> concentrations over Southern Hebei, China in  
1943 severe winter haze episodes. *Front. Environ. Sci. Eng.* 12, 13. <https://doi.org/10.1007/s11783-018-1014-2>.
- 1945 Wang, Z., Huang, X., Ding, A., 2019. Optimization of vertical grid setting for air quality modelling  
1946 in China considering the effect of aerosol-boundary layer interaction. *Atmos. Environ.* 210, 1-  
1947 13. <https://doi.org/10.1016/j.atmosenv.2019.04.042>.
- 1948 Wang, Z., Huang, X., Ding, A., 2018. Dome effect of black carbon and its key influencing factors:  
1949 a one-dimensional modelling study. *Atmos. Chem. Phys.* 18, 2821. <https://doi.org/10.5194/acp-18-2821-2018>.
- 1950
- 1951 Wang, Z.F., Li, J., Wang, Z., Yang, W., Tang, X., Ge, B., Yan, P., Zhu, L., Chen, X., Chen, H., 2014.  
1952 Modeling study of regional severe hazes over mid-eastern China in January 2013 and its  
1953 implications on pollution prevention and control. *Sci. China Earth Sci.* 57, 3-13.  
1954 <https://doi.org/10.1007/s11430-013-4793-0>.
- 1955 Wang, Z., Wang, Zhe, Li, Jie, Zheng, H., Yan, P., Li, J., 2014. Development of a meteorology-  
1956 chemistry two-way coupled numerical model (WRF-NAQPMS) and its application in a severe  
1957 autumn haze simulation over the Beijing-Tianjin-Hebei area, China. *Clim. Environ. Res.* 19,  
1958 153-163. <https://doi.org/10.3878/j.issn.1006-9585.2014.13231>.
- 1959 Wendisch, M., Keil, A., Müller, D., Wandinger, U., Wendling, P., Stifter, A., Petzold, A., Fiebig, M.,  
1960 Wiegner, M., Freudenthaler, V., 2002. Aerosol-radiation interaction in the cloudless  
1961 atmosphere during LACE 98 1. Measured and calculated broadband solar and spectral surface  
1962 insulations. *J. Geophys. Res. Atmos.* 107, LAC-6. <https://doi.org/10.1029/2000JD000226>.
- 1963 Wilcox, E.M., 2012. Direct and semi-direct radiative forcing of smoke aerosols over clouds. *Atmos.*  
1964 *Chem. Phys.* 12, 139. <https://doi.org/10.5194/acp-12-139-2012>.
- 1965 Wong, D.C., Pleim, J., Mathur, R., Binkowski, F., Otte, T., Gilliam, R., Pouliot, G., Xiu, A., Young,  
1966 J.O., Kang, D., 2012. WRF-CMAQ two-way coupled system with aerosol feedback: software  
1967 development and preliminary results. *Geosci. Model Dev.* 5, 299. <https://doi.org/10.5194/gmd-5-299-2012>.
- 1968
- 1969 Wu, J., Bei, N., Hu, B., Liu, S., Zhou, M., Wang, Q., Li, X., Lang, L., Tian, F., Liu, Z., 2019a.  
1970 Aerosol-radiation feedback deteriorates the wintertime haze in the North China Plain. *Atmos.*  
1971 *Chem. Phys.* 19, 8703-8719. <https://doi.org/10.5194/acp-19-8703-2019>.
- 1972 Wu, J., Bei, N., Hu, B., Liu, S., Zhou, M., Wang, Q., Li, X., Liu, L., Feng, T., Liu, Z., Wang, Y., Cao,  
1973 J., Tie, X., Wang, J., Molina, L.T., Li, G., 2019b. Is water vapor a key player of the wintertime  
1974 haze in North China Plain? *Atmos. Chem. Phys.* 19, 8721-8739. <https://doi.org/10.5194/acp-19-8721-2019>.



- 1975 19-8721-2019
- 1976 Wu, L., Su, H., Jiang, J.H., 2013. Regional simulation of aerosol impacts on precipitation during the
- 1977 East Asian summer monsoon. *J. Geophys. Res. Atmos.* 118, 6454-6467.
- 1978 <https://doi.org/10.1002/jgrd.50527>.
- 1979 Wu, W., Zhang, Y., 2018. Effects of particulate matter (PM<sub>2.5</sub>) and associated acidity on ecosystem
- 1980 functioning: response of leaf litter breakdown. *Environ. Sci. Pollut. Res.* 25, 30720-30727.
- 1981 <https://doi.org/10.1007/s11356-018-2922-1>.
- 1982 Wu, Y., Han, Y., Voulgarakis, A., Wang, T., Li, M., Wang, Y., Xie, M., Zhuang, B., Li, S., 2017. An
- 1983 agricultural biomass burning episode in eastern China: Transport, optical properties, and
- 1984 impacts on regional air quality. *J. Geophys. Res. Atmos.* 122, 2304-2324.
- 1985 <https://doi.org/10.1002/2016JD025319>.
- 1986 Xie, M., Liao, J., Wang, T., Zhu, K., Zhuang, B., Han, Y., Li, M., Li, S., 2016. Modeling of the
- 1987 anthropogenic heat flux and its effect on regional meteorology and air quality over the Yangtze
- 1988 River Delta region, China. *Atmos. Chem. Phys.* 16, 6071. [https://doi.org/10.5194/acp-16-6071-](https://doi.org/10.5194/acp-16-6071-2016)
- 1989 2016.
- 1990 Xing, J., Mathur, R., Pleim, J., Hogrefe, C., Gan, C.-M., Wong, D.-C., Wei, C., Gilliam, R., Pouliot,
- 1991 G., 2015a. Observations and modeling of air quality trends over 1990-2010 across the Northern
- 1992 Hemisphere: China, the United States and Europe. *Atmos. Chem. Phys.* 15,
- 1993 <https://doi.org/10.5194/acp-15-2723-2015>.
- 1994 Xing, J., Mathur, R., Pleim, J., Hogrefe, C., Gan, C., Wong, D.C., Wei, C., Wang, J., 2015b. Air
- 1995 pollution and climate response to aerosol direct radiative effects: A modeling study of decadal
- 1996 trends across the northern hemisphere. *J. Geophys. Res. Atmos.* 120, 12-221.
- 1997 <https://doi.org/10.1002/2015JD023933>.
- 1998 Xing, J., Mathur, R., Pleim, J., Hogrefe, C., Gan, C.M., Wong, D.C., Wei, C., 2015c. Can a coupled
- 1999 meteorology-chemistry model reproduce the historical trend in aerosol direct radiative effects
- 2000 over the Northern Hemisphere? *Atmos. Chem. Phys.* 15, 9997-10018.
- 2001 <https://doi.org/10.5194/acp-15-9997-2015>.
- 2002 Xing, J., Wang, J., Mathur, R., Pleim, J., Wang, S., Hogrefe, C., Gan, C.-M., Wong, D.C., Hao, J.,
- 2003 2016. Unexpected benefits of reducing aerosol cooling effects. *Environ. Sci. Technol.* 50,
- 2004 [7527-7534. https://doi.org/10.1021/acs.est.6b00767](https://doi.org/10.1021/acs.est.6b00767).
- 2005 Xing, J., Wang, J., Mathur, R., Wang, S., Sarwar, G., Pleim, J., Hogrefe, C., Zhang, Y., Jiang, J.,
- 2006 Wong, D.C., 2017. Impacts of aerosol direct effects on tropospheric ozone through changes in
- 2007 atmospheric dynamics and photolysis rates. *Atmos. Chem. Phys.* 17, 9869.
- 2008 <https://doi.org/10.5194/acp-17-9869-2017>.
- 2009 Yahya, K., Wang, K., Gudoshava, M., Glotfelty, T., Zhang, Y., 2015. Application of WRF/Chem
- 2010 over North America under the AQMEII Phase 2: Part I. Comprehensive evaluation of 2006
- 2011 simulation. *Atmos. Environ.* 115, 733-755. <https://doi.org/10.1016/j.atmosenv.2014.08.063>.
- 2012 Yan, J., Wang, X., Gong, P., Wang, C., Cong, Z., 2018. Review of brown carbon aerosols: Recent
- 2013 progress and perspectives. *Sci. Total Environ.* 634, 1475-1485.
- 2014 <https://doi.org/10.1016/j.scitotenv.2018.04.083>.
- 2015 Yang, J., Duan, K., Kang, S., Shi, P., Ji, Z., 2017. Potential feedback between aerosols and
- 2016 meteorological conditions in a heavy pollution event over the Tibetan Plateau and Indo-
- 2017 Gangetic Plain. *Clim. Dyn.* 48, 2901-2917. <https://doi.org/10.1007/s00382-016-3240-2>.
- 2018 Yang, J., Kang, S., Ji, Z., Chen, D., 2018. Modeling the origin of anthropogenic black carbon and
- 2019 its climatic effect over the Tibetan Plateau and surrounding regions. *J. Geophys. Res. Atmos.*
- 2020 123, 671-692. <https://doi.org/10.1002/2017JD027282>.
- 2021 Yang, T., Liu, Y., 2017a. Mechanism analysis of the impacts of aerosol direct effects on a rainstorm.
- 2022 *J. Trop. Meteorol.* 33, 762-773. <https://doi.org/10.16032/j.issn.1004-4965.2017.05.019>.
- 2023 Yang, T., Liu, Y., 2017b. Impact of anthropogenic pollution on “7.21” extreme heavy rainstorm. *J.*
- 2024 *Meteorol. Sci.* 742-752. <https://doi.org/10.3969/2016jms.0074>.
- 2025 Yang, Y., Fan, J., Leung, L.R., Zhao, C., Li, Z., Rosenfeld, D., 2016. Mechanisms contributing to
- 2026 suppressed precipitation in Mt. Hua of central China. Part I: Mountain valley circulation. *J.*
- 2027 *Atmos. Sci.* 73, 1351-1366. <https://doi.org/10.1175/JAS-D-15-0233.1>.
- 2028 Yang, Y., Tang, J., Sun, J., Wang, L., Wang, X., Zhang, Y., Qu, Q., Zhao, W., 2015. Synoptic Effect
- 2029 of a Heavy Haze Episode over North China. *Clim. Environ. Res.*
- 2030 <https://doi.org/10.3878/j.issn.1006-9585.2015.15018>.
- 2031 Yang, Y., Zhao, C., Dong, X., Fan, G., Zhou, Y., Wang, Y., Zhao, L., Lv, F., Yan, F., 2019. Toward



- 2032 understanding the process-level impacts of aerosols on microphysical properties of shallow  
2033 cumulus cloud using aircraft observations. *Atmos. Res.* 221, 27-33.  
2034 <https://doi.org/10.1016/j.atmosres.2019.01.027>.
- 2035 Yao, H., Song, Y., Liu, M., Archer-Nicholls, S., Lowe, D., McFiggans, G., Xu, T., Du, P., Li, J., Wu,  
2036 Y., 2017. Direct radiative effect of carbonaceous aerosols from crop residue burning during the  
2037 summer harvest season in East China. *Atmos. Chem. Phys.* 17, 5205.  
2038 <https://doi.org/10.5194/acp-17-5205-2017>.
- 2039 Yasunari, T.J., Yamazaki, K., 2009. Impacts of Asian dust storm associated with the stratosphere-to-  
2040 troposphere transport in the spring of 2001 and 2002 on dust and tritium variations in Mount  
2041 Wrangell ice core, Alaska. *Atmos. Environ.* 43, 2582-2590.  
2042 <https://doi.org/10.1016/j.atmosenv.2009.02.025>.
- 2043 Yiğit, E., Knížová, P.K., Georgieva, K., Ward, W., 2016. A review of vertical coupling in the  
2044 Atmosphere-Ionosphere system: Effects of waves, sudden stratospheric warmings, space  
2045 weather, and of solar activity. *J. Atmos. Solar-Terrestrial Phys.* 141, 1-12.  
2046 <https://doi.org/10.1016/j.jastp.2016.02.011>.
- 2047 Yoo, J.-W., Jeon, W., Park, S.-Y., Park, C., Jung, J., Lee, S.-H., Lee, H.W., 2019. Investigating the  
2048 regional difference of aerosol feedback effects over South Korea using the WRF-CMAQ two-  
2049 way coupled modeling system. *Atmos. Environ.* 218, 116968.  
2050 <https://doi.org/10.1016/j.atmosenv.2019.116968>.
- 2051 Yoon, J., Chang, D.Y., Lelieveld, J., Pozzer, A., Kim, J., Yum, S.S., 2019. Empirical evidence of a  
2052 positive climate forcing of aerosols at elevated albedo. *Atmos. Res.* 229, 269-279.  
2053 <https://doi.org/10.1016/j.atmosres.2019.07.001>.
- 2054 Yu, H., Kaufman, Y.J., Chin, M., Feingold, G., Remer, L.A., Anderson, T.L., Balkanski, Y., Bellouin,  
2055 N., Boucher, O., Christopher, S., 2006. A review of measurement-based assessments of the  
2056 aerosol direct radiative effect and forcing. *Atmos. Chem. Phys.* 6, 613-666.  
2057 <https://doi.org/10.5194/acp-6-613-2006>.
- 2058 Yuan, T., Chen, S., Huang, J., Wu, D., Lu, H., Zhang, G., Ma, Xiaojun, Chen, Z., Luo, Y., Ma,  
2059 Xiaohui, 2019. Influence of dynamic and thermal forcing on the meridional transport of  
2060 Taklimakan Desert dust in spring and summer. *J. Clim.* 32, 749-767.  
2061 <https://doi.org/10.1175/JCLI-D-18-0361.1>.
- 2062 Zhan, J., Chang, W., Li, W., Wang, Y., Chen, L., Yan, J., 2017. Impacts of meteorological conditions,  
2063 aerosol radiative feedbacks, and emission reduction scenarios on the coastal haze episodes in  
2064 southeastern China in December 2013. *J. Appl. Meteorol. Climatol.* 56, 1209-1229.  
2065 <https://doi.org/10.1175/JAMC-D-16-0229.1>.
- 2066 Zhang, B., Wang, Y., Hao, J., 2015. Simulating aerosol-radiation-cloud feedbacks on meteorology  
2067 and air quality over eastern China under severe haze conditions in winter. *Atmos. Chem. Phys.*  
2068 15, 2387-2404. <https://doi.org/10.5194/acp-15-2387-2015>.
- 2069 Zhang, H., Cheng, S., Li, J., Yao, S., Wang, X., 2019. Investigating the aerosol mass and chemical  
2070 components characteristics and feedback effects on the meteorological factors in the Beijing-  
2071 Tianjin-Hebei region, China. *Environ. Pollut.* 244, 495-502.  
2072 <https://doi.org/10.1016/j.envpol.2018.10.087>.
- 2073 Zhang, X.Y., Gong, S.L., Shen, Z.X., Mei, F.M., Xi, X.X., Liu, L.C., Zhou, Z.J., Wang, D., Wang,  
2074 Y.Q., Cheng, Y., 2003a. Characterization of soil dust aerosol in China and its transport and  
2075 distribution during 2001 ACE-Asia: 1. Network observations. *J. Geophys. Res. Atmos.* 108.  
2076 <https://doi.org/10.1029/2002JD002632>.
- 2077 Zhang, X.Y., Gong, S.L., Zhao, T.L., Arimoto, R., Wang, Y.Q., Zhou, Z.J., 2003b. Sources of Asian  
2078 dust and role of climate change versus desertification in Asian dust emission. *Geophys. Res.*  
2079 *Lett.* 30. <https://doi.org/10.1029/2003GL018206>.
- 2080 Zhang, Xin, Zhang, Q., Hong, C., Zheng, Y., Geng, G., Tong, D., Zhang, Y., Zhang, Xiaoye, 2018.  
2081 Enhancement of PM<sub>2.5</sub> Concentrations by Aerosol-Meteorology Interactions Over China. *J.*  
2082 *Geophys. Res. Atmos.* 123, 1179-1194. <https://doi.org/10.1002/2017JD027524>.
- 2083 Zhang, Y., 2008. Online-coupled meteorology and chemistry models: history, current status, and  
2084 outlook. *Atmos. Chem. Phys.* 8, 2895-2932. <https://doi.org/10.5194/acp-8-2895-2008>.
- 2085 Zhang, Y., Chen, Y., Fan, J., Leung, L.-Y.R., 2015a. Application of an online-coupled regional  
2086 climate model, WRF-CAM5, over East Asia for examination of ice nucleation schemes: part  
2087 II. Sensitivity to heterogeneous ice nucleation parameterizations and dust emissions. *Climate*  
2088 3, 753-774. <https://doi.org/10.3390/cli3030753>.



- 2089 Zhang, Yue, Fan Shuxian, Li Hao, Kang Boshi, 2016. Effects of aerosol radiative feedback during  
2090 a severe smog process over eastern China. *Acta Meteorol.* 74.  
2091 <https://doi.org/10.11676/qxxb2016.028>.
- 2092 Zhang, Y., Karamchandani, P., Glotfelty, T., Streets, D.G., Grell, G., Nenes, A., Yu, F., Bennartz, R.,  
2093 2012. Development and initial application of the global-through-urban weather research and  
2094 forecasting model with chemistry (GU-WRF/Chem). *J. Geophys. Res. Atmos.* 117.  
2095 <https://doi.org/10.1029/2012JD017966>.
- 2096 Zhang, Y., Wang, K., He, J., 2017. Multi-year application of WRF-CAM5 over East Asia-Part II:  
2097 Interannual variability, trend analysis, and aerosol indirect effects. *Atmos. Environ.* 165, 222-  
2098 239. <https://doi.org/10.1016/j.atmosenv.2017.06.029>.
- 2099 Zhang, Y., Zhang, X., Cai, C., Wang, K., Wang, L., 2014. Studying Aerosol-Cloud-Climate  
2100 Interactions over East Asia Using WRF/Chem, in: *Air Pollution Modeling and Its Application*  
2101 XXIII. Springer, pp. 61-66. [https://doi.org/10.1007/978-3-319-04379-1\\_10](https://doi.org/10.1007/978-3-319-04379-1_10).
- 2102 Zhang, Y., Zhang, X., Wang, K., He, J., Leung, L.R., Fan, J., Nenes, A., 2015b. Incorporating an  
2103 advanced aerosol activation parameterization into WRF-CAM5: Model evaluation and  
2104 parameterization intercomparison. *J. Geophys. Res. Atmos.* 120, 6952-6979.  
2105 <https://doi.org/10.1002/2014JD023051>.
- 2106 Zhang, Yang, Zhang, X., Wang, K., Zhang, Q., Duan, F., He, K., 2016a. Application of WRF/Chem  
2107 over East Asia: Part II. Model improvement and sensitivity simulations. *Atmos. Environ.* 124,  
2108 301-320. <https://doi.org/10.1016/j.atmosenv.2015.07.023>.
- 2109 Zhang, Yang, Zhang, X., Wang, L., Zhang, Q., Duan, F., He, K., 2016b. Application of WRF/Chem  
2110 over East Asia: Part I. Model evaluation and intercomparison with MM5/CMAQ. *Atmos.*  
2111 *Environ.* 124, 285-300. <https://doi.org/10.1016/j.atmosenv.2015.07.022>.
- 2112 Zhao, B., Liou, K., Gu, Y., Li, Q., Jiang, J.H., Su, H., He, C., Tseng, H.-L.R., Wang, S., Liu, R.,  
2113 2017. Enhanced PM<sub>2.5</sub> pollution in China due to aerosol-cloud interactions. *Sci. Rep.* 7, 1-11.  
2114 <https://doi.org/10.1038/s41598-017-04096-8>.
- 2115 Zhao, B., Wang, Y., Gu, Y., Liou, K.-N., Jiang, J.H., Fan, J., Liu, X., Huang, L., Yung, Y.L., 2019.  
2116 Ice nucleation by aerosols from anthropogenic pollution. *Nat. Geosci.* 12, 602-607.  
2117 <https://doi.org/10.1038/s41561-019-0389-4>.
- 2118 Zhong, M., Chen, F., Saikawa, E., 2019. Sensitivity of projected PM<sub>2.5</sub>- and O<sub>3</sub>-related health  
2119 impacts to model inputs: A case study in mainland China. *Environ. Int.* 123, 256-264.  
2120 <https://doi.org/10.1016/j.envint.2018.12.002>.
- 2121 Zhong, M., Saikawa, E., Liu, Y., Naik, V., Horowitz, L.W., Takigawa, M., Zhao, Y., Lin, N.-H.,  
2122 Stone, E.A., 2016. Air quality modeling with WRF-Chem v3.5 in East Asia: sensitivity to  
2123 emissions and evaluation of simulated air quality. *Geosci. Model Dev.* 9, 1201-1218.  
2124 <https://doi.org/10.5194/gmd-9-1201-2016>.
- 2125 Zhong, S., Qian, Y., Zhao, C., Leung, R., Wang, H., Yang, B., Fan, J., Yan, H., Yang, X.-Q., Liu, D.,  
2126 2017. Urbanization-induced urban heat island and aerosol effects on climate extremes in the  
2127 Yangtze River Delta region of China. *Atmos. Chem. Phys.* 17. <https://doi.org/10.5194/acp-17-5439-2017>.
- 2129 Zhong, S., Qian, Y., Zhao, C., Leung, R., Yang, X., 2015. A case study of urbanization impact on  
2130 summer precipitation in the Greater Beijing Metropolitan Area: Urban heat island versus  
2131 aerosol effects. *J. Geophys. Res. Atmos.* 120, 10-903. <https://doi.org/10.1002/2015JD023753>.
- 2132 Zhou, C., Gong, S., Zhang, X., Liu, H., Xue, M., Cao, G., An, X., Che, H., Zhang, Y., Niu, T., 2012.  
2133 Towards the improvements of simulating the chemical and optical properties of Chinese  
2134 aerosols using an online coupled model-CUACE/Aero. *Tellus B Chem. Phys. Meteorol.* 64,  
2135 18965. <https://doi.org/10.3402/tellusb.v64i0.18965>.
- 2136 Zhou, C., Gong, S.L., Zhang, X.Y., Wang, Y.Q., Niu, T., Liu, H.L., Zhao, T.L., Yang, Y.Q., Hou, Q.,  
2137 2008. Development and evaluation of an operational SDS forecasting system for East Asia:  
2138 CUACE/Dust. *Atmos. Chem. Phys.* 8, 787-798. <https://doi.org/10.5194/acp-8-787-2008>.
- 2139 Zhou, C., Zhang, X., Gong, S., Wang, Y., Xue, M., 2016. Improving aerosol interaction with clouds  
2140 and precipitation in a regional chemical weather modeling system 145-160.  
2141 <https://doi.org/10.5194/acp-16-145-2016>.
- 2142 Zhou, D., Ding, K., Huang, X., Liu, L., Liu, Q., Xu, Z., Jiang, F., Fu, C., Ding, A., 2018. Transport,  
2143 mixing and feedback of dust, biomass burning and anthropogenic pollutants in eastern Asia: a  
2144 case study. *Atmos. Chem. Phys.* 18, 16345-16361. <https://doi.org/10.5194/acp-18-16345-2018>.
- 2145 Zhou, M., Zhang, L., Chen, D., Gu, Y., Fu, T.-M., Gao, M., Zhao, Y., Lu, X., Zhao, B., 2019. The



- 2146 impact of aerosol-radiation interactions on the effectiveness of emission control measures.  
2147 Environ. Res. Lett. 14, 24002. <https://doi.org/10.1088/1748-9326/aaf27d>.  
2148 Zhuang, B., Jiang, F., Wang, T., Li, S., Zhu, B., 2011. Investigation on the direct radiative effect of  
2149 fossil fuel black-carbon aerosol over China. Theor. Appl. Climatol. 104, 301-312.  
2150 <https://doi.org/10.1007/s00704-010-0341-4>.